2008-04-10

Automatic Classification of Long Term Involuntary Spontaneous EMG

Jeffrey Winslow
University of Miami, jwinslow@cableone.net

UNIVERSITY OF MIAMI

AUTOMATIC CLASSIFICATION OF LONG TERM INVOLUNTARY SPONTANEOUS EMG

By

Jeffrey S. Winslow

A DISSERTATION

Submitted to the Faculty
of the University of Miami
in partial fulfillment of the requirements for
the degree of Doctor of Philosophy

Coral Gables, Florida

May 2008

UNIVERSITY OF MIAMI

A dissertation submitted in partial fulfillment of
the requirements for the degree of
Doctor of Philosophy

AUTOMATIC CLASSIFICATION OF LONG TERM INVOLUNTARY SPONTANEOUS EMG

Jeffrey S. Winslow

Approved:

_____ Dr. Dejan Tepavac Assistant Professor of Biomedical Engineering	_____ Dr. Terri A. Scandura Dean of the Graduate School
_____ Dr. Ozcan Ozdamar Professor of Biomedical Engineering	_____ Dr. Jorge Bohorquez Assistant Professor of Biomedical Engineering
_____ Dr. Weizhao Zhao Associate Professor of Biomedical Engineering	_____ Dr. Christine Thomas Professor of Neurological Surgery

WINSLOW, JEFFREY S. (Ph.D., Biomedical Engineering)

Automatic Classification of Long Term Involuntary Spontaneous EMG (May 2008)

Abstract of a dissertation at the University of Miami.

Dissertation supervised by Assistant Professor Dejan Tepavac and Dr. Christine Thomas.
No. of pages in text. (198)

Involuntary electromyographic (EMG) activity has been recorded in the thenar (thumb) muscles of spinal cord injured (SCI) subjects for only short time periods (minutes), but it is unknown if this motor unit activity is ongoing. Longer duration EMG recordings can investigate the physiological significance of this neuromuscular activity. Analysis of these data is complex and time consuming. Since no software is currently capable of classifying 24 hours of data at a single motor unit level, the goal of this research was to devise an algorithm to automatically classify motor unit potentials over 24-hours.

Twenty-four-hour, 2-channel thenar muscle EMG recordings were obtained from four different SCI subjects with cervical level injuries using a data logging device with custom software. The automatic motor unit classification algorithm used to classify the 24-hour recordings was a procedure consisting of four stages that included segmentation, clustering, and motor unit template uniting. All individual potentials were then classified and any superimposed potentials were resolved into their constituent classes. Finally, the algorithm found the firing patterns for each of the stable motor unit classes.

The classification algorithm performance was compared to the analysis of a human operator and assessed in 2 ways: Tracking global classes over the 24

hours and correctly classifying individual motor unit potentials as to belonging to particular global classes. The algorithm was able to track an average of 13 global classes in four 24-hour recordings with a mean accuracy of 92 %. It was also able to classify individual potentials with a mean accuracy of 86% over four recordings, greater than the inter-rater reliability of two human operators (79%). The activities of the motor units tracked by the algorithm ranged from tonic firing to sporadic activity. The algorithm could analyze 24 hours of data in 2-3 weeks, while a human operator was estimated to take more than 2 years. In conclusion, the motor unit classification algorithm accomplished its goal of automatically tracking motor unit classes over a 24-hour recording with high accuracy. The 24-hour classification method developed here could be applied towards classifying long term recordings of other biological signals.

This is dedicated to HAH and Mr. Pesty

Acknowledgements

I would like to thank Dejan Tepavac for his guidance throughout this long process. I had to rub my eyes and blink a few times, but when I clearly saw the faint glow at the end of that long tunnel, it was really Dejan shining that light the whole time.

I would also like to thank Christine Thomas for helping me revise the dissertation, along with the rest of the hardworking members of her lab for manually classifying all the EMG data. I really appreciate all their efforts to make this project what it was.

This project was funded by the State of Florida (Appropriation # 677) and the Miami Project to Cure Paralysis, USPHS grant # 30226.

TABLE OF CONTENTS

LIST OF FIGURES

Page

LIST OF TABLES

Chapter 1: Introduction

Spinal cord injured (SCI) individuals have no voluntary control over some of their skeletal muscles, generally those innervated from spinal segments below the lesion. These paralyzed muscles contract involuntarily (spasm) however in response to various stimuli such as vibration or changes in temperature [Karamura et al., 1989], [Little et al., 1989]. In other situations, involuntary contractions appear to be spontaneous in that no obvious stimulus generates the motor unit activity. These different types of muscle activity can be recorded as electromyographic (EMG) activity.

Spontaneous EMG activity has been observed by different investigators after spinal cord injury. While studying the use of EMG biofeedback to improve hand muscle function, Stein et al. [1990] showed some first dorsal interosseus and thenar muscles were spontaneously active. No apparent mechanism triggered this activity. Zijdewind and Thomas [2001] and Zijdewind et al. [2004] similarly have studied spontaneously active motor units in thenar muscles in humans with spinal cord injury. The spontaneously active motor units had two activity patterns – either firing tonically at around 6 Hz or sporadically at rates around 2 Hz. The authors found that these motor unit firing patterns were present in 2-minute and 30-minute recordings. Since there have been no long-term recordings of such spontaneous EMG activity, it is unknown if the motor unit activity takes place over extended time periods.

Long-term EMG recordings, for example over 24 hours, are important because they can provide detailed information about motor unit activity and

muscle behavior. They can aid in investigating the concept that only small amounts of neuromuscular activity are required to sustain muscle and motor unit properties as well as show activity differences between awake and sleep times. The effectiveness of spasm reducing medications can also be investigated through long-term EMG recordings. The duration of a drug's activity over time can be investigated by comparing muscle and motor unit activity before and after the medication is taken.

To analyze single motor unit behavior, it is critical to identify the action potentials that belong to a single motor unit and to follow that unit activity over time. A computerized method is required to accomplish this analysis because it is not practical to do these tasks manually. A classification expert requires a complete 40 hour week to manually classify 12 minutes of EMG even with software support. If extrapolated to the entire 24-hour recording, the time required skyrockets to more than two years. The overall objective of this research is to devise methods to automatically classify and analyze involuntary single motor unit activity in EMG recordings that are 24 hours in length.

Chapter 2: Objectives

The overall objective of this research is to automatically analyze involuntary motor unit activity from surface EMG records with minimal intervention from the human operator. The EMG arises from human thenar muscles that have been paralyzed chronically (>1 year) by cervical SCI. Two channels of EMG were recorded from the thenar muscles in order to provide additional motor unit potential features to aid in classification.

While there are currently several computerized classification tools available that are capable of analyzing EMG data for time periods ranging from several minutes to several hours [McGill et al., 2005], [Zennaro et al., 2003], there is presently no software package that can classify and track motor unit activity over a full 24-hour period. Automation is also an integral feature of the classification and analysis of 24-hour EMG recordings because the task is complex and time consuming.

Specifically, the aims in developing the classification algorithm are:

1) To segment individual potentials from the continuous EMG recording.
2) To cluster all of the motor units with stable templates shapes over the 24-hour time period.
3) To classify the potentials that belong to these most stable motor units over the 24-hour time period.
4) To resolve any superimposed potentials into their constituent motor units using a modified peel-off method developed by Stashuk [2001].

5) To determine the number of trackable units and their firing behavior. The final output of the algorithm will also provide the motor unit potential template waveforms.

6) To assess the performance of the automated classification algorithm and compare its outcome to motor unit classification completed by an EMG expert. Four 3-minute records were classified manually for each of four, 24-hour recordings for a total of 16 gold standard classifications.

7) To assess the trackability of the motor unit templates over 24 hours by comparing the results of the algorithm to the results of an expert classifier. Gold standards detailing the presence of each global class in each 3-minute EMG portion were manually produced using the specially EMG classification software.

Hypotheses:

1) Automatic (software-based) classification of motor unit potentials is as accurate as manual (user-based) analysis of motor unit potentials.

2) Automatic (software-based) classification of motor unit potentials is faster than manual (user-based) analysis of motor unit potentials.

The first hypothesis will be tested by computing the classification performance against the inter-rater reliability of manually constructed gold standards for individual potential classification (as described above). The second hypothesis will be tested by comparing the computing time of the algorithm

against the estimated time to generate a gold standard of the correct motor unit classifications for a 24-hour recording.

Chapter 3: Background

3.1 Electromyography (EMG)

3.1.1 Whole Muscle EMG

The motor unit is the basic unit of contractile force produced by a muscle and consists of a motoneuron, its axon, and all of the muscle fibers that the motoneuron innervates [Sherrington CS, 1929]. Each muscle fiber in the motor unit produces a muscle fiber action potential (MFAP) that results from the propagation of an action potential along the excitable membrane of a muscle fiber. The motor unit action potential (MUAP), which consists of the superposition of all individual MFAP produced in the motor unit, can be recorded as electromyographic activity, or EMG. [Stashuk DW, 2001], [Loeb and Gans, pg. xvii, 1986].

When recording EMG from the skin surface, individual MUAPs can be seen during weak contractions. As the strength of the contraction increases, these potentials overlap to produce an interference pattern which makes identification of potentials impossible.

In 1965, Henneman et al. [1965] proposed the size principle to describe how motor units are recruited (activated). The initial input signals to muscles only activate the weakest motor units. As the strength of the input signal grows, stronger and stronger motor units are activated. In summary, the weaker units composed of fatigue resistant fibers are activated, followed by units with more fatigable fibers when even more force is required.

Force can be produced by muscles in two different ways – motor unit recruitment and firing rate modulation. As more motor units are recruited, or activated, more force is generated. The central nervous system also controls muscle force by motor unit firing rate modulation, where increases in firing rates yield more force [Farina et al., 2002]. Muscle force builds from its component individual twitch contractions of single motor units into a fused contraction where each new contraction occurs before the preceding contraction ends. At a certain point, the successive contractions are so rapid (firing frequencies become high enough), they fuse together to produce a smooth and continuous contraction.

The balance between motor unit recruitment and firing rate modulation varies in different muscles. Kukulka CG and Clamann HP [1981] have shown that hand muscles like the adductor pollicis muscle rely primarily on recruitment of motor units to produce weak contractions (up to 30% of maximal force) and then more on firing rate modulation for production of stronger forces. In contrast, in limb muscles (e.g. the biceps brachii) motor units are recruited up to high forces (70-80% maximal muscle force).

3.1.2 Motor Unit Action Potentials (MUAPs)

The shape, amplitude, and duration of the motor unit action potential depend on many anatomical and physiological characteristics of the muscle fibers [Bekka RE et al., 2002]. Muscle fiber diameter and the number of fibers active affect the amplitude of the resulting MUAP. Larger muscle fibers will generate higher amplitude signals. The diameter of muscle fibers impacts the

MUAP conduction velocities, which are inversely proportional to the MUAP duration. Larger diameter muscle fibers will have MUAPs with greater conduction velocities, and therefore MUAPs with shorter durations.

The recording system also shapes the surface EMG that is recorded. The tissue in between the electrodes and the muscle fibers influences the frequency spectrum of the resulting EMG signal by creating a low-pass filtering effect. The electrodes themselves have their own filtering properties and the placement of the electrodes with respect to the innervation zone also determines the resulting EMG signal. For example, the electrode configuration in Westling et al. [1990] and Thomas [1997] recorded two channels of EMG from the thenar muscles in unipolar configurations (see Figure 4.4, section 4.1.2). The positive electrodes were positioned at the distal and proximal ends of the muscles with the common electrode for both channels positioned across belly of the muscles, close to the motor unit end plates, or in other words, where the muscles are innervated. The distal and proximal EMG channels in this situation are of opposite polarities because the electrical signals originating from the motor end plates propagate towards the positive electrodes of each channel.

3.1.3 Involuntary and Spontaneous EMG

After spinal cord injury, paralyzed muscles (under no voluntary control) still exhibit EMG, and by definition, this EMG is involuntary. Involuntary EMG can be in the form of muscle spasms brought about by some type of stimulus or there may be just spontaneously active motor units. Involuntary EMG has been studied at the single motor unit level, as muscle spasms or in long term recordings. These types of activity have only been explored in the laboratory environment over short time periods.

3.1.3.1 Single Motor Unit Activity

Stein et al. [1990] found more spontaneous activity when investigating the contractile properties of paralyzed muscles (in incomplete injuries in humans). The authors characterized the active motor units that they observed into three discrete types. The first category of motor units was those that were under voluntary control and had clear activation thresholds and a range of firing rates comparable to those of normal motor units. The second category included those units that could only be slowly and weakly activated. The final category consisted of those units that were not under voluntary control but were spontaneously active. These motor units represented about 20% of all units that were studied and tended to fire at rates less than 5 Hz. Although subjects could not activate these motor units voluntarily, their firing rates could increase when the muscle was stretched or undergoing a spasm.

Zijdewind and Thomas [2001] have observed two patterns of spontaneously active motor unit activity in SCI subjects during 2 minute recordings. The motor units either fired tonically at a mean frequency of 6 Hz or fired more sporadically at a rate of 2 Hz. Zijdewind et al. [2004] also recorded these spontaneously active motor units for 30-minute periods. Motor units that fired with high variability were significantly stronger than those firing with low variability. Irregularly firing motor units were also higher threshold units.

Spontaneous EMG activity has been observed in healthy animals as well as able-bodied humans. Tonic single unit firing has been recorded in the soleus muscles of cats without being accompanied by discernible movement of the hindlimbs, almost mirroring the spontaneously active motor units in SCI thenar motor units [Hensbergen E and Kernell D, 1997]. Eken [1998] also observed tonic motor unit firing activity in rats when they were standing still or asleep.

Sporadically firing spontaneous units may be driven by synaptic noise. Matthews [1996] showed that the exponential decay on the right tail of motor unit interpotential interval histograms provides evidence that synaptic noise may be responsible for some motor unit firings. Figure 3.1 shows interpotential interval histograms of motor unit data from two different muscles.

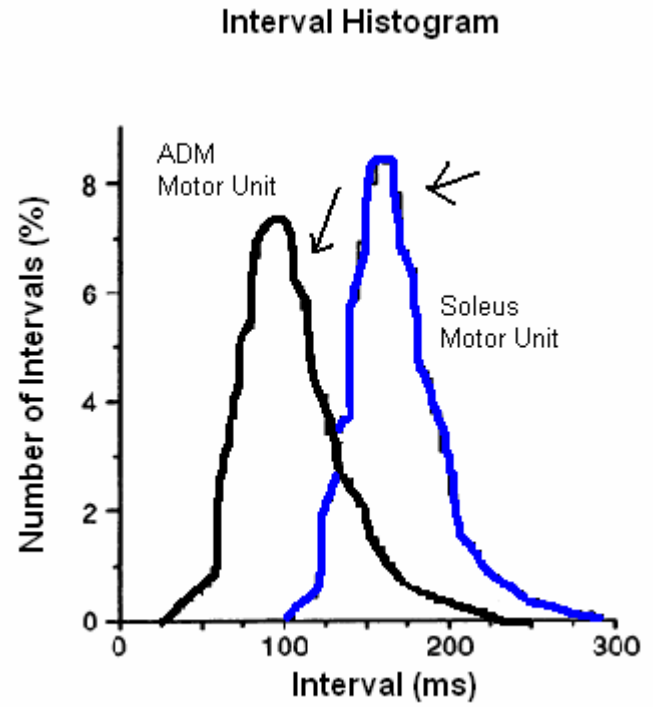

Figure 3.1 Example histogram of slow firing motor units in two different muscles. Interpotential intervals (the time between each motor unit firing) are shown for individual motor units in the soleus and abductor digiti minimi (ADM) muscles. The mean firing rate for the soleus motor unit is about 5 Hz while that for the ADM is about 10 Hz. The right tails of each of these histograms appear to decay exponentially, providing some evidence that synaptic noise may be causing some firings. The arrows indicate the start of the exponential decay behavior. [Modified from Matthews PBC, 1996]

Matthews transformed the interpotential interval histogram of a motor unit into a probability function, thus revealing the probabilities of future motor unit firings. As the interpotential intervals become longer and longer, the probability that another firing will occur steadily increases up to a certain point. This is the point where exponential decay behavior in the histogram begins (as indicated by the arrows in Figure 3.1). After this point, the probability remains constant, meaning that the probability of the next firing becomes a random process. This can be interpreted as the motoneuron firing being randomly excited by noise. The afterhyperpolarization (AHP), the process in which the motoneuron membrane potential drops below its resting value after a firing, is important in this

process. If the AHP is shorter than the time between firings, synaptic noise can enable the generation of an action potential [Matthews PBC, 1996].

Persistent inward currents, or PICs, may be related to spontaneous EMG activity. Motoneurons were once thought to be merely passive structures in the nervous system, conveying a signal generated elsewhere, but are now thought to contribute an active component in the form of persistent inward currents. A PIC is a depolarizing current generated by voltage sensitive ion channels that tend not to inactivate and are primarily generated in the dendritic regions of neurons [Heckman CJ et al., 2005]. PICs are involved in normal motoneuron activation in humans and have the ability of amplifying synaptic inputs by a factor of 5 [Gorassini et al., 2004]. These currents can be inhibited in the able-bodied with the help of neurotransmitters originating from the brainstem, so that the actions of PICs are controlled. In SCI individuals, PICs are less controlled by inhibition, and allow the production of excessive and undesired muscle contractions, like muscle spasms and can produce self-sustained firing of neurons.

PICs or synaptic noise may be responsible for spontaneously active motor units in SCI individuals that fire tonically or sporadically. PICs are more likely to be the source of spontaneously firing motor units that fire tonically at relatively low frequencies. The firing rate histograms for these motor units resemble normal distributions.

3.1.3.2 Spasm Activity

Thomas and Ross [1997] and Gorassini et al. [2004] both observed motor unit activity during muscle spasms in SCI subjects. Recording from the medial and lateral gastrocnemius, Thomas and Ross saw that the firing rate of most motor units (54%) increased up to the spasm peak and then decreased after the peak. The firing rates observed were similar to those seen in ramp-force voluntary contractions of able-bodied subjects. The remaining units fired doublets (two potentials close together) or at almost constant rates, around 6 Hz, with little rate modulation. Gorassini et al. recorded from the first dorsal interosseus, tibialis anterior, soleus, quadriceps, and hamstring muscles and theorized that 40% of the motor unit activity during spasms was produced by PICs. The firing rates towards the end of a muscle spasm were very low on average (around 3 Hz). Hamstring motor units exhibited steady firing rates (in-between 5 Hz and 11 Hz) with low variability.

3.2 Long Term EMG recordings

Long term EMG recordings are essential for gaining insight into muscle properties and usage. Aside from obtaining information on which muscles are active during daily activity, 24-hour EMG recordings on able-bodied individuals can also provide data as to how muscle activity is involved in maintaining muscle health and preserving its properties. In spinal cord injured individuals, long term EMG recordings can quantify spasms, a severe impairment to quality of life, and yield data on 24-hour involuntary EMG activity. In addition, long term recordings

of single motor units can reveal how the activity of individual motor units relates to the gross activity of the entire muscle. For example, a certain medication may only dampen the activity of the whole muscle by a small amount because it influences some but not all of the motor units.

3.2.1 Data Storage in Long Term Recordings

A critical issue in the history of long-term EMG recording is the inability to store large amounts of data. This has been dealt with in a number of ways. In many studies, the raw EMG is not directly recorded. Instead, the raw EMG is processed into integrated EMG (iEMG), which is simply the EMG smoothed via low pass filtering, rectified, and integrated in sequential, equal time divisions. iEMG reduces the amount of data that has to be recorded because only one iEMG data point is stored for each time division. These time divisions are always longer than the sampling period, thus effectively reducing the sampling rate of the EMG data. The ability to reduce the amount of data that is recorded over long time periods makes iEMG recording a common long-term EMG recording technique in that net EMG activity can still be recorded over long periods of time, at the expense of losing some duration and intensity information.

In their 24 hour EMG recordings, Tepavac et al. [1992] used an analog processing unit to compute the iEMG from the raw EMG before a microprocessing unit stored the processed data. Since iEMG can be interpreted as the product of EMG amplitude and duration, the true value of either of these quantities is lost during a recording. High iEMG values either means that there

was high amplitude raw EMG for a brief duration, or low amplitude raw EMG for a long duration or some combination of these possibilities. In this way, critical information is lost with this data reducing technique. In addition, any noise that is present is integrated as well and integrated noise can be mistaken for actual EMG activity.

To resolve these situations in which EMG information has been lost, raw EMG must be recorded for the total duration of the recording period. We now have the ability to store large amounts of data (greater than 1.0 Gigabytes) on flashcards, small media that act as hard disks, but without moving parts. If storage space is still limited, a lossless compression routine can be performed by a microprocessor-driven data logger to compress the data online as it is sampled.

There have been a number of advances that have made it possible to record raw EMG over long time periods. Advances in flashcard design have enabled large quantities of data to be stored, enough to store two channels of raw EMG at high sampling rates suitable for the identification of single motor units. A data logging device capable of recording 24 hours of raw, uncompressed EMG to a compact flashcard will be used in this study to collect long-term recordings. In addition, data loggers have become small enough for subjects to wear for long durations. Their processing power has also increased. Now that the raw EMG can be stored in long-term recordings, EMG intensity and duration information that was lost when recording iEMG can now be recovered for later analysis.

3.2.2 Previous Work in Long Term EMG Recording

Hensbergen and Kernell [1997] applied a different data reducing technique to examine daily EMG activity in cat ankle muscles. They recorded raw EMG through FM telemetry, but for only 4-minute periods every half hour, for a total of 192 minutes of raw EMG over a 24 hour period, before later generating iEMG for offline analysis. The authors recorded two channels of EMG simultaneously - one channel for the full hour and one channel for only 4 minutes. Upon comparing the iEMG obtained from these two sample times, the authors explained that these 4-minute samples were faithfully representative of an entire hour of activity.

Alaimo et al. [1984] similarly recorded iEMG from ankle muscles of healthy and spinalized cats for a 24 hour period. They only recorded the first 10 minutes of each hour, for a total of 240 minutes of iEMG over a 24-hour period. The authors “assumed” that this first 10 minutes of each hour was representative of the daily activity of the cats and do not discuss the possibility of incorrectly estimating the daily activity. A cat’s activity over the portion of the hour during which the EMG is not recorded, may be totally different than the period during which the EMG is recorded. A cat maybe extremely active during the actual recording period, and mostly inactive when the recording ceases, or the cat maybe inactive for the recording period, while being extremely active when the EMG is not being recorded. These examples illustrate the potential for overestimation and underestimation of electromyographic activity by sampling for a few minutes each hour.

Authors have used different methods to store large amounts of data. Boose et al. [1996] simultaneously recorded surface EMG from the extensor carpi radialis and flexor carpi ulnaris muscles of both forearms, using ECG electrodes for 24 hours so that they could quantify essential tremors through frequency analysis. They used a medilog tape recorder to record the raw EMG in an analog fashion, and then later digitized the data by sampling at 200 Hz using a personal computer. Sporrong et al. [1999] recorded two hours of surface EMG from the trapezius muscle with a portable device to investigate the workload of construction workers doing ceiling fitting tasks. They used their portable device to compute the average rectified value and the mean power frequency of the EMG online, which was recorded using a sampling period of 2 seconds.

Pozzo M et al. [2004] developed a 64-channel long term EMG recording system similar to the data logging system described by Mavoori et al. [2005] in order to assess neuromuscular functioning in elderly workers to ameliorate the affects of neuromuscular disorders. This system similarly records on type II flashcards, but samples each channel at 2 KHz and no online processing is done. This limits the recording times to two hours at most on 1.0 Gigabyte flashcards.

Airakisenen et al., [2005] and Mork and Westgaard [2004] both made long term EMG recordings from shoulder muscles to investigate chronic neck pain. Both sets of research groups recorded EMG from the skin surface over 24 hours in order to correlate EMG activity with neck pain. Mork and Westgaard showed

that there was no direct, simple correlation between neck pain and sustained low-level muscle activity during sleep.

Mavoori et al. [2005] utilized an implantable device called a neurochip in macaque monkeys to both process and record brain neuron activity. Their neurochip had 4 megabits of onboard memory, making it capable of recording 140 milliseconds of activity every 9 minutes for a total of 36 hours of neuron recording. This implantable device also had a built in spike discriminator that initiated recording whenever activity was present. With low power consumption, the neurochip was able to record 60 hours of data and the authors were able to record nine days of data with battery changes.

3.3 Muscle Health

It has been hypothesized that small amounts of neuromuscular activity, such as the spontaneous tonic firing of individual motor units, are required to sustain muscle properties. Healthy human leg muscles are only active for about 14% of the day in any case [Kern DS et al., 2001]. Hodgson et al., [2001] attempted to determine how much muscle activity was necessary to preserve muscle properties by recording EMG from the hind limbs of Rhesus monkeys for 24 hours. They found that the soleus muscles were active for approximately 9% of the day whereas the other muscles studied (lateral gastrocnemius and tibialis anterior muscles) were only active for approximately 4% of the day. The authors also analyzed the raw EMG intensities recorded from the hind limbs of healthy Rhesus monkeys over a 24 hour period and found that there were only brief

periods (less than one minute a day) when high-amplitude EMG activity was present in the soleus muscle. The authors suggested that only brief durations of activity were required to maintain the normal functional properties of the skeletal muscles of healthy Rhesus monkeys. This suggests that spontaneous motor unit firing in paralyzed muscles may serve a function in maintaining muscle health.

Hodgson et al. [2005] conducted 24-hour EMG recordings in the leg muscles of rats to determine the relationship between muscle properties and the daily muscle activity. Like the previously mentioned studies, this study found that most muscles were inactive for large portions of the day, including the more active soleus muscle that contains a large proportion of slow fibers. It also showed that there was a poor correlation between the daily duration of muscle activation and the percentage of slow fibers in a muscle. The general conclusion was that muscle fiber composition is maintained even when fibers are only activated for brief periods of time. It is still unknown if muscle activity, manifesting itself in the form of spontaneously generated motor activity or muscle spasms, is important for the health of paralyzed muscles.

Roy et al. [2007] studied spinal cord isolation as a model of disuse, a situation where the spinal cord is transected at two levels and all inflow to these spinal regions is eliminated by bilateral dorsal root section. Despite this attempt to remove all activity to leg muscles, short, high amplitude activity bursts were present in all the muscles they studied plus sporadic bursts in individual muscles. They proposed that the paralyzed muscle activity could be due to several possibilities. The first possibility was that rat motoneurons and interneurons may

be exhibiting enhanced excitability, thereby causing spontaneous activity. Another possibility was that the increased excitability may have been due to enhanced excitability of the muscle fibers themselves.

3.4 American Spinal Injury Association (ASIA) SCI Classification

Spinal cord injuries are classified by injury level and the severity of the injury as established by the American Spinal Injury Association (ASIA) [ASIA, 2006]. The spinal cord consists of four segmental levels – cervical (neck), thoracic (chest), lumbar (back), and sacral (tail). There are 7 cervical vertebrae, 12 thoracic vertebrae, 5 lumbar vertebrae, and 5 sacral vertebrae. The level of the injury can be established by testing: 1) the dermatomes and finding the corresponding spinal level at which there is or isn't sensation; 2) muscle function at these same spinal levels.

A dermatome is patch of skin that is innervated by a given spinal cord level. A chart is given in Figure 3.2 that describes the skin regions innervated by the associated spinal cord levels.

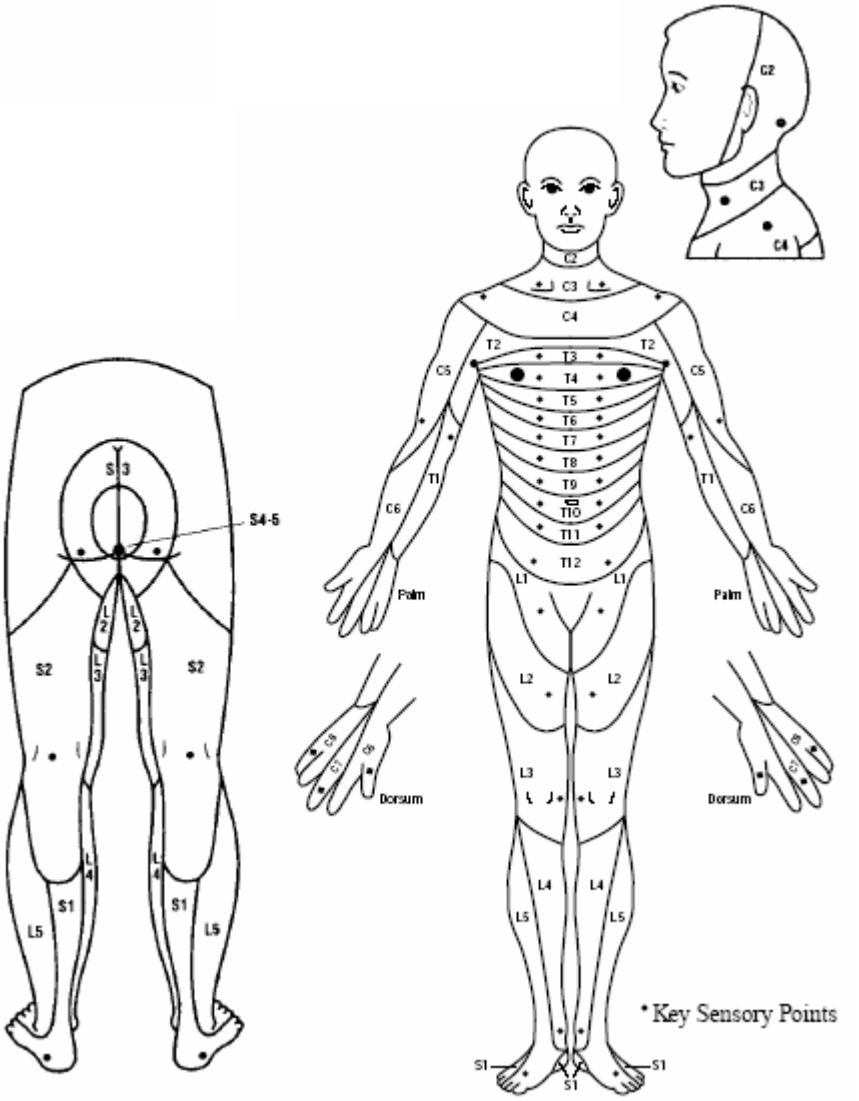

Figure 3.2 Dermatomes and their corresponding spinal levels. A dermatome is a patch of skin innervated by a given spinal cord level as shown in the figure. [Modified from ASIA, 2006]

The C2 to C4 levels cover the dermatomes from the top part of the neck to the area just below the clavicle, respectively. The C5 to T1 levels are situated in the arms, L1 to L5 represent the hip and groin area, and S2 to S5 represent the backs of the legs and the feet. According to the ASIA worksheet [2006] for injury classification, there are three basic ratings for each of these dermatomes: 0 for absent sensation, 1 for impaired sensation, and 2 for normal sensation.

Ten regions of motor function can similarly be examined (Figure 3.3). The figure shows that 10 sets of muscles which correspond to the spinal levels C5 through C8, T1, L2 through L5, and S1. There are five degrees of classification for motor function: A score of 5 means that there is active movement against full resistance; a score of 4 means that there is active movement against some resistance; a score of 3 means that there is active movement against gravity; a score of 2 means that there is active movement without respect to gravity; a score of 1 means that there is palpable or visible contraction; and, a score of 0 indicates total paralysis.

In this study, the thenar muscles investigated have no voluntary control or function, were paralyzed completely, and were rated as a 0. The level of injury was either C4, C5, or C6. Shoulder muscles can be used voluntarily when a SCI is at C4. Biceps brachii and wrist extensor muscles can also be used when the SCI is at C5 or C6, respectively.

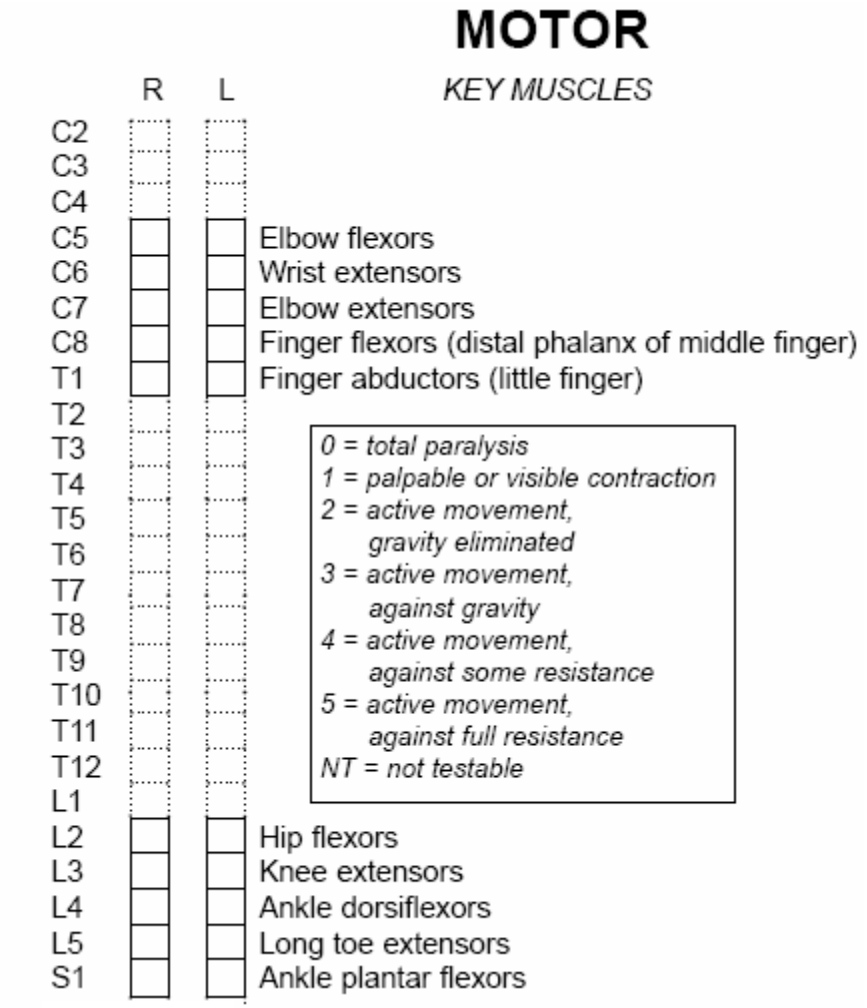

Figure 3.3 Key muscles and their corresponding spinal levels. Ten key groups of muscles are listed along with their corresponding spinal levels. [Modified from ASIA, 2006]

ASIA also has an impairment scale based on five classifications, A through E. Class A describes a complete injury – no motor or sensory function is preserved in the sacral segments S4 and S5. Individuals with complete SCI will be used in this study. Classes B through D describe incomplete injuries. In a class B injury, sensory but not motor function is preserved below the neurological level and includes the sacral segments S4 and S5. In a class C injury, motor function is preserved below the neurological level and more than half of the key muscles mentioned earlier have a muscle grade less than 3. In class D injuries,

motor function is preserved below the neurological level and at least half of the muscles below the neurological level have a muscle grade of 3 or greater. Finally, class E is normal, meaning that both motor and sensory function is normal.

3.5 Spasticity: A Problem for SCI Individuals

SCI individuals are commonly afflicted by spasticity, but the way spasticity manifests itself varies greatly and depends on the level and completeness of the injury. Spasticity is a complex phenomenon and may consist of hyperreflexia, clonus, increased muscle tone and spontaneous muscle spasms. The severity and distribution of such spastic activity can change over time. [Little JW et al., 1989]

Spasticity degrades the quality of life of the SCI individuals that it afflicts. In one questionnaire-based study consisting of 60 SCI subjects who complained about spasticity of the lower extremities, 91 % reported that spasms interfered with their activities to some extent. 65 % stated that the spasms disrupted their sleep. Half of the patients reported that their spasms contributed to pain. [Little JW et al., 1989] A similar study was conducted regarding the spasticity experienced by SCI subjects with a cervical cord injury [Karamura J et al., 1989]. 11 out of 13 patients stated that spasms interfered with their daily activities.

Muscle spasms for both complete and incomplete SCI were almost always accompanied by triggers. The list of triggers includes [Karamura J et al., 1989], [Little JW et al., 1989]:

1. Transfers from one position to another
2. Bladder and bowel evacuation
3. Voluntary motion like yawns and coughs
4. Physical stimuli such as vibration and cold breezes
5. Emotional stimuli such as excitement and emotional tension.

Treatment methods must be developed in order to ease SCI individual's daily struggle with spasticity, particularly the muscle spasms. For example, the severity and frequency of spasms in the SCI subjects with a cervical level seemed to decrease after exercise [Karamura J et al., 1989].

Although the negative effects of spasms have been mentioned so far, some SCI individuals use spasms to their advantage. For example, a SCI individual may know how to trigger a spasm and that contraction can act to shift his or her position in bed without any additional help. The involuntary muscle contractions may also be beneficial, helping to maintain muscle properties like strength, for example.

Anti-spasm medications serve as a pharmacological treatment for muscle spasms. Baclofen (which works on GABA-b receptors), diazepam, and clonidine are drugs that have been used individually or in combination to lessen the effects of spasticity on the spinal cord injured by dampening involuntary muscle activity. While there have been several studies to assess the effects of these drugs [Taricco et al., 2006], the outcome measures have varied between studies. This leaves much doubt about the true effectiveness of treatment regimes of these drugs.

The only way to evaluate treatments for spasticity is the development of some form of quantifiable measure of spasticity. According to the Karamura J et

al. [1989] and a study assessing the effects of a muscle relaxant in reducing muscle spasms in SCI individuals, 24-hour EMG recording is the only way to quantitatively evaluate patient spasticity in order to develop treatments and assessments of spasticity. One advantage of long term EMG recordings is that they capture all of the contractions, even the problematic muscle spasms that occur at night when laboratory experiments are not normally performed.

3.6 EMG Signal Decomposition

EMG signal decomposition is a complicated multi-step procedure of resolving compound EMG signals into their constituent trains of MUAPs. Some basic assumptions are needed when accomplishing EMG decomposition [Stashuk DW, 2001]:

1) MUAPs produced by the same motor unit must be more similar in shape than the MUAPs produced by different motor units.
2) Differences in MUAP shapes must be distinguishable.
3) Each MUAP must occur enough times without superpositions and with MUAPs from other motor units so that the respective template shapes of each active motor unit can be determined.

The basic process of decomposition involves the following fundamental steps:

1) Segmentation, or candidate selection
2) Clustering
3) Superposition resolution

The EMG decomposition system must be able to resolve 2 or more units with similar shapes, frequent superpositions of MUAPs, and variability in shapes due to biological noise and variability [Stashuk DW, 2001].

3.6.1 Segmentation

The first step in EMG decomposition is segmentation of the signal into MUAP candidate waveforms. The segmentation procedure is extremely important, as it will determine which potentials will be included in the analysis and the ease in their classification in later decomposition stages.

The simplest method to isolate MUAP candidate waveforms is by means of an amplitude threshold. The actual threshold value can be determined by the EMG signal frequency components, characteristics of the signal and noise components, or even a human operator [Fang J et al., 1999]. The choice of threshold can introduce bias against smaller MUAPs, but it is essential to consistently select those waveforms that can be successfully categorized [Stashuk DW, 2001]. Only those waveforms that are discernable by a human operator should be retained as candidate MUAPs to ensure that when an algorithm detects a candidate MUAP, it actually is a MUAP.

Filtering can also be done to accentuate the prominence of candidate MUAPs and thus make candidate waveforms more discriminable. Low-pass differentiation (LPD) filters have been used on raw EMG to reduce both the high frequency noise and the low frequency baseline noise, along with enhancing peak sharpness [Hassoun MH et al., 1994]. LPD filters also shorten the duration

of MUAPs, reducing their possible temporal overlap, decreasing the number of superimposed waveforms [Stashuk DW, 2001].

Alignment is also a crucial factor in segmentation. All candidate MUAPs that are segmented from the EMG signal on a per channel basis must be aligned in a consistent manner. Most systems either initially align peak values of either the amplitude or slope signal. If consistency in alignment during segmentation is not maintained, the clustering steps that follow may fail to categorize similar candidate MUAPs. Figure 3.4 demonstrates this situation.

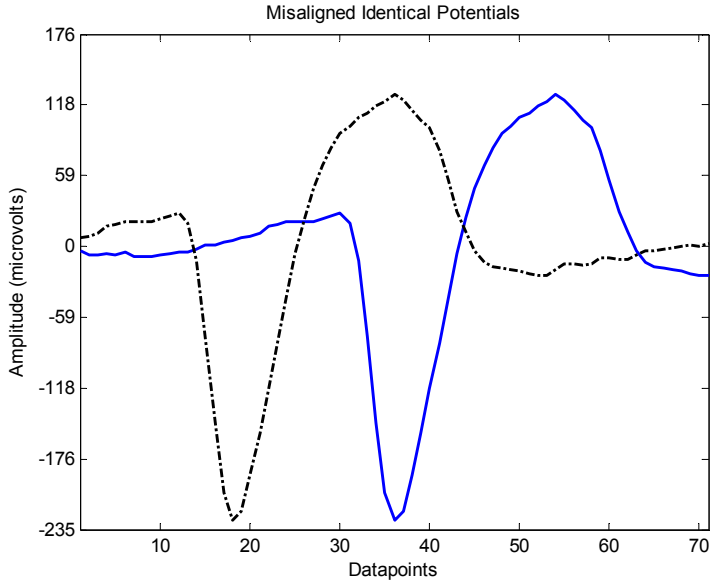

Figure 3.4 Misaligned potential example. Both the solid and dotted lines represent an identical potential that was segmented at 2 different alignments, the maximum and the minimum. Although these are identical potentials, when distance measures, like the Euclidean distance, are applied, they will result in large distances, meaning that the potentials are not similar. If they had been both segmented with the same alignment, a Euclidean distance measure would result in a value of zero, meaning that they were identical. It is in this way that incorrect classifications can result.

The same potential was segmented (or extracted) from the raw EMG recording with different alignments. The blue instance of segmentation was extracted from the recording with its most negative point at the center of the window, while the black instance was segmented with the maximum point at the center of the

window. If these two potentials were compared using a distance measure such as Euclidean distance, their distance would be large. The distance between them would be zero if they had been aligned by segmenting them both so that they were aligned at either the potential's maximum or minimum points. Major initial alignment errors can sometimes not be corrected later [Stashuk DW, 2001].

3.6.2 Clustering

After the EMG signal has been segmented into candidate MUAP waveforms, they must be grouped into clusters, with each cluster ideally representing the motor unit that produced the MUAPs. Clustering is defined as the partitioning of a set of objects (the MUAPs) into a number of similar classes or clusters [Stashuk DW, 2001]. If the number of active motor units is not known in advance, as is the case most of the time, the exact number of clusters is not known. Each cluster also has a centroid, also known as a cluster mean or template shape that is also unknown. The clustering algorithm must first determine the correct number of clusters and then correctly assign as many MUAPs as possible to the correct clusters so that template MUAP shapes can be recovered [Stashuk DW, 2001].

Many different clustering algorithms exist and have been used for clustering candidate MUAPs. Hierarchical, K-means, and artificial neural networks (ANN) clustering methods have been employed in clustering EMG signals for decomposition and classification. MUAP firing pattern information has

also been used in conjunction with shape-based clustering to make categorization more robust [Schalk G et al., 2002].

Except for ANN methods, clustering algorithms routinely use a distance measure for comparing candidate MUAPs. Some distance measures commonly used include Euclidean, normalized Euclidean (based on waveform energies), and correlational distances. Sections 3.6.2.1 and 3.6.2.2 describe clustering methods that utilize distance measures for clustering.

3.6.2.1 Hierarchical Clustering

Hierarchical clustering is a distance-based clustering method in which a nested sequence of partitions is formed to divide the input set of objects into clusters. The basis for hierarchical clustering is the proximity matrix. [Jain AK and Dubes RC, pg. 11, 1988] The proximity matrix contains distances between the different objects that must form clusters. In the case of multi-dimensional vectors, the distance between vectors can be a sum of the distances between vector components. Typically, the proximity matrix is a dissimilarity matrix, meaning that the smaller a distance value between two objects, the more similar the objects are. The columns and rows of the proximity matrix represent the different objects in the group that must be clustered (Figure 3.5).

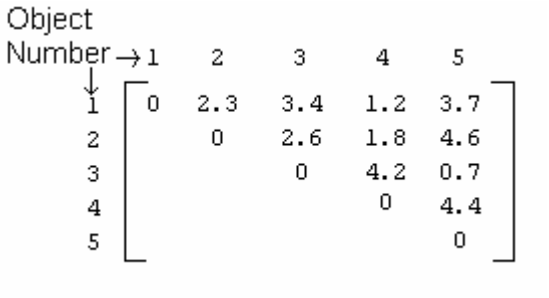

Figure 3.5 Example proximity matrix. The proximity matrix shows the difference between objects in a dataset. For example, the distance between objects 4 and 2 is 1.8.

The proximity matrix is a triangular matrix, meaning that the lower triangle of the two-dimensional matrix mirrors the upper triangle, and its diagonal is undefined. The values in the matrix are distances. In Figure 3.5, for example, the distance between object 2 and object 4 is 1.8.

In the agglomerative method of clustering, each object is given its own cluster, and through a sequence of combinations, these clusters are merged into larger clusters. As the combination is done, the proximity matrix is updated to reflect the absence of the previous objects and the addition of the new clusters.

Two algorithms that conduct object merging in this hierarchical fashion are single-linkage and complete linkage clustering. In both clustering methods, the two most similar objects are first found. The rows and columns corresponding to the smallest distance value represent the objects to be merged into a cluster. The two objects are then merged into an individual cluster. The two algorithms differ in how the proximity matrix is updated to reflect the new clustering. In the single linkage algorithm, the distances between the new cluster and the previous objects are replaced by the smaller of the two distances of the original objects that were just combined to form new objects.

In Figure 3.6A, the single-linkage algorithm is used to update the proximity matrix, forming a new cluster by combining objects 3 and 5 and replacing the distances from 3 and 5 to all other objects with the smaller of the two corresponding values from the previous proximity matrix (Figure 3.5).

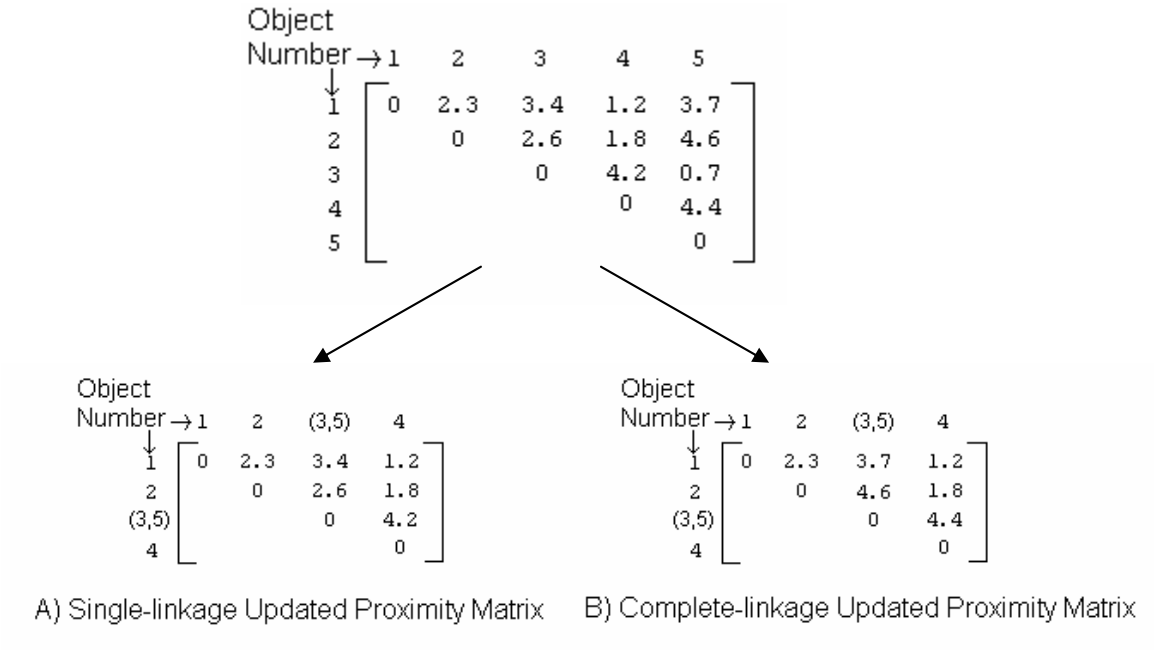

Figure 3.6 Proximity matrix update for hierarchical clustering algorithms. A) Single linkage algorithm. B) Complete linkage algorithm.

In Figure 3.6B, the complete-linkage algorithm similarly updates the proximity matrix, but the larger of the two corresponding values from the previous proximity matrix are used to replace the distances from objects 3 and 5 to all other objects.

Since the new distance values replaced are the smaller of the groupings, it can be seen as a nearest neighbor method. In complete-linkage clustering, the distances between the new cluster and the previous objects are replaced by the larger of the two distances of the original objects. For example, in Figure 3.6B,

the larger of the 2 corresponding values from the previous proximity matrix are used to replace the distances from object 3 and 5 to all other objects.

In the single-linkage and complete-linkage clustering algorithms, the same merging process is continued until there are no individual objects remaining. The result of these linkage algorithms is a dendrogram. The dendrogram (Figure 3.7) is a tree-like diagram displaying which objects or clusters of objects have been merged.

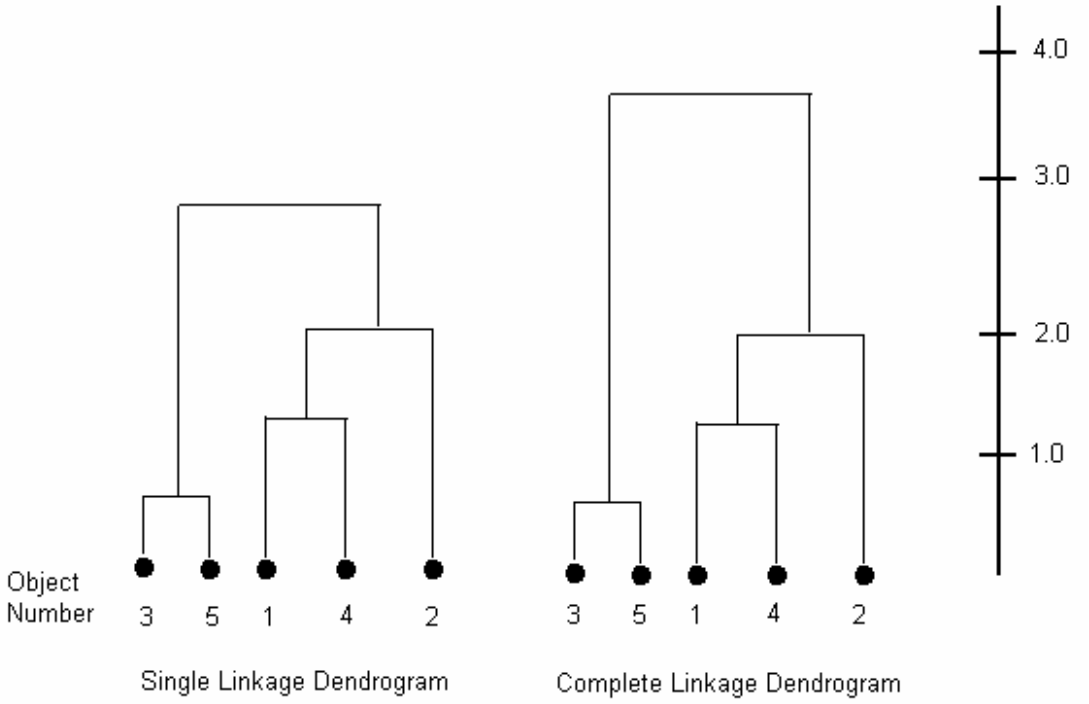

Figure 3.7 Resulting dendrograms for single and complete linkage hierarchical clustering algorithms. Slightly different dendrograms result from combining objects in the proximity matrix from Figure 3.5. Objects are grouped by distances from each other, with the closest objects joined by branches on the dendrogram. [Modified from Jain AK, pg 73, 1988].

The number of clusters obtained from these types of hierarchical clustering depends on the distance level, or distance threshold, at which the dendrograms are cut. For example, when the complete linkage dendrogram in Figure 3.7 is cut at distance levels of 3.0, 2.0, and 0.8, the number of resulting clusters is 2, 3, and

4, respectively (Figure 3.8, A,B, and C). The order in which the objects are merged does not affect the final resulting dendrogram.

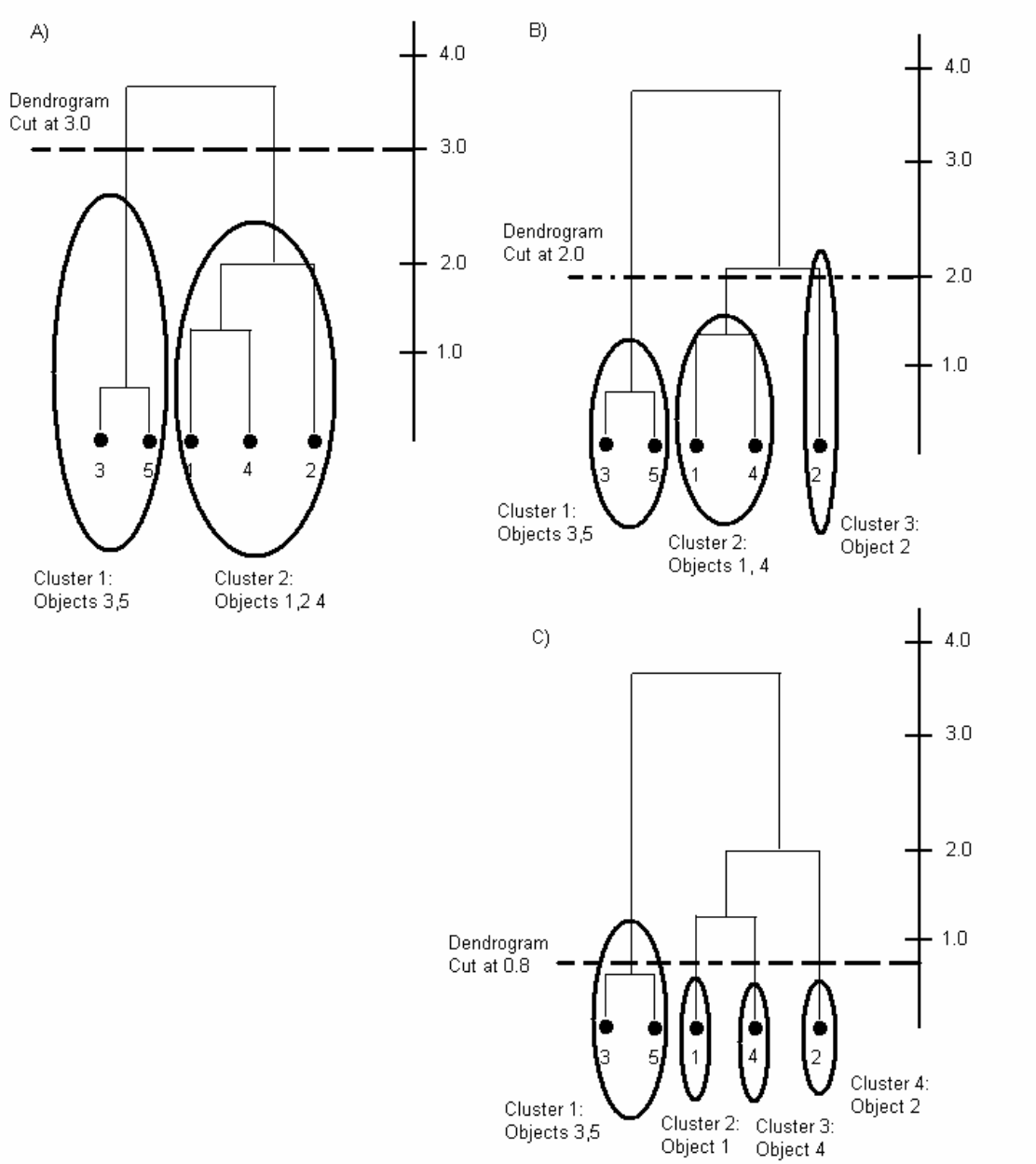

Figure 3.8 Resulting Clusters from cutting dendrograms for complete linkage algorithm. When the Dendrogram is cut at distance levels of A)3.0, B) 2.0, and C) 0.8, cluster numbers of 2, 3, and 4, result, respectively. [Modified from Jain AK, pg 73, 1988]

3.6.2.2 K-means Clustering

Partitional clustering methods, like K-means clustering, when given a known number of clusters, K, beforehand, attempt to create K cluster set partitions to separate each cluster [Stashuk DW, 2001]. The partitions are found through the minimization of a specified function, usually an error function.

In partitional clustering methods, object vectors are assigned to the cluster whose centroid (equation 3.1), or mean vector, is closest.

$$\vec{m}^{(k)} = \frac{1}{n_k} \sum_{i=1}^{n_k} \vec{x}_i^{(k)} \qquad (3.1)$$

In equation 3.1, $\vec{m}^{(k)}$ is the centroid of cluster k, n_k is the number of vectors that are contained in cluster k, and $\vec{x}_i^{(k)}$ is an individual vector belonging to cluster k.

The K-means iterative partitioning algorithm does object vector assignments based on the total squared error, the error function (equation 3.2).

$$E_k^2 = \sum_{k=1}^{K} e_k^2 = \sum_{k=1}^{K} \sum_{i=1}^{n_k} (\vec{x}_i^{(k)} - \vec{m}^{(k)})^T (\vec{x}_i^{(k)} - \vec{m}^{(k)}) \qquad (3.2)$$

The K-means algorithm [Jain AK and Dubes RC, pg.96-97] follows the following steps:

1) Select initial partitions with K clusters. The initial clusters can contain object vectors selected at random or those vectors that are a good estimate to the actual cluster means. Hierarchical clustering can even be used to set an initial partition.
2) Generate new partitions by assigning each object vector to its closest cluster centroid.
3) After all object vectors are assigned, recompute the cluster centroids and the total squared error. Each run through assignment of all object vectors is known as a pass. Cluster centroids can also be recomputed after each individual object vector assignment.
4) Repeat steps 2) and 3) until a global minimum of the error function is reached, or the computed squared error stabilizes.

Additional steps can be added to the K-means algorithm to improve its versatility. New clusters can be created if certain conditions are met. Clusters can be split if too many object vectors become members of a cluster and there is a large variance along a vector component with the largest spread. Small clusters can be viewed as outliers and removed from clustering entirely [Jain AK and Dubes RC, pg.96-97].

In partitioning methods, the order in which the data are considered can change the final results. Typically the K-means algorithm can be run a series of times to try to reduce the minimum error and achieve the global minimum of the

error function to improve the clustering. Since the K-means algorithm can become “trapped” in a local minimum, a forcing pass can be used to perturb the partitions to avoid ensnarement in a global minimum [Jain AK, pg.96-97].

3.6.2.3 Fuzzy Clustering

The clustering methods in the preceding sections have discussed “hard clustering” methods. In “hard clustering” an object or pattern is a member of a particular cluster, or it is not. In fuzzy clustering, however, cluster membership is not binary, but assumes a range of values. In this way, the “degree” of cluster membership is addressed for each pattern. Fuzzy K-means clustering is similar to K-means clustering in that K clusters are formed and K is known beforehand. However, the output of the fuzzy K-means clustering is a membership function that describes the degree to which each object is a member of each cluster. These membership function values can range from 0 to 1, and all membership function values for a particular object for all of the K clusters, must sum to 1. This is demonstrated in equation 3.3, where μ_{ij} is the membership function value of pattern j to cluster i and K is the total number of clusters.

$$\sum_{i=1}^{K} \mu_{ij} = 1 \qquad (3.3)$$

The fuzzy K-means algorithm is an iterative procedure that continually recomputes membership function values, then uses these values to find the cluster centroids, and compares the change in the distance between centroids

from one iteration to the next. Once the change is less than a given value, then the algorithm is terminated.

The iterative version of the fuzzy K-means proceeds as follows:

Step 1) Random values are assigned to the membership function so that equation 3.3 is true.

Step 2) The fuzzy centroids, $\vec{V}_i$, for each cluster I are computed, where $\vec{X}_j$ is the pattern and there are N patterns (equation 3.4). q is the fuzziness index which is determined empirically and usually q > 1 [Zouridakis G and Tam DC, 2000].

$$\vec{V}_i = \frac{\sum_{j=1}^{N} (\mu_{ij})^q \vec{X}_j}{\sum_{j=1}^{N} (\mu_{ij})^q} \qquad (3.4)$$

Step 3) Compute the updated membership function values based on the new centroids obtained (equation 3.5). $d^2(X_j, V_i)$ is the squared Euclidean distance between each pattern and the cluster centroid, and is given by equation 3.6. In equation 3.6, each pattern has M points and $X_j(n)$ is the point by point representation of the pattern $\vec{X}_j$, and $V_i(n)$ is the point by point representation of the centroid $\vec{V}_i$.

$$\mu_{ij} = \frac{[\frac{1}{d^2(X_j, V_i)}]^{\frac{1}{q-1}}}{\sum_{i-1}^{K} [\frac{1}{d^2(X_j, V_i)}]^{\frac{1}{q-1}}} \qquad (3.5)$$

$$d^2(X_j V_i) = \sum_{n=1}^{M} (X_j(n) - V_i(n))^2 \qquad (3.6)$$

Step 4) Compute the total error, E_{Total} by summing the Euclidean distances the previous cluster centroid, $\vec{V}_i$, and the updated cluster centroid, $\vec{V}_i^*$.

$$E_{Total} = \sum_{i=1}^{K} \left\| \vec{V}_i - \vec{V}_i^* \right\| \qquad (3.7)$$

Step 5) If the total error is less than a given small value, then stop. Otherwise, go back to step 2.

The fuzzy partitions created by fuzzy K-means clustering are not the end of the algorithm. The fuzzy membership values generated must be defuzzified to achieve crisp centroids and classifications. The defuzzification can simply be accomplished by using a threshold value for the membership function. If the membership value for a particular pattern is greater than some value μ_T for some cluster i, then the pattern is a member of that cluster i for which the threshold is exceeded.

A validity criterion can be used to address the correctness of clusters. Equation 3.8 shows a clustering validity function, S, for fuzzy clustering. This validity function is expressed as the ratio of the compactness to the separation of clusters.

$$S = \frac{\sum_{i=1}^{K}\sum_{j=1}^{N}(\mu_{ij})^{q}\left\|\vec{V}_i - \vec{V}^{*}_i\right\|^2}{N\min\left\|\vec{V}_i - \vec{V}^{*}_i\right\|^2} \qquad (3.8)$$

A smaller S value means a more compact, separate partition and thus a better clustering [Zouridakis G and Tam DC, 2000].

3.7 Previous Attempts at Classifying EMG

There have been many past endeavors at automatically classifying EMG recordings at the motor unit level. They have used ANNs and complex algorithms. Christodoulou and Pattichis [1999] used a multi-step process involving ANNs to decompose EMG signals in order to diagnose neuromuscular diseases. After preprocessing and segmentation, their system consisted of a self-organizing map type ANN followed by a learning vector quantization stage to fine tune the ANN, and finally yield a motor unit potential classification (Figure 3.9).

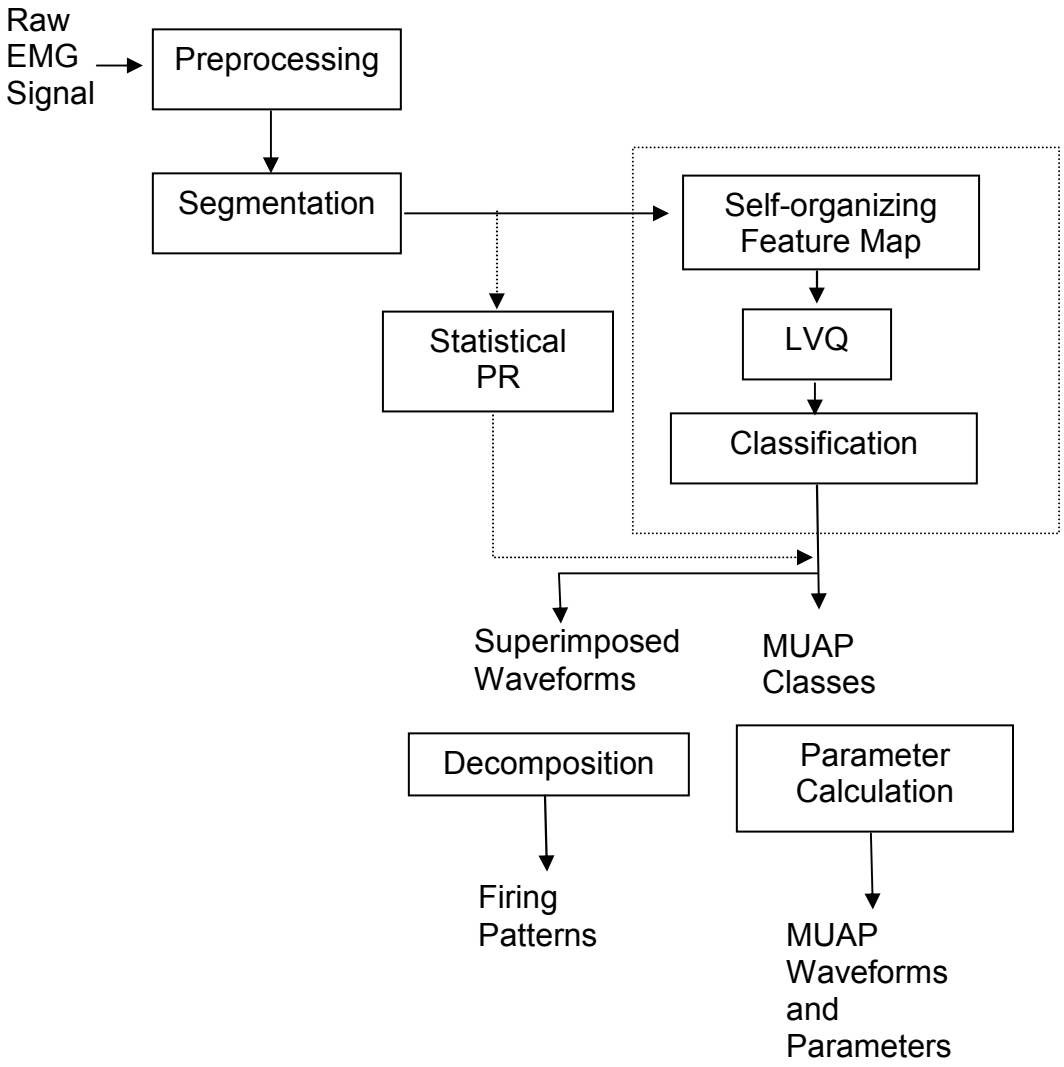

Figure 3.9 Christodoulou and Pattichis' EMG classification system. After preprocessing and segmenting potentials, a self-organizing map ANN along with one stage of learning vector quantization classifies motor unit potentials into different classes. The system then determines parameters such as peak-to-peak amplitude and duration and resolves superimposed potentials by means of an iterative peel-off method. [Modified from Christodoulou CI and Pattichis CS. 1999]

Superimposed potentials were resolved using an iterative peel-off algorithm that cross-correlated each superimposed potential with a class template and then applied a Euclidean distance measure to verify which template potentials were contained within the superposition.

Fang, Agarwval, and Shahani [1999] used a method based in the wavelet domain to classify multi-unit EMG signals. The authors segmented potentials

using wavelet coefficients to select the proper threshold and then classified potentials based on similar wavelet coefficients.

Hassoun et al.'s [1994] NNERVE system utilized an auto-associative ANN with specially designed training rules for automated EMG decomposition. After linear predictive filtering, segmented potentials were aligned and combined with several features, such as amplitude and the norm of the dataset, to constitute input patterns for training examples for an ANN. The ANN's targets for the training examples were the training examples themselves, so that the ANN, using a special pseudo-unsupervised training algorithm, could learn binary patterns to represent several classes of motor unit potentials, instead of memorizing the individual potentials themselves. Hamming distances, or bitwise differences between binary numbers, from the binary patterns were used to classify motor unit potentials. Finally, an inter-potential-interval analysis was conducted to refine classification.

Stashuk [1999] used a "certainty-based" method for classification. First, a modified K-means shape algorithm and an error-filtered estimation algorithm that attempted to estimate firing rate information are used to cluster similar potentials. The author then used a certainty-based method, which involves fuzzy values for further classification. The certainty-based method attempts to emulate the job of a human classifier by looking at several characteristic features of a potential and weighing each one against specified rules to determine if classifications are appropriate.

Several authors have attempted motor unit classification in EMG using timing based methods. Schalk et al. [2002] used interpotential interval (IPI) based clustering to classify MUAPs. The interpotential interval is the time between firings of MUAPs. They mapped MUAP trains into a two dimensional feature space consisting of a mean IPI and a time offset relative to an arbitrary starting time (Figure 3.10).

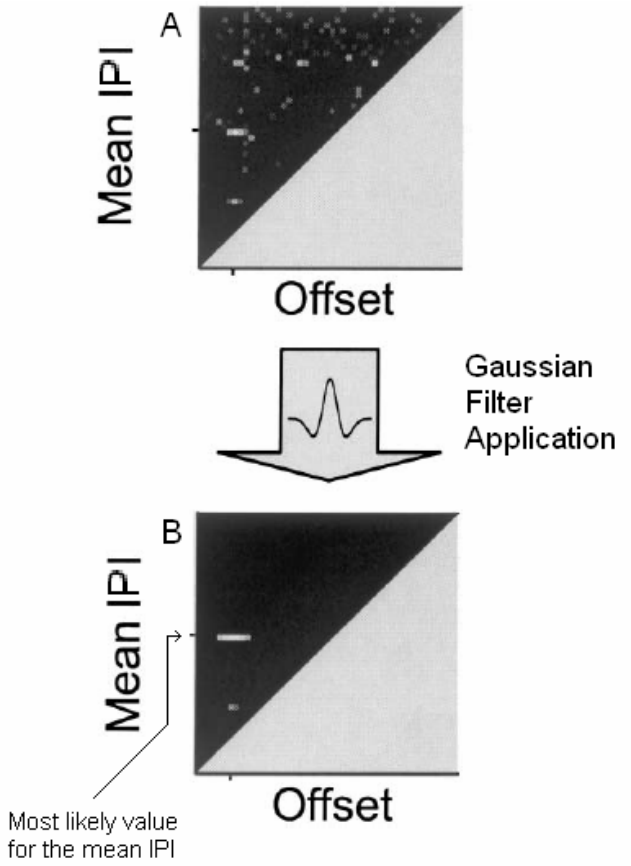

Figure 3.10 MUAP classification by means of mapping MUAP trains to a feature space. MUAP trains are mapped to a two dimensional feature space by iteratively subtracting a mean IPI from the firing time of each potential and repeating this process for different mean IPIs. After plotting the values in A, a 1-dimensional filter is applied that works along the mean IPI axis with the offset value being held constant for each offset value (to obtain B). The bright patterns in the graph are those MUAP trains that are most likely to have the mean IPI as indicated on the mean IPI axis. [Modified from Schalk G, Carp JS, and Wolpaw JR. 2002]

By iteratively subtracting a number of mean IPI from the firing time of a given potential, the corresponding nonzero offset for each potential can be determined so that mean IPI – offset ordered pairs can be computed for plotting in the new feature space. The offset/mean IPI information can then be plotted and filtered with a 1-dimensional Gaussian function that operates by holding the offset constant and filtering along the mean IPI axis. The resulting graph in Figure 3.10 shows which trains of MUAPs are likely to have a given mean IPI. The lower triangle of the graph is undefined because the offset cannot be greater than the mean IPI. The bright patterns in the Offset vs. mean IPI graph are those MUAP trains that are most likely to have potentials that belong to a MUAP train with a mean IPI as indicated on the mean IPI axis. However, there can be "ghost" bright lines on the graph at 0.5 multiples of the mean IPI, complicating IPI determination.

Chauvet et al. [2003] sequentially extracted MUAP waveforms based on the mean IPI and largest peak to peak value over an entire recording before using fuzzy classification on the extracted waveforms. First, the IPI histogram of the entire recording would be constructed and it was filtered using a zero-phase filter to reduce fluctuations. The representative IPI was that which produced the maximum value of the filter. The representative peak to peak value was determined similarly by constructing a peak to peak value histogram over the entire recording. The representative waveform was finally determined by selecting the MUAP whose peak to peak value best matched the representative peak to peak value. Fuzzy logic based classification was then applied using 3

inputs: relative IPI, relative peak to peak value, and the crosscorrelation value computed between the current waveform and the representative waveform. The relative IPI and peak to peak values were computed as the percentage difference between the IPI and peak to peak values of the current waveform and those values of the representative waveform (equations 3.9 and 3.10).

$$\Delta IPI = \frac{\left| IPI_{current} - IPI_{representative} \right|}{IPI_{representative}} \tag{3.9}$$

$$\Delta PtP = \frac{\left| PtP_{current} - PtP_{representative} \right|}{PtP_{representative}} \tag{3.10}$$

In equation 3.9, ΔIPI is the relative IPI value, $IPI_{representative}$ is the representative IPI value, and $IPI_{current}$ is the current potential's IPI. In equation 3.10, ΔPtP is the relative peak to peak value, $PtP_{representative}$ is the representative peak to peak value, and $PtP_{current}$ is the current potential's peak to peak value. The fuzzy values obtained from the membership functions applied to these inputs are then used in conjunction with rules in a decision table to determine class membership. After all potentials have been classified in this manner, those potentials that fit into the class of the representative potential are removed from the input recording, and the process is repeated to obtain more representative values for different MUAP classes. The authors admit that this algorithm can only successfully function with at most four different classes.

McGill [2002] developed an "optimal" method to resolve superpositions of MUAPs into their constituent potentials. This method is called optimal because it

can resolve high level combinations (greater than two constituents) of superimposed potentials and also because it uses interpolation to overcome inherent misalignment errors in digitally sampling waveforms.

McGill also incorporated this method into EMGLAB, an interactive EMG decomposition tool written in Matlab [McGill KC et al., 2005]. This method utilized one or more channels of multi-unit EMG recorded from healthy muscles of able-bodied individuals using needle and wire electrodes. The signals were sampled at 10 KHz. The algorithm accomplished clustering by assigning symbols to windowed waveforms that were based on relative amplitudes, durations and slopes [Florestal JR et al., 2006]. The authors used a novel similarity metric known as the pseudo-correlation to match potentials.

Zennaro et al. [2003] tackled the problem of EMG decomposition of EMG recordings ranging from three minutes to several hours. The authors applied wavelet-based classification to three channels of intramuscular EMG along with a weighted averaging technique to track changes in the shapes of MUAP templates. Figure 3.11 details the classification algorithm.

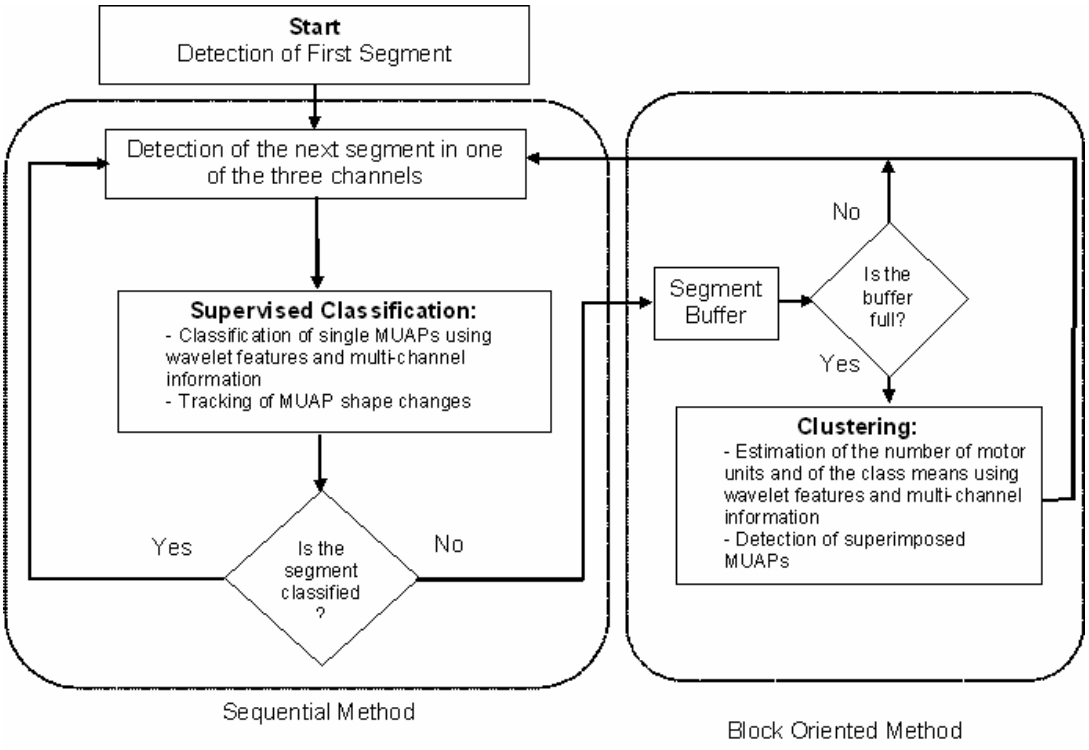

Figure 3.11 Zennaro et al.'s flowchart for wavelet-based EMG classification. Three channels of EMG were analyzed simultaneously according to the decision making in the flow chart above. If a detected motor unit action potential could not be classified it was sent to a buffer where it would be saved for clustering of other similar unclassifiable potentials. Newly computed clusters are then used to classify subsequent potentials that are detected. [Modified from Zennaro, 2003]

In order to isolate individual MUAPs, segments of activity were found and defined as deviations from the signal baseline. The three channels of EMG were analyzed simultaneously, with each active segment considered as coming from a pool of segments within a single channel. Wavelet transforms were applied to the MUAPs and only several bands of frequency components were retained for classification. The specific frequency bands were retained based on optimization criteria for this given application. The authors achieved a mean rate of 96.1% of correctly classified MUAPs with a standard deviation of 2.6%.

Several 24 hour studies recording EMG have been done, but few have actually attempted analysis at the single motor unit level. Even then, the descriptions of motor unit behavior are qualitative [Eken, 1998], [Hennig and

Lomo, 1985]. No studies have addressed classification of motor unit action potentials for 24 hours of data. Thus, 24-hour recording exploits have largely involved analysis at the whole muscle level.

Chapter 4: Methods

4.1 Experimental Protocol

4.1.1 Electrode configuration and 24-hour EMG Recording Setup

The subject pool consisted of 4 SCI subjects with cervical level injuries that were 1 year or more post injury. The thenar muscles (abductor pollicis brevis, flexor pollicis brevis, and opponens pollicis, Figure 4.1) of at least one hand were not under voluntary control as confirmed by manual muscle examination [Thomas CK, 1997]. All subjects signed informed consent forms approved by the University of Miami IRB. One 24-hour recording was made per subject.

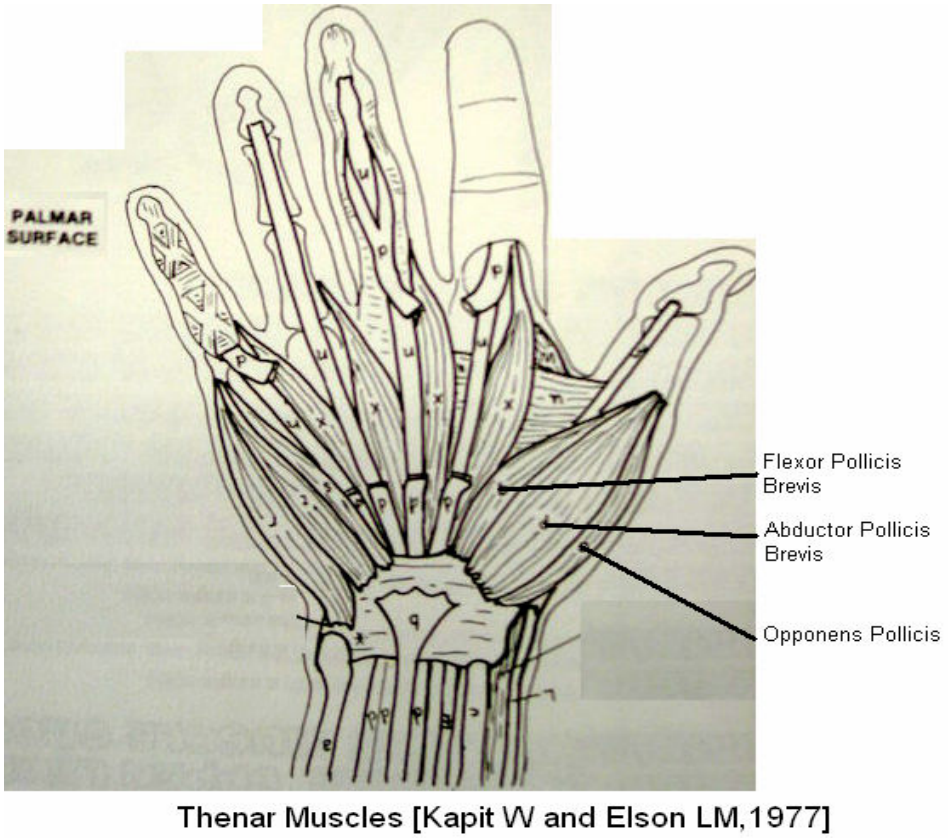

Figure 4.1 Structure of the thenar muscle (right hand). The thenar muscle consists of three muscles: Flexor pollicis brevis, abductor pollicis brevis, and opponens pollicis [Modified from Kapit W and Elson LM, 1977].

Subject histories are presented below in Table 4.1. This table details the age and sex of each subject, the hand used in the experimental, injury information, and any anti-spasm medications that each subject was taking. Only subject 3 took no anti-spasm medication.

Table 4.1 Subject history.

Recording	Side Studied	Age (yrs)	Sex	Injury Duration (yrs)	Injury Cause	Level	ASIA	Spasm medications
Subject 1	Left	30	M	1	Diving	C5	A	Neurontin (1500 mg/day) and Klonopin (5 mg/day)
Subject 2	Left	49	F	9	Horseback Riding	C4	A	Baclofen (150 mg/day) and Klonopin (0.75 mg/day)
Subject 3	Right	27	M	10	Diving	C4	A	None
Subject 4	Right	60	M	38	Motor Vehicle Accident	C6	A	Diazepam (60 mg/day)

Five new self-adhesive electrodes (Superior Silver electrodes, Uni-Patch, MN) were trimmed to approximately 1 cm x 2.5 cm using scissors so that they could be positioned across the thenar muscles. The distal electrode was positioned across the metacarpal-phalangeal joint, the proximal electrode at the base of the thenar muscles, and two closely spaced electrodes across the muscle bellies at their midpoint (Figure 4.2). Another electrode was placed just proximal to the wrist as a ground, distally and proximally over the thenar muscle to yield a 2-channel unipolar recording setup.

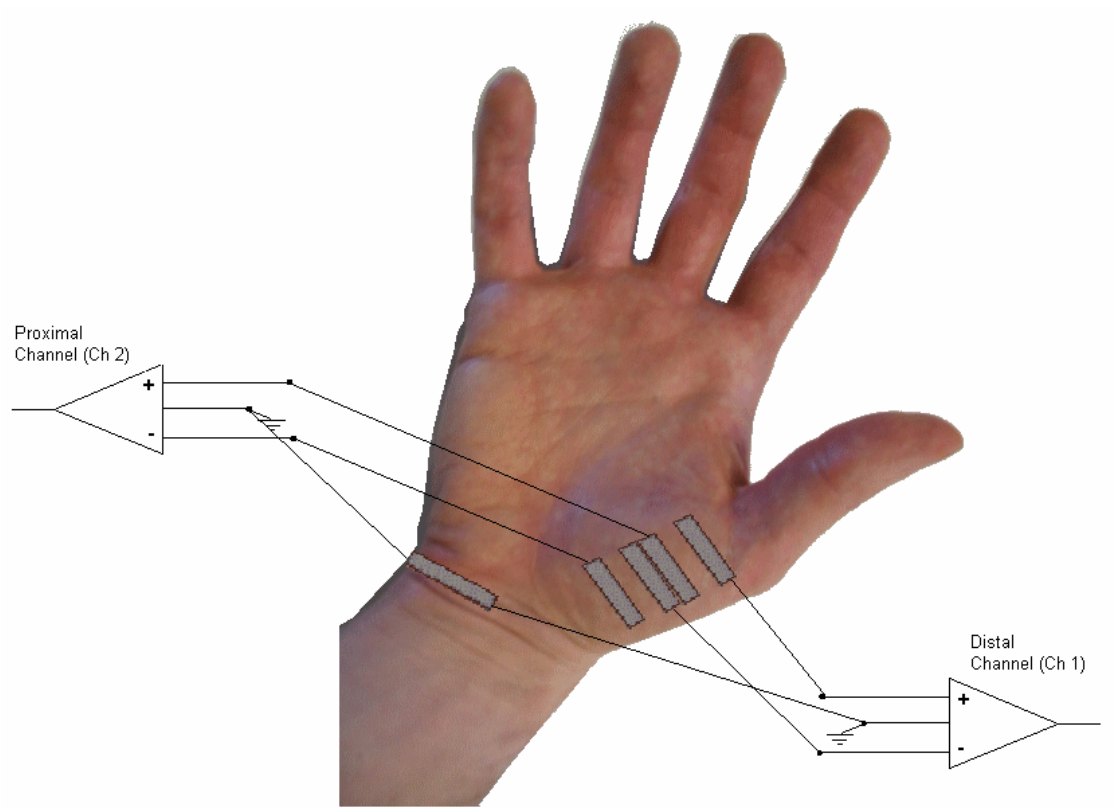

Figure 4.2 Electrode configurations for recording two surface EMG channels from the thenar muscle on the right hand. Each differential EMG premamplifier had three inputs: a positive electrode , a negative electrode, and a common electrode. A wrist electrode was utilized as the common for both preamplifier channels. Channel 1 served as the distal channel while Channel 2 was the proximal channel. The negative electrodes were placed very closely next to the common electrode so that the differential amplifiers could emulate unipolar electrodes.

The electrodes were then secured to the thumb skin overlying the thenar muscles using a layer of hypafix medical tape, followed by several wrappings of athletic tape and co-flex to make sure that the electrodes maintained the same position on the skin during the EMG recording.

The electrodes were connected to the inputs of two differential preamplifiers as shown in Figure 4.2. These preamplifiers were manufactured by

Motion Control (Salt Lake City, UT) and have gains of approximately 400. An electrode was positioned on the wrist to serve as the ground for both preamplifiers.

The preamplifier outputs were first connected to a preprocessing unit. The preprocessing unit was responsible for scaling the signal to an approximate 2 V baseline and further amplifying the signal to fill the input range of the data logger. The net gain of the additional amplifiers in the preprocessing unit was 1.5 for each channel. The preprocessing unit was also equipped with analog bandpass filters with cutoff frequencies of 10 Hz and 1000 Hz.

The preprocessing unit out put was then connected to a portable, battery-powered data logging device with a 12-bit analog-to-digital converter that accepts input signals from 0 Volts to 4.096 Volts (Figure 4.3).

Figure 4.3 Battery powered data-logging device for recording two channels of EMG at 3200 Hz. The device stores the data on a type II PCMCIA flashcard or compactflash card, which acts as a hard disk drive.

The data logging device consisted of the Tattletale 8 Logger, manufactured by Onset Computer Corporation, driven by specially designed software. The software acquired data through a two input analog-to-digital

converter (ADC) and permanently stored the data on a 1.0 Gigabyte type I compact flashcard for later analysis. Computers recognize these compact flashcards as hard disk drives, although they have no moving parts. The ADC used a sampling frequency of 3.2 KHz and a 7.2 volt rechargeable battery was used to power the logger.

The data logger was calibrated prior to starting the 24 hour recording. A 100 Hz, 1 mV peak to peak sine wave obtained from a signal generator was supplied directly to each EMG preamplifier channel for about a minute and a recording was made on the data logger. The recorded sine wave was used to relate the input voltage to the recorded voltage for both channels. The same calibration procedure was done after the recording because the calibration changes over time as the data logger's batteries drain. Table 4.2 shows a list of the results of the 1-minute calibration recordings for all four test recordings

Table 4.2 Calibration values for the data logger. The values in the table are the number of millivolts in the recorded signal that correspond to a 1millivolt input signal for each channel, distal and proximal. The pre-recording calibration values were before the 24-hour recording had started and the post-recording calibration values were found after the recording had ended. The mean of the pre- and post- calibration values are also shown.

Recording	Recorded Peak to Peak Sine Wave (in mV)					
	Distal Pre-recording	Proximal Pre-recording	Distal Post-recording	Proximal Post-recording	Mean Distal	Mean Proximal
Subject 1	686	653	679	649	682.5	651
Subject 2	683	653	681	650	682	651.5
Subject 3	681	653	679	647	680	650
Subject 4	692	651	689	651	690.5	651

4.1.2 Stimulation Protocol

Before and after the 24-hour recording was started, maximal compound action potentials (M-wave) were recorded from the thenar muscles in response to

supramaximal stimulation of the median nerve. Comparison of the maximal evoked M-wave before and after each 24-hour recording was used to gauge the stability of the recording electrodes and to normalize all template potential amplitudes so that they could be compared across recordings.

The stimulation protocol in Thomas [1997] is again presented here. Each SCI subject positioned their wheelchair alongside a platform that supported the forearm of the hand to be studied. The forearm was supinated, extended, and resting in a vacuum cast supported by a platform (Figure 4.4).

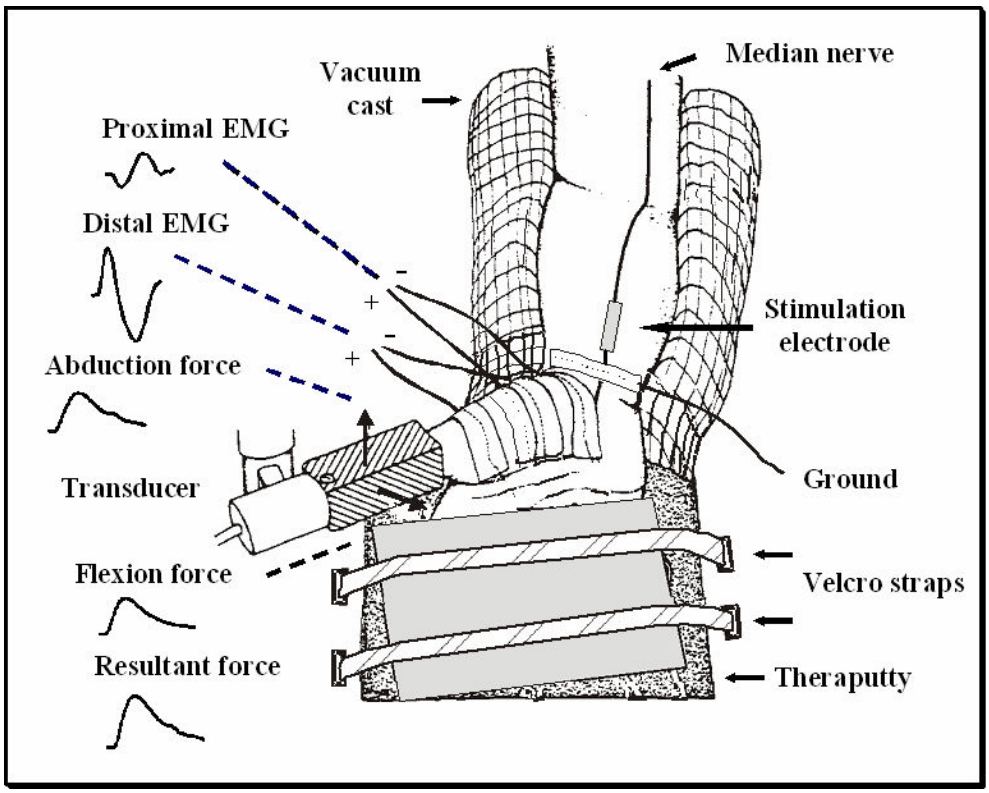

Figure 4.4 Stimulation setup.

Clay was molded to the shape of the hand to stabilize it. A metal plate lay on the fingers to restrain them. A custom-made transducer was aligned along the

length of the thumb so that approximately 0.5 N of resting tension was applied in both the abduction and flexion directions. Force was registered in both of these directions at right angles so the resultant force could be calculated. Single pulses (50 μs duration) were delivered to the median nerve at increasing intensities until the M-wave was maximal. All subsequent stimuli were 120 % maximal. The following stimuli were delivered to the nerve: *1*) 5 single pulses to elicit initial maximal M-waves (distal and proximal) and initial twitches. *2*) A train of stimuli at 50 Hz for 1 s to determine the maximal evoked force. *3*) 5 single pulses to elicit twitches after posttetanic potentiation [Thomas et al. 1990]; *4*) 2 min of stimulation at 40 Hz (13 pulses each second) to induce fatigue [Burke et al. 1973; Thomas et al. 1991]; *5*) post fatigue responses including single pulses and trains of pulses at 5–100 Hz as before fatigue. The stimuli that induced muscle fatigue and post fatigue responses (4, 5 above) were only delivered after the 24-hour recording.

EMG was recorded from the distal and proximal surfaces of the thenar muscles, and the abduction and flexion forces were each sampled on-line at 3,200 Hz and 400 Hz, respectively, using SC/Zoom (Physiology Section, IMB, Umeå University, Sweden). All data analyses were done off-line. The vector sum of the measured abduction and flexion force components represented the magnitude of the evoked forces. Three M-waves and twitches recorded before and after the stimuli at 50 Hz were measured. The EMG potentials obtained from both the distal and the proximal channels were characterized by peak to peak amplitude.

4.1.3 24-hour Recording Initiation

After a subject had undergone the stimulation protocol, the 24-hour recording was started. The data logger was stored in a belt bag and could be moved for transfers. A light on the data logger flashed to indicate that EMG was being recorded.

4.2 EMG Preprocessing

24-hour EMG data were preprocessed before any analysis was done. The raw EMG data could assume integer values from 0 through 4095, since the ADC was 12-bit and accepts voltages between 0 and 4.095 V. The baseline of the signal was level shifted so that it appeared at about a value of 2048, or (2.048 V as acquired). Before any processing, all EMG data were demeaned and then smoothed using a simple 3-point, symmetric moving average filter. The recording was next filtered with a 60 Hz second order notch filter and was applied twice (reversing the order of the input signal the second time) to prevent phase distortion. The last filtering step depended on the quality of the recording and either involved high pass filtering at 30 Hz, or bandpass filtering. One of the raw EMG recordings was clean so only a highpass filter was applied (subject 1). Frequency spectra of portions of the remaining recordings were inspected and upper cutoff frequencies for bandpass filters were determined individually. Table 4.3 shows which additional filters were applied to each recording.

Table 4.3 Additional filtering for each 24-hour EMG recording. Individual recordings were additionally filtered by either highpass or bandpass filters depending on the quality of the raw EMG signal.

Recording	Filter parameters
Subject 1	30 Hz Highpass
Subject 2	30-500 Hz Bandpass
Subject 3	30-1075 Hz Bandpass
Subject 4	30-500 Hz Bandpass

The filtered EMG was divided by 100 as the final step before processing. The classification routines utilized by the overall classification algorithm worked best with amplitude values in between -2.0 and 2.0 The division by 100 shifted the amplitude values of most discernible potentials into the target range of -2.0 to 2.0. The actual recorded signal of interest therefore translated into a signal of +/- 200 mV, or 400 mV peak to peak.

The voltage at the skin surface of the signal of interest can be determined using the calibration values from Table 4.2.

(400 mV logger) x (1 mV EMG input / 682 mV logger) = 0.5865 mV EMG input (4.1)

(Note: the 682 mV calibration factor was taken from Table 4.1 and used as an example). The maximum recordable range (before saturation) is actually 10 times that amount, or 5.865 mV peak to peak, because the upper limits of the data logger's recording range is actually 4000 mV peak to peak.

4.3 Motor Unit Action Potential Classification Algorithm

All data were processed using Matlab 7.0 and 7.4, a programming suite capable of performing complex computations to simple processing tasks. Matlab also has the capability of creating stand-alone applications without the requirement of having Matlab installed on the target system.

The motor unit action potential classification algorithm utilized two channels of EMG and consisted of four processing passes through the 24-hour recording. Since two channels of EMG were used instead of one, the algorithm was provided with twice the information to classify motor unit potentials. For example, the motor unit action potential waveforms in each channel were unique with differences in potential amplitude, duration, shape and polarity. These features also added an extra layer of differences to be categorized. The algorithm first broke the recording into 480, 3-minute portions and processed the EMG at the 3-minute level before finalizing the procedure by uniting all classifications.

Figure 4.5 shows the steps of the classification algorithm.

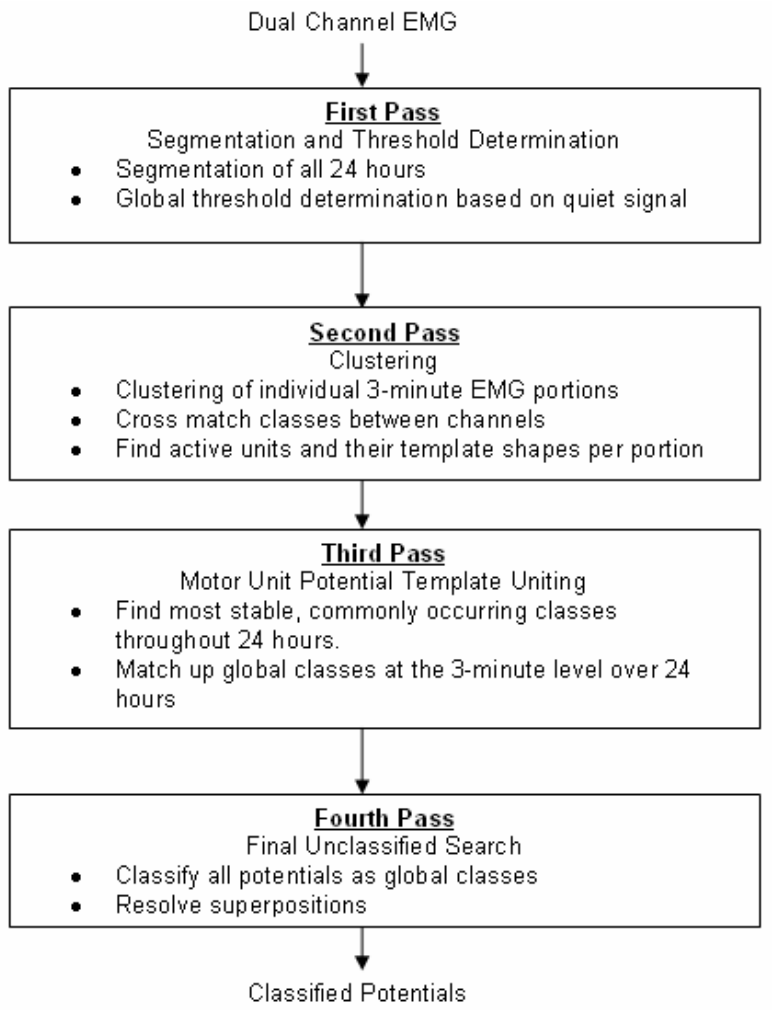

Figure 4.5 Block diagram for motor unit potential classification. Automated classification of motor unit potentials is a process consisting of four major passes.

These steps included: 1) segmentation and threshold determination, in which a global threshold was computed in order to isolate individual motor unit potentials; 2) clustering, in which similar potentials were grouped into their respective motor unit classes; 3) motor unit template uniting where the most stable, commonly occurring classes were found throughout the 24-hour recording; 4) final unclassified search, where all unclassified potentials were compared to the

global motor unit templates in order to either achieve a classification with or without the need for superposition resolution.

4.3.1 EMG Segmentation

Segmentation represents the method of breaking up the EMG signal into individual motor unit potentials. This is done by windowing, or keeping track of the potential by extracting the datapoints that comprise the potential, for later classification. Segmentation occurred in three phases and on both the distal and proximal channels independently. In the first phase, all 480, 3-minute EMG portions were segmented to find amplitude thresholds at which to extract potentials. Three minutes was found to offer the best recording length for clustering and provided feasible recording lengths for manual classification and processing. In the second phase, all the 3-minute EMG portion thresholds were utilized to compute a global segmentation threshold. The third and final phase actually segmented candidate motor unit potentials using the global segmentation threshold.

4.3.1.1 Segmentation Phase 1

The 3-minute thresholds for segmentation were found by computing an estimate of the baseline thickness based on a windowed peak to peak value signal, for both the distal and proximal channels independently. Motor unit potentials resemble spikes, so filtering was done to emphasize the peak to peak value of these spikes and also get an estimate of the baseline width. A simple

peak to peak filter determined the peak to peak EMG value (maximum value – minimum value) in consecutive windows of 32 data points (10 ms) (Figure 4.6). This time length was used because it was approximately half the duration of a MUAP and approximately captured the outline of the baseline of a rectified EMG signal.

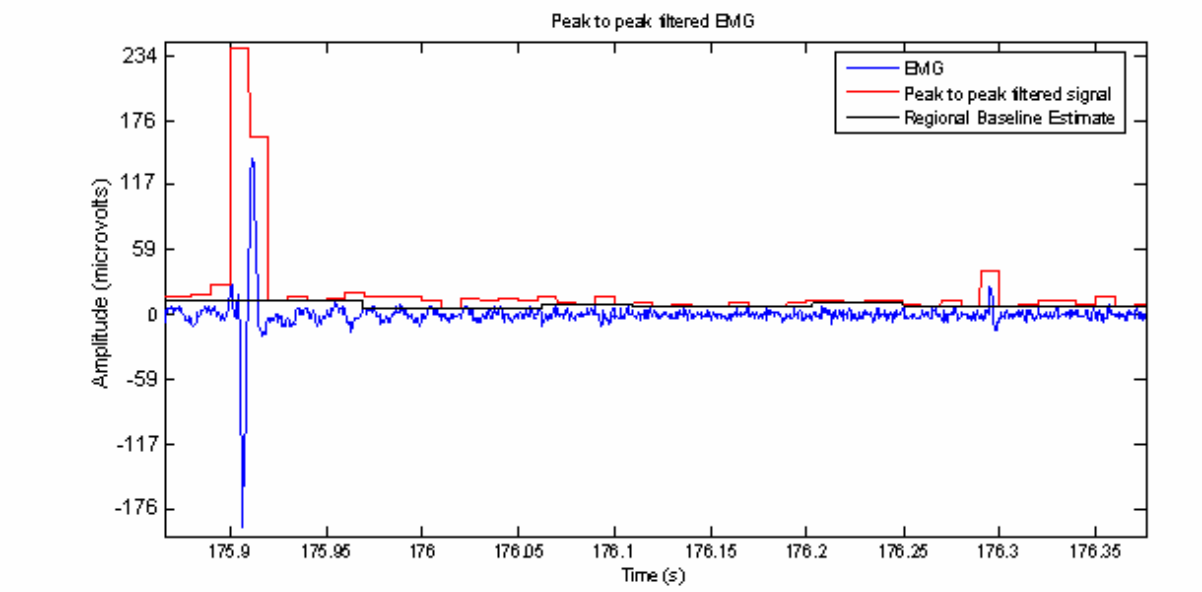

Figure 4.6 Peak to peak filtered EMG signal and regional baseline estimate. A peak to peak filter determined the peak to peak EMG value (red trace) in consecutive 32 point windows (10 ms). The regional baseline value (black trace) was next computed by finding the lowest value in fixed 150 point (47 ms) consecutive windows.

The regional baseline value was next computed by finding the smallest value within fixed windows of 150 points (47 ms). This value was assumed to be a regional representation of the baseline and the 150 point width proved to be the width that best represented the regional EMG activity. The mean and standard deviation of all the regional baseline signals for every 3-minute EMG portion, plus the actual regional baseline signals themselves, were used to find the global segmentation threshold.

4.3.1.2 Segmentation Phase 2

To determine the global threshold, all regional baseline means were ordered from least to greatest. Their corresponding standard deviations were arranged according to the order of the sorted means (Figure 4.7).

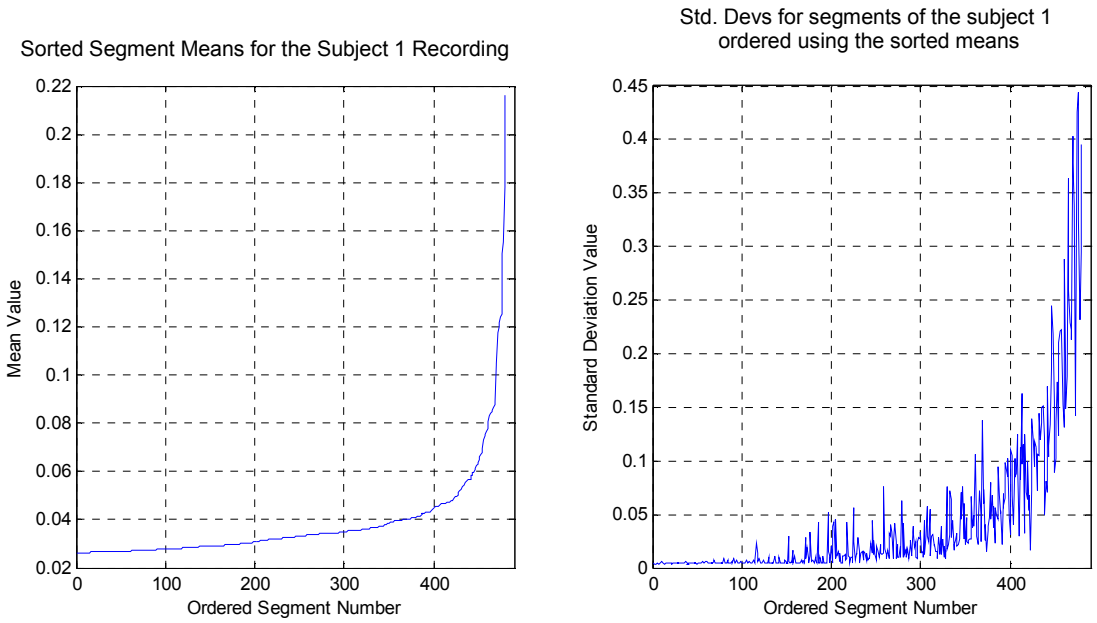

Figure 4.7 Threshold selection method using recording from subject 1, distal channel. The left pane shows the mean values of the regional baseline signal found in each 3-minute EMG portion sorted from least to greatest. The right pane shows the standard deviations of those same EMG portions according to the sorted order from the left pane.

The goal in finding the global threshold that represents the "quiet signal" was to find the location where the variability, or standard deviation, becomes too large. A running standard deviation was calculated using the baseline signal values from each 3-minute EMG portion. In Figure 4.8 for example, the first standard deviation point was the standard deviation of the estimated baseline value for the 3-minute EMG portion with the least variability (least baseline noise); the second standard deviation point is the standard deviation of the combined values of the estimated baseline signal of the first two 3-minute

portions, and so on, continually adding the next 3-minute baseline estimate to perform the computation.

A running mean of this constructed signal was calculated simultaneously and the ratio of the running standard deviation to the running mean was computed. When the ratio of the running standard deviation to its corresponding running mean changes abruptly, then a limiting point is found. Figure 4.8 shows a plot of this ratio.

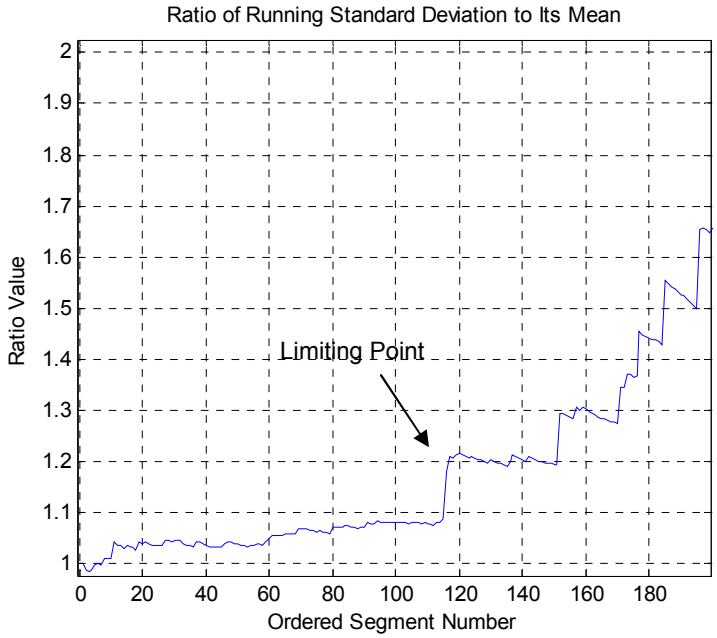

Figure 4.8 Ratio of the running standard deviation value to its mean. In this example, there was a significant increase at around segment number 120, so this is the cutoff point. The 120 3-minute EMG portions with the smallest baseline means were used to compute the mean and standard deviation to be used for the threshold for this channel.

This abrupt change represents the presence of reasonably sized MUAPs and thus the quiet signal baseline value. After processing all 480 3-minute EMG portions from the four recordings, the best target ratio for the limiting point was 1.2. The mean estimated baseline signal value at the 3-minute EMG portion number where the limiting point occurs was used in conjunction with its

corresponding standard deviation for a given channel's global threshold. The final global threshold was the mean plus 2 standard deviations, a value commonly used in biological studies.

4.3.1.3 Segmentation Phase 3

Phase 3 of the segmentation procedure used the global thresholds obtained for each channel to segment motor unit potentials from each 3-minute EMG portion. This phase operates on each channel's data independently and also features noise rejection as will be described in section 4.3.1.4.

During the segmentation process, the peak to peak signal was computed twice. The first time the peak to peak signal was computed with 32 datapoint windows as it was done in phase one, but the second time it was done at a shift of 16 data points so that the two peak to peak signals overlapped (Figure 4.9).

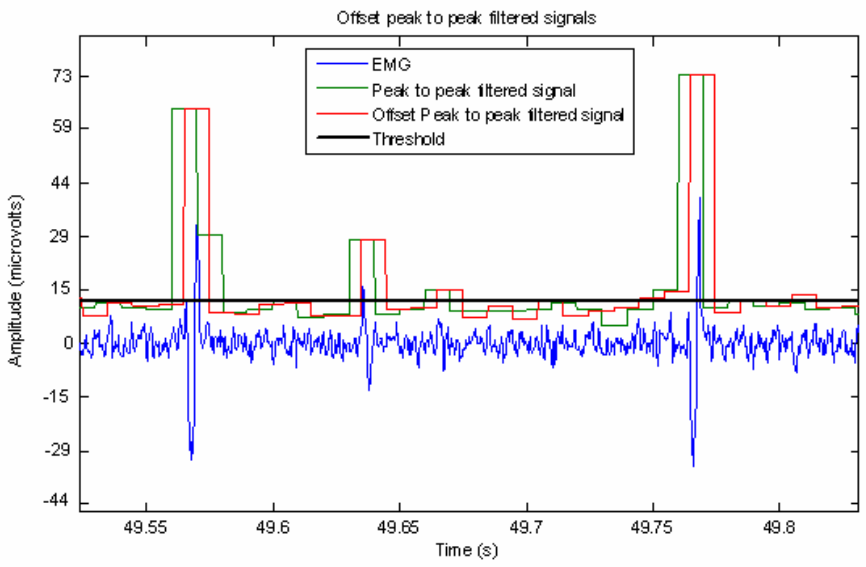

Figure 4.9 Offset peak to peak filtered signals used in segmentation phase 3. 2 peak to peak filtered signals are computed from the EMG, with one offset from the other by 16 points (5 ms), or half a window, so that all potentials were found. All potentials that were above the threshold (solid black trace) were segmented.

The offset peak to peak filtered signal was additionally utilized so that no potentials were missed due to the positioning of the 32 point windows. In other words, overlapping windows would prevent the case that the full peak to peak value of a potential could be erroneously computed due to the positioning of the windows. All regions of the peak to peak filtered signals that had values above the global threshold (black trace in Figure 4.9) were marked for inspection by the potential segmentation procedure.

The potential segmentation procedure took each marked region and defined a candidate potential by locating the maximum positive amplitude value. Each candidate potential was aligned by centering its potential window at the minimum EMG amplitude value. This fiducial centering point was then used to construct a 71 data point window (22 millisecond time window) around each candidate for later classification (35 datapoints to the left and to the right of the centering point). If two potentials were segmented whose centerpoints occurred less than 35 datapoints apart, only the candidate potential with the larger peak to peak value was retained.

The alignment criterion is crucial, for it critically affects the later stages of classification (as described in section 3.6.1). The valley of each potential was selected as the fiducial point so that all 3-phase potentials (two positive phases) were aligned correctly. Every potential had a negative phase. If the maximum peak of each candidate potential were chosen for alignment instead, ambiguity is introduced for three phase potentials: One positive phase may be slightly larger than the other in different potentials belonging to the same class or group. In this

case, the valley would fall either to the left or right of the aligned maximum peak, depending on which positive potential phase is larger (Figure 4.10).

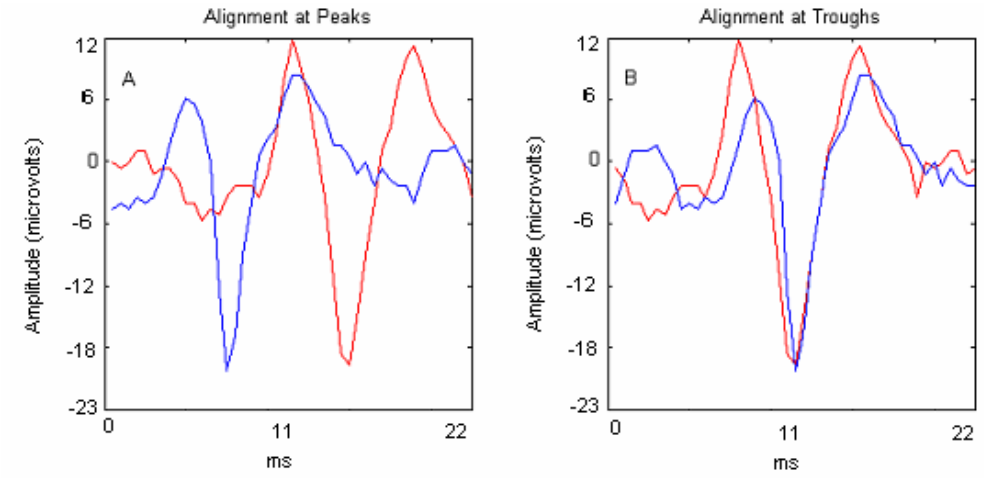

Figure 4.10 Three phase ambiguity when aligning at peaks. A) If 3 phase potentials are aligned at their peaks, one positive phase can be alternately larger than the other phase, even within the same class of potentials. B) If the 3 phase potentials are aligned at their valleys, the relative size of either positive phase is inconsequential and the classification of these two potentials is straight forward for any classification algorithm.

The net effect would be that potentials belonging to the same class would be classified differently, simply due to the fact that their initial alignments were different.

The negative peak alignment helps remedy the situation in Figure 4.10, but problems arise when there are two negative phases. To alleviate some problems that this introduces, all comparisons were done after candidate potentials and template shapes were optimally aligned (section 4.3.7).

After each channel had been segmented, the candidate potentials of each channel were matched in time so that each candidate potential was a single entity with one representation in each channel. When a candidate potential existed in one channel with no corresponding potential in the opposite channel, a

new candidate potential was segmented in that opposite channel using the corresponding time window.

4.3.1.4 Noise rejection

Noise that was incorrectly segmented was eliminated using two methods. The first method was frequency based and was done during segmentation, while the second compared what potentials were segmented with those that were not segmented.

The frequency based noise elimination procedure determined which segmented potentials were actually noise (noise potentials) by investigating frequency content. The frequency spectra of motor unit potentials consisted mostly of low frequency components while noise potentials consisted mostly of high frequency components or had a flat frequency spectrum. Noise potentials also had low maximum magnitudes in the frequency domain. Figure 4.11 shows an example with two relatively small waveforms, one is noise while the other is a motor unit potential.

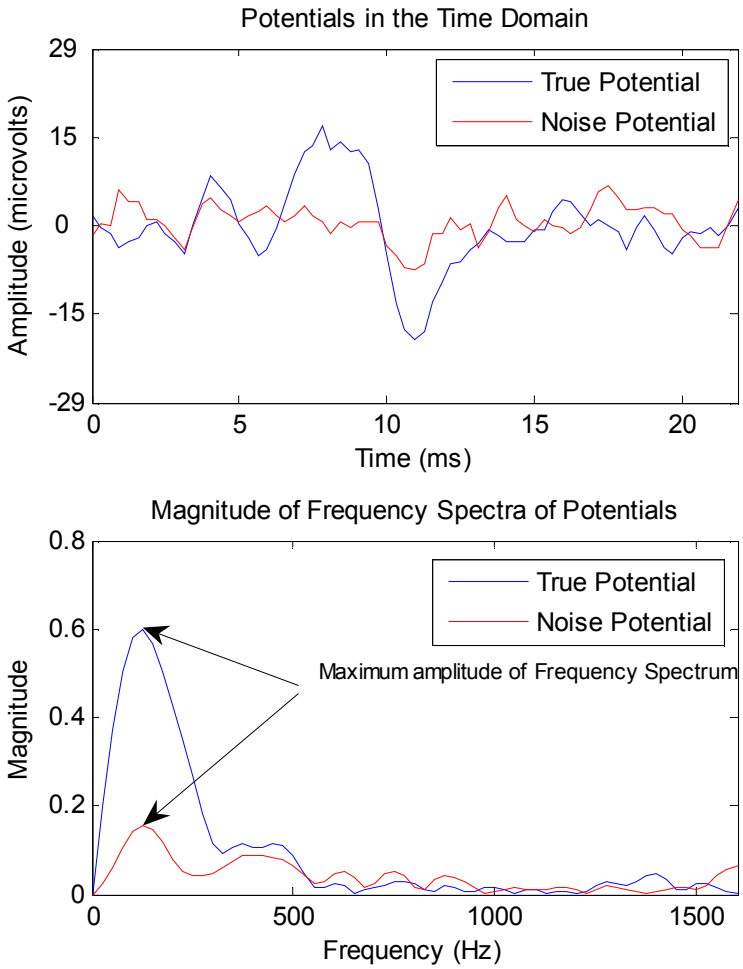

Figure 4.11 Spectra of motor unit potentials and noise. Not only will the percentage of area under the curve under 310 Hz be larger for true potentials than noise, but the maximum magnitude value for the true potential will be much larger than that of the noise.

A large portion of the area beneath a motor unit potential's frequency spectrum occurs below 310 Hz. The percentage of area of the frequency spectrum below 310 Hz was utilized as a noise elimination criterion.

Figure 4.12 shows a scatter plot with area ratios (the area of the frequency spectrum below 310 Hz to the total area beneath the frequency spectrum, or in other words, an area percentage) plotted on the x-axis along with maximum magnitudes of the frequency spectrum plotted on the y-axis. Each point represents one motor unit potential or one noise potential.

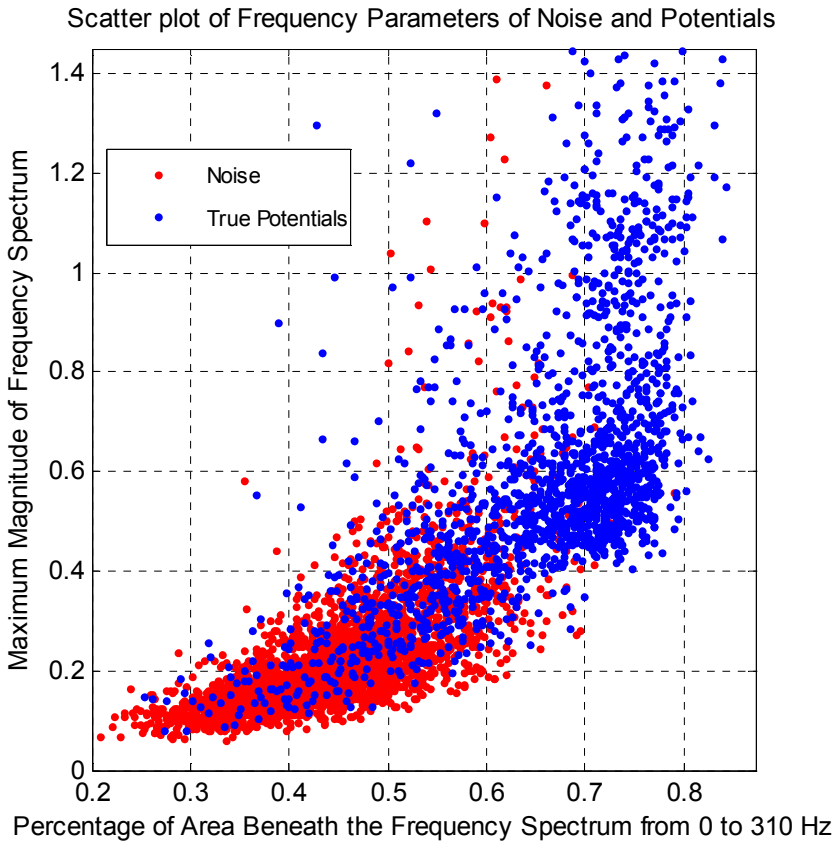

Figure 4.12 Scatter plot of area ratios vs. maximum magnitudes of frequency spectra for HR 16 MIN 45 of the subject 1 recording. Each point represents a potential. Most noise lies beneath an area ratio value of about 0.55 and a maximum magnitude value of about 0.5.

Figure 4.12 shows that for most motor unit potentials, the percentage of area below 310 Hz was greater than 0.55. The maximum magnitude value for most potentials was above 0.5. Thus two thresholds were set – segmented noise that had spectral area percentages less than 0.55 and maximum magnitudes (of their frequency spectra) less than 0.5. This frequency based noise elimination procedure is performed on each candidate potential as they were segmented. A candidate potential was eliminated as noise only if it met the criteria above in both channels.

The second noise elimination procedure was based on the distributions of the peak to peak values of EMG that were segmented versus the distribution of the peak to peak values of what was not segmented. Figure 4.13 shows example distributions of the peak to peak values in both channels of a 3-minute EMG portion.

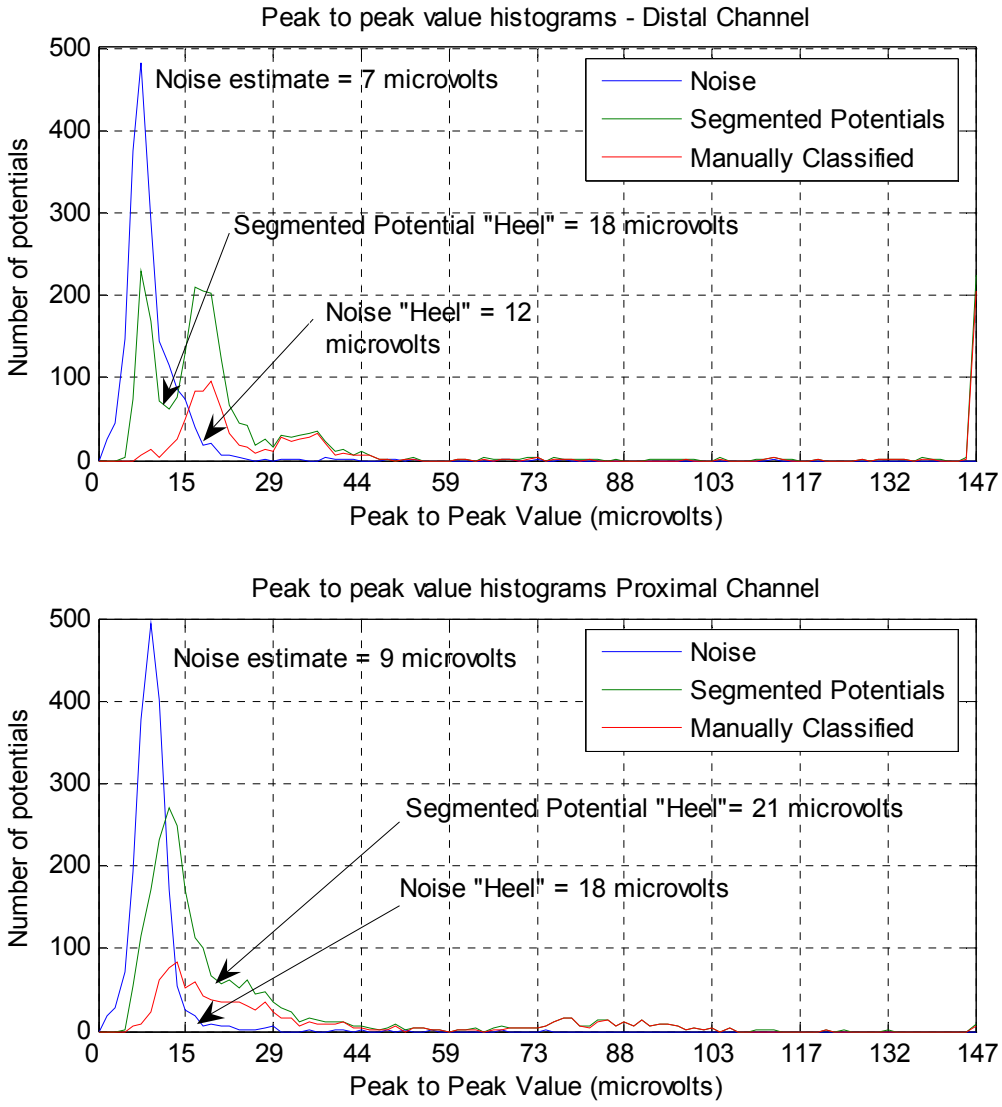

Figure 4.13 Histograms of the peak to peak values for the subject 1 recording, HR 16, MIN 45. The three traces in each plot represent distributions for the noise, the segmented potentials, and those potentials that were manually classified. The “heels,” or the first relative minima after the peaks of the noise and segmented potential distributions are labeled.

The three traces in the figure consist of the peak to peak value histograms of the potentials that were segmented, the potentials that were manually classified, and windowed data that were not segmented (noise). The noise distribution was computed by taking the peak to peak value of those EMG regions between candidate potentials that were segmented.

The idea was to eliminate all of the segmented potentials whose peak to peak values lay within the noise distribution plus within the first peak of the segmented potential distribution. This assumed that the first peak of the segmented potential distribution was also noise. The actual threshold line was drawn depending on where the first peaks of both distributions end, or in other words, the right “heel” of the noise peak and the first peak of the segmented potential distributions. The lower amplitude “heel” between the two was selected as the threshold for each channel. For example, the heels of both histogram peaks in each channel are labeled in Figure 4.13. Since the segmented potential heel was located at a peak to peak value of 18 μV and the noise heel was located at 12 μV, the distal channel threshold is chosen as 12 μV. In the proximal channel, the threshold is chosen to be 18 μV because the noise heel value was less than the segmented potential heel value (21 μV).

Only potentials with peak to peak values below the thresholds in both channels were eliminated. In summary, this method used dynamic thresholds for noise elimination – the ability to adapt thresholds based on the EMG data that were recorded.

4.3.2 Artifact and Spasm Exclusion

Artifact is a form of large amplitude noise and arises from external interference, such as electric bed noise. Spasms were also problematic in classification and in revealing the true nature of spontaneous motor unit activity. EMG during spasms typically results in an interference pattern when recorded using surface electrodes. The automated classification algorithm was not designed for areas where there was too much EMG activity and no discrete observable potentials (Figure 4.14, bottom pane). The automated classification algorithm was designed to classify discrete visible potentials as shown in the top pane of Figure 4.14.

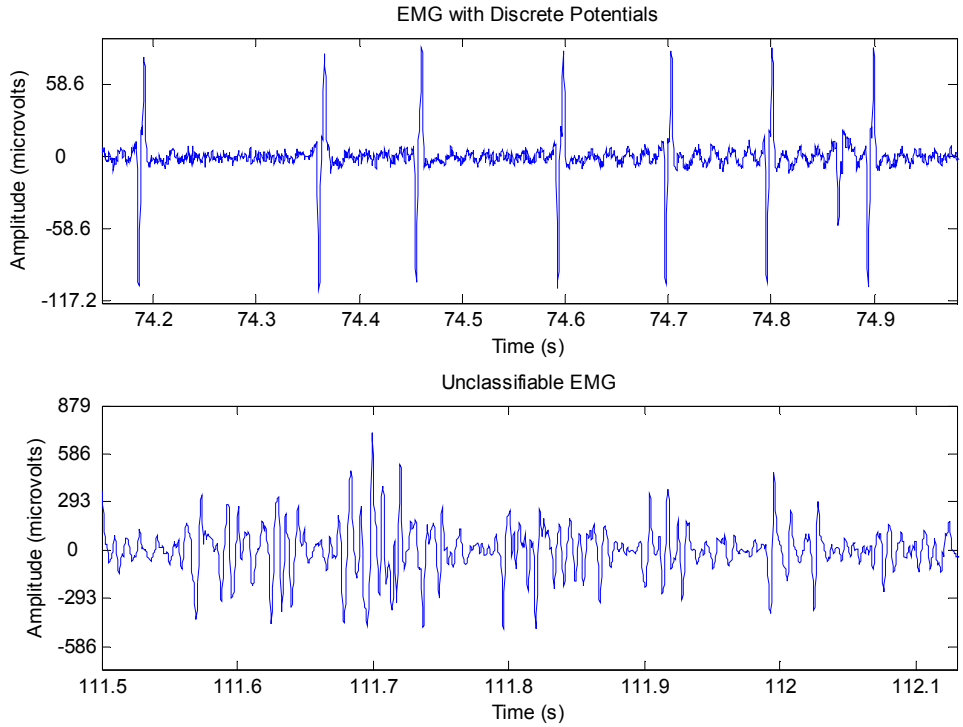

Figure 4.14 Classifiable vs. unclassifiable EMG examples.

The observation of motor unit activity can be contaminated by the presence of spasms, even if visually classifiable potentials are close to spasm activity. Two

methods were designed to exclude these EMG regions from consideration: An amplitude threshold method and a method that deals with the density of potentials in a region.

The first method used a simple dual amplitude threshold. All four recordings were visually inspected and it was found that EMG values with relative amplitude values of greater than 2.0 and less than -2.5 represented spasms or artifact. The regions marked as artifact consisted of the locations where these thresholds were exceeded at the beginning of a stable baseline signal (Figure 4.15).

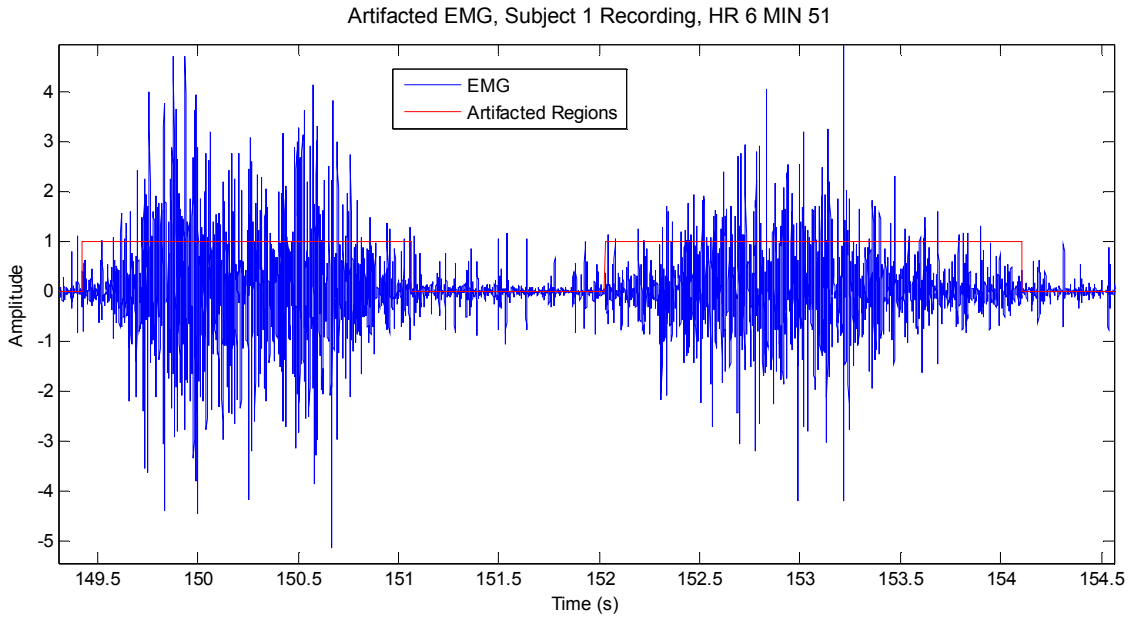

Figure 4.15 Spasms and artifact labeling. The regions where the red trace assumes a non zero value were excluded from classification and segmentation. The regions that are artifacted are indicated by values exceeding the amplitude thresholds of 2.0 and -2.5. The artifact regions end where the EMG returns to a stable baseline. The amplitude values in this figure are relative, meaning that the raw recorded logger signal was divided by 100.

The baseline was defined as a region that remained at a relative amplitude of +/- 0.15 for at least 40 data points. The regions marked as artifact were neither segmented nor classified.

The second method used to mark regions of EMG “overactivity” dealt with the endpoint values of segmented potentials on a per channel basis for each 3-minute EMG portion. A potential was temporarily marked as a spasm potential when it met one of two criteria. The first was that the absolute values of at least one endpoint of a segmented potential exceeded the template endpoint threshold. The second criterion involved the presence of a relative maximum or minimum that lay within several data points outside the edge of a potential’s window. In Figure 4.16, the box drawn around the potential at the center of the figure shows the windowed potential that is temporarily marked as a spasm potential.

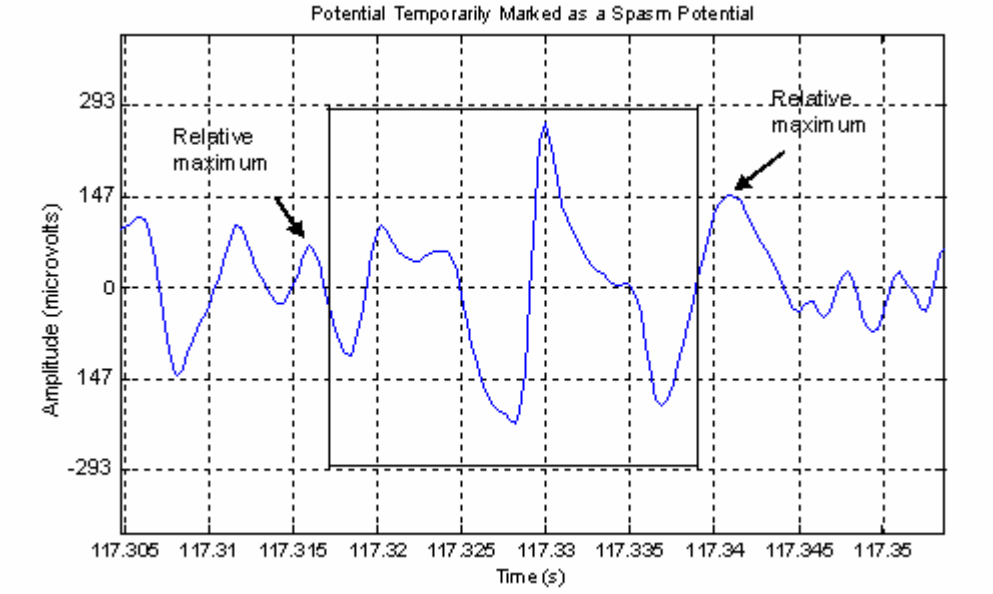

Figure 4.16 Possible spasm potential.

At least one of this segmented potential’s endpoints exceeds the template endpoint threshold so it is temporarily marked as a spasm potential. There are also relative maxima that exist within a few points of the edge of the potential’s window. The template endpoint threshold was the largest absolute endpoint

value of all the class template potentials in a 3-minute segment (Figure 4.17) (see section 4.3.3 for class template formation).

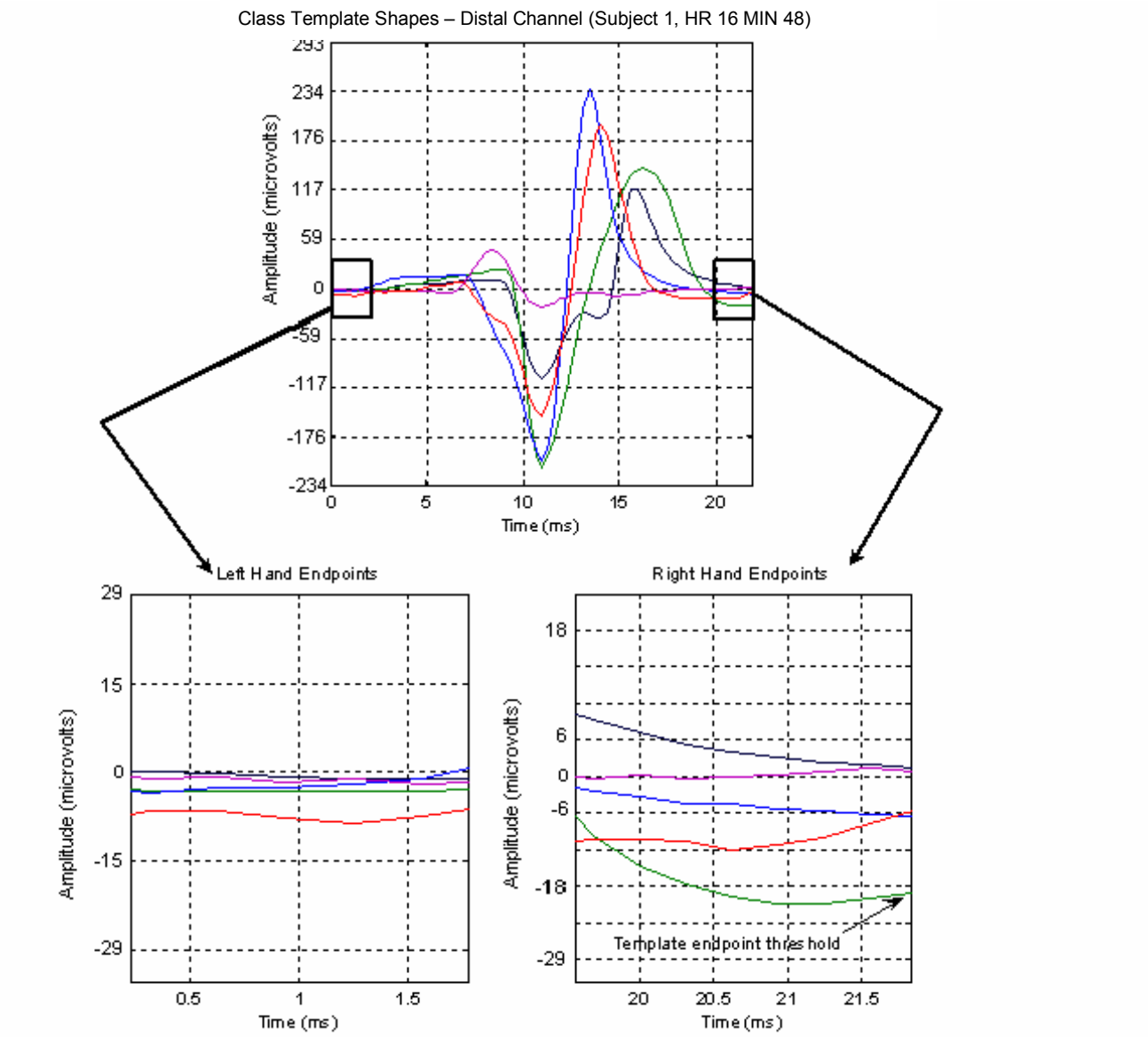

Figure 4.17 Template endpoint threshold for five class template shapes or the distal channel of an EMG segment.

The top pane shows a collection of class template shapes for the distal channel of an EMG segment. The bottom two panes show the magnified regions of the top pane. The template endpoint threshold is the template endpoint that has the

greatest absolute value. This value indicated by the arrow on the bottom right pane and is approximately -18 microvolts. If 10 consecutive potentials were marked in this manner, all of them were labeled as spasm potentials. If there were less than 10 consecutive marked potentials, they remained untouched.

While the above method helped eliminate unclassifiable potentials within spasms, an additional automated method was created to identify the remaining spasms that contaminated discrete motor unit activity. An expert manually identified spasms within the subject 1 recording to provide a gold standard, which was used to construct an automatic method to emulate the work of the expert spasm identifier.

The automatic spasm identification method was based on finding regions where the area under the rectified EMG was greater than a certain threshold. Additionally, the area was normalized by the area beneath the average rectified template potential within the current 3-minute EMG portion. Since peak spasm activity was largely marked with this method, time safety factors were added just before and just after the previously identified spasm regions to extend the spasm regions to encompass the entire contraction and were derived from the manual labeling of spasm activity in the subject 1 recording. That is, the expert marked the spasm onset and end, as well as the quiet time prior to and after each spasm (pre-time and post time). There were four different time safety factors attempted, each based on statistical measures of the pre-spasm times in the manually classified spasms (Table 4.4).

Table 4.4 Different spasm pre-times for four different spasm removal methods. There were four different pre-time values attempted based on statistical measures of the pre-spasm times for the manually classified spasms. The pre-time was the time safety factor taken immediately before the peak spasm onset to ensure that no spontaneous motor unit activity was included with spasm activity.

Spasm Identification Removal Method	Time Safety Factor Employed
1	Median of pre-time values
2	Mean of pre-time values
3	Mean of pre-time values + 1 standard deviation
4	Mean of pre-time values + 2 standard deviations

The pre-time was the time safety factor taken before the peak spasm onset to reduce spontaneous motor unit activity was included with spasm activity. The post-time was the time safety factor taken after the peak spasm had occurred and was always chosen to be the average value of 1.48 times the pre-time. Table 4.5 shows the performance of the automatic method with different safety factor times with respect to the gold standard spasm locations. Figure 4.18 shows a graphical representation of the Table 4.5 data.

Table 4.5 Automatic spasm identification procedure performance on the subject 1recording.

Spasm Identification Removal Method	% Correct	Time correctly found	Actual Spasm Time (seconds)	Total Classified Potentials Lost (FPs)	Total Spasm Potentials Missed
1	49.4%	1781.71	3606.44	5456	11334
2	58.2%	2099.30	3606.44	8495	9211
3	69.6%	2511.38	3606.44	14033	6694
4	75.7%	2731.29	3606.44	18612	5725

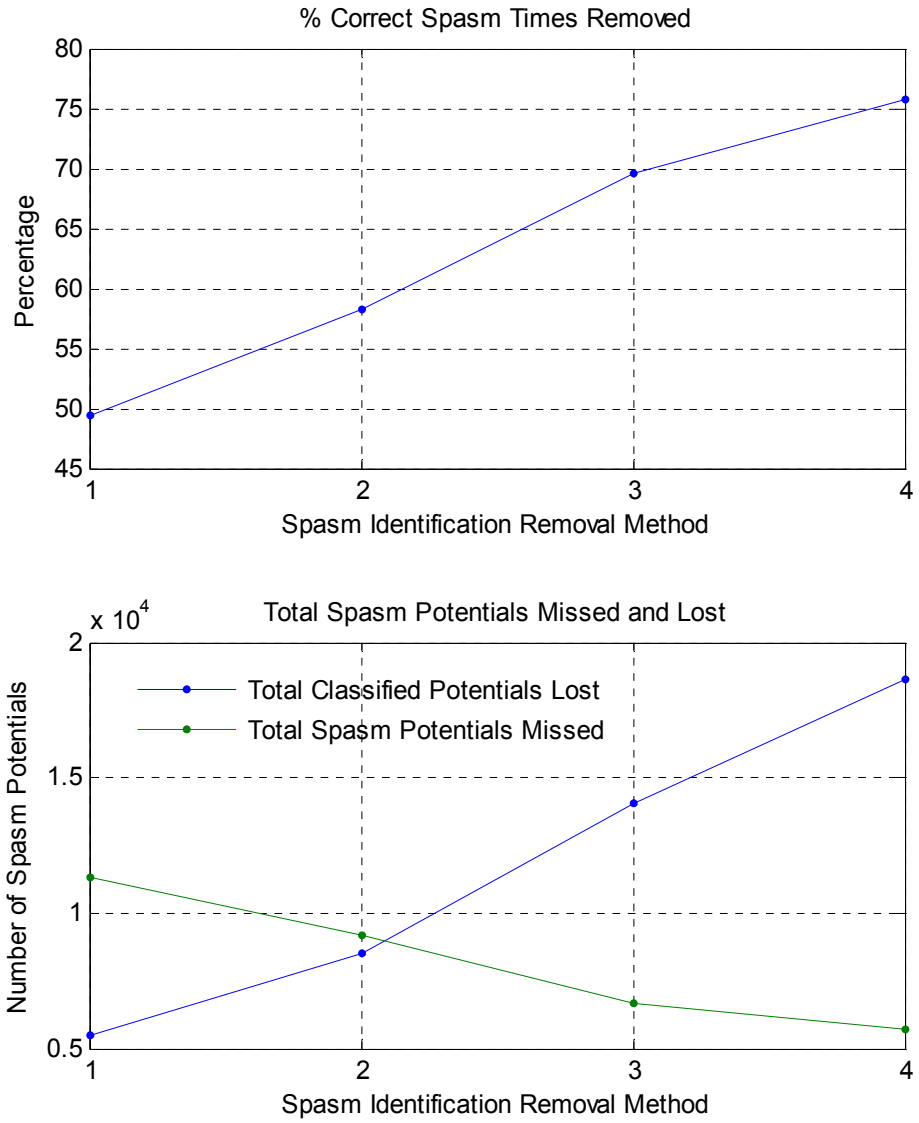

Figure 4.18 Automatic spasm identification procedure performance on the subject 1recording (graph format). The top pane shows the percentage of spasm times correctly identified by each of the 4 methods. The bottom pane shows the total classified potentials lost (false positives) and the total number of spasm potentials missed for each method. Method 1 has the shortest time safety factors while method 4 has the largest time safety factor. Even though method 4 has the highest percent correct, there were still large numbers of spasm potentials erroneously included (missed) and large numbers of false positives

Method 1 has the shortest time safety factors while method 4 has the largest time safety factor. Even though method 4 has the highest percent correct, there were still large numbers of spasm potentials erroneously included (missed) and large numbers of false positives erroneously excluded.

While these automated spasm identification procedures found different percentages of correct spasm regions, with method 4 the best, there were still large numbers of spasm potentials that were not identified and large numbers of false positive spasms. Figure 4.19 illustrates how the automated spasm finding affected the histogram of the firing frequency for global class 6 from the subject 1 recording, by plotting the histograms before any spasm potentials were removed, and after the spasm potentials identified by method 4 were removed. These histograms were normalized with respect to the number of potentials that belonged to global class 6.

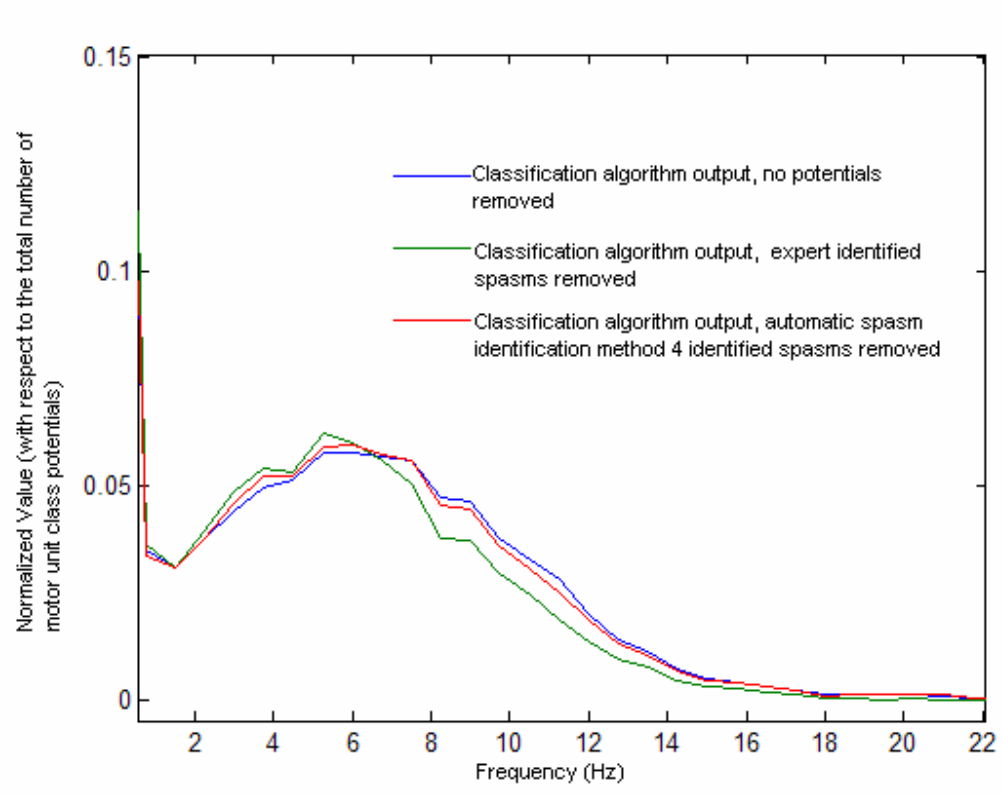

Figure 4.19 Automatic spasm identification effects on the firing rate histogram global class 6 in the subject 1 recording. Three different normalized histograms were plotted: The output of the classification algorithm (blue), the classification algorithm output after the expert identified spasms have been removed (green), and the classification algorithm output after method 4 identified spasms have been removed (red). The histograms were normalized with respect to the total number of potentials that belonged to global class 6.

Although 75 % of the correct spasm regions were found using method 4, the resulting histogram of global class 6 more resembled the original histogram without any spasms removed than it did the histogram with the gold standard spasm potentials removed. This behavior was seen with the remaining global classes in the subject 1 recording as well. Due to this behavior, the automated spasm identification procedure was not employed and instead an expert identified the spasms for the remaining recordings. The automated spasm identification procedure could be further developed, however, and pursued as a future project.

4.3.3 Clustering

Candidate potentials were clustered as part of the second phase of the automatic motor unit classification algorithm. "Transitive clustering" was used to cluster potentials in each channel independently to form classes. From this point on, the terms "cluster" and "class" are used interchangeably. Both terms refer to groupings of potentials that are similar according to distance metrics. These groups of potentials were produced by the same motor unit.

In transitive clustering, distance matrices were formed using all segmented potentials. The distances from any given potential to all other potentials were computed using two distance metrics, the Euclidean distance and the correlation coefficient (here after referred to as simply the correlation). The Euclidean distance is given by equation 4.2 and the correlation coefficient is given by equation 4.3.

$$d_{euclidean} = \sqrt{\sum_{n=1}^{N}(x_n - y_n)^2} \quad (4.2)$$

$$correlation = \frac{\sum_{n=1}^{N}(x_n - \bar{x})(y_n - \bar{y})}{(N-1)\sigma_x\sigma_y} \quad (4.3)$$

In both equations, x_n and y_n are components of the vectors **x** and **y** which have N components and represent 2 different potentials. σ_x and σ_y are the standard deviations of the vectors **x** and **y**, respectively, while $\bar{x}$ and $\bar{y}$ are the means of the vectors. All potential pairings that met the correlation and Euclidean distance thresholds of 0.95 and 0.25, respectively, were retained in a similarity list. These threshold values were chosen because they produced clusters that were the most compact and distant from each other. In other words, cluster members were the most similar to each other while cluster centers were furthest from each other. The retained potential pairings were then transitively grouped according to their similarity list. Table 4.6 shows an example similarity list and the classes that result.

Table 4.6 Transitive grouping example. The table shows pairings of templates that are the same based on the Euclidean and correlation distance metrics. There are 3 colors that highlight the numbers, representing 3 different global classes that are formed by transitively grouping the list.

1	2
1	3
2	5
4	6
10	11

Classes:
Class 1: 1, 2, 3, 5
Class 2: 4, 6
Class 3: 10, 11

Transitive clustering is based on the transitive property (if A=B, and B=C, then A=C). Since potential 1 is similar to potential 2 and 3, and potential 2 is similar to potential 5, then potential 1 must be similar to potential 2, 3, and 5. Class 1 then consists of potentials 1, 2, 3, and 5. The final two classes consist of potentials 4 and 6, and potentials 10 and 11, respectively. The transitive grouping procedure found all matches between pairings over the entire 3-minute EMG portion. All clusters formed had to have at least 3 potentials to prevent noise from being incorrectly clustered. Template potentials were then computed for each cluster by averaging all the potentials of each cluster (at the 3-minute level), to obtain the mean, or cluster centroid.

The last stage of transitive clustering refined the classes that were formed by comparing the distances between all clustered potentials. Again correlation and Euclidean distance measures are used, but this time the Euclidean distance was normalized using the norm of the template potential (equation 4.4).

$$norm = \sqrt{(x_1^2 + x_2^2 + \ldots + x_N^2)} \qquad (4.4)$$

In equation 4.4, x_1 through x_N are the data points of the template potential, where N is the number of points in the template potential. This way, Euclidean distance measures relative to the size of the potentials in question were used instead of an absolute distance measure. Member potentials remained in a given class only if the potential correlated to at least 0.95 with all other member potentials

plus was closer than 0.45 away from all other member potentials according to the normalized Euclidean distance metric.

The classes produced by the clustering method were extremely refined (using high thresholds) so that no misclassifications would be made. The end result was that a unique class could be clustered as several separate classes. These separate classes were merged in a later stage of the classification algorithm. Figure 4.20 shows a clustering example that has several motor unit classes found as individual classes (classes 2 and 12 would later be combined to represent the template for one motor unit class).

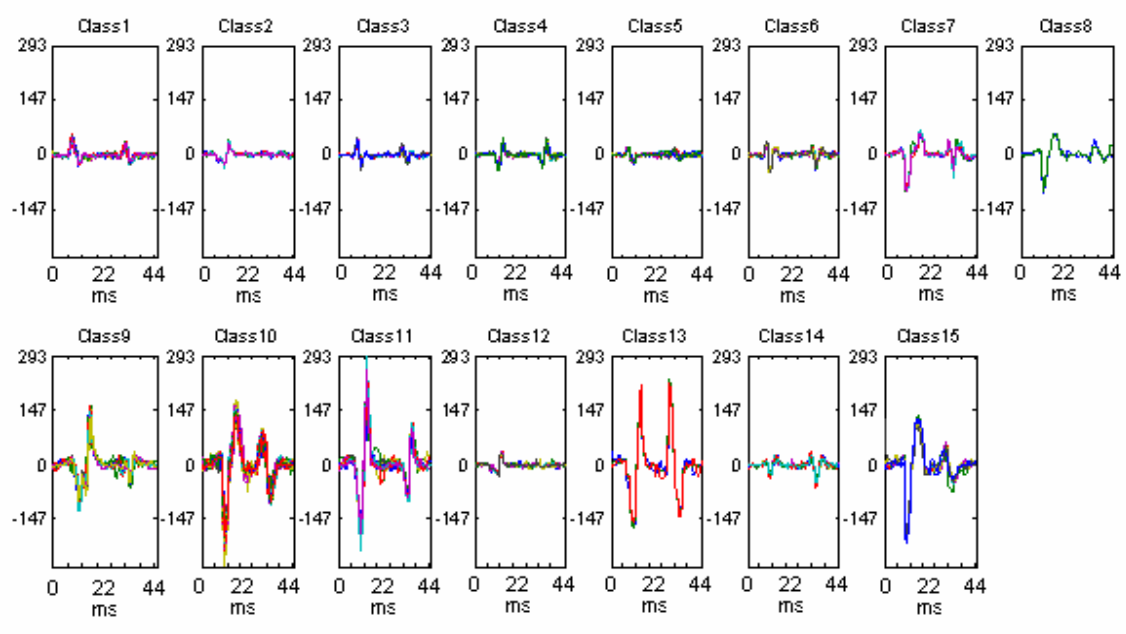

Figure 4.20 Clustering stage output example. Fifteen classes were obtained from clustering the subject 1 recording, HR 16 MIN 45. The left side of each pane constitutes distal channel potentials while proximal channel potentials constitute the right side of each pane. The result of each clustering may be that a unique class appears as several individual classes. In this case, classes 2 and 12 represent the same class. These classes will be merged by a later stage of the classification algorithm. All amplitudes are in microvolts.

In the figure, the left side of each pane is distal channel potentials while the right side of each pane is proximal channel potentials. The third and fourth passes of the classification algorithm performed the required merging so that one unique class is clustered as one individual class.

4.3.4 Cross Channel Class Matching

The cross channel class matching procedure matched the classes found in each channel independently to yield the net classes for a 3-minute EMG portion. Since thenar fibers probably go from one end of the muscle to the other (Westling et al., 1990), and the EMG electrodes lay across the bellies of the muscles in a distal/proximal configuration, motor unit potential potentials were recorded simultaneously in the two channels so that each channel had a representation of a single motor unit potential. However, the actual shapes of the potentials for any one motor unit were different between channels, due to the difference in the positioning of the recording electrodes and because the potentials traveled away from the motor end plates in opposite directions.

In cross channel class matching, the classes in one channel were matched with classes in the opposite channel (Figure 4.21).

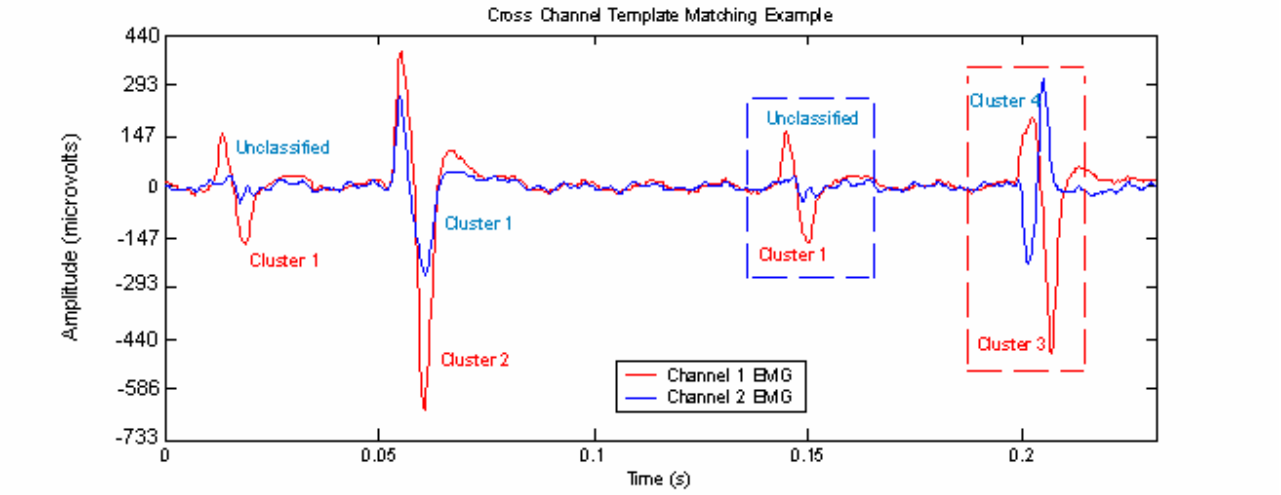

Figure 4.21 Cross channel template matching example. Both channels were clustered independently, yielding different cluster numberings between channels. Correspondences between clusters in each channel were then found.

Both channels were clustered independently, yielding different cluster numberings between channels. In most cases, each class in one channel had a direct match with a corresponding class in the opposite channel. If there were no direct class match between channels, classes were retained based on distance metric thresholds. For example in Figure 4.21, cluster 2 in channel 1 was paired with cluster 1 in channel 2, thus forming a (cluster 2/1 pairing). Similarly, there is a cluster 3/4 pairing between channels 1 and 2. Cluster 1 in channel 1 doesn't correspond to a cluster in channel 2, as shown by the dotted blue rectangle. The corresponding potential to the cluster 1 potential is unclassified. Therefore, a new corresponding cluster is created in channel 1. Corresponding member potentials in the opposite channel had to correlate to at least 0.95 with each other and have a normalized Euclidean distance closer than 0.5. If the distance criteria were not met, the class was discarded.

There were some instances where a legitimate class existed in one channel, whereas the opposite channel had corresponding potentials that appear to be noise and failed the distance measure criteria (Figure 4.22).

This exception was accounted for in the following way: Below a peak to peak potential value of about 22 μV, distance criteria were not used. Although removing the distance criteria in this instance can produce misclassification problems later, it did enable the tracking of motor unit classes that were very stable in only one channel.

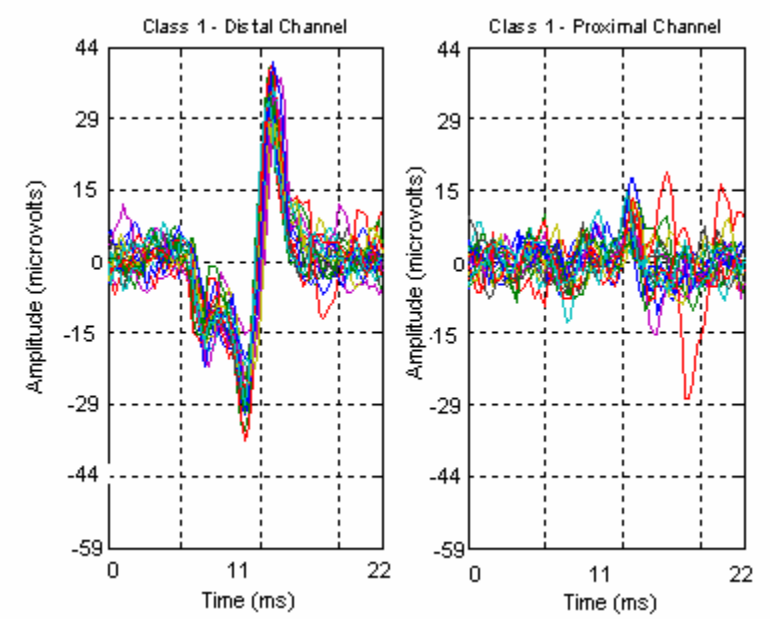

Figure 4.22 Potential representation in one channel fails distance measures. The above class has a repeatable, stable potential in the distal channel, while the proximal channel's representation appears to be noise. The noise-like potentials in the proximal channel fail the distance measure criteria. In order for the above class to be correctly clustered and additional criterion is added. Distance measure criteria are not applied if the peak to peak value of the class template potential is less than a threshold value.

4.3.5 Motor Unit Classification Viewing Software Package

A comprehensive, user-friendly software package was created in order to view and modify classified EMG data at both the 3-minute segment level and the 24-hour (global) level because no other available software packages are capable of handing these large data sets or analyzing all of these data at the single motor unit level. For the same reasons, a user-friendly interface was also designed for manually verifying the tracking of templates over the 24-hour recording. The viewing software was GUI based and written in Matlab 7.0 just as the processing software.

Individual 3-minute EMG segment viewing and modification was provided with a set of GUI tools developed in Matlab 7.0. Figure 4.23 shows the front end of the viewing software package. The primary purpose of this package was to allow a user to view the two channels of raw data and to evaluate the accuracy of the algorithm-based classification of motor unit potentials.

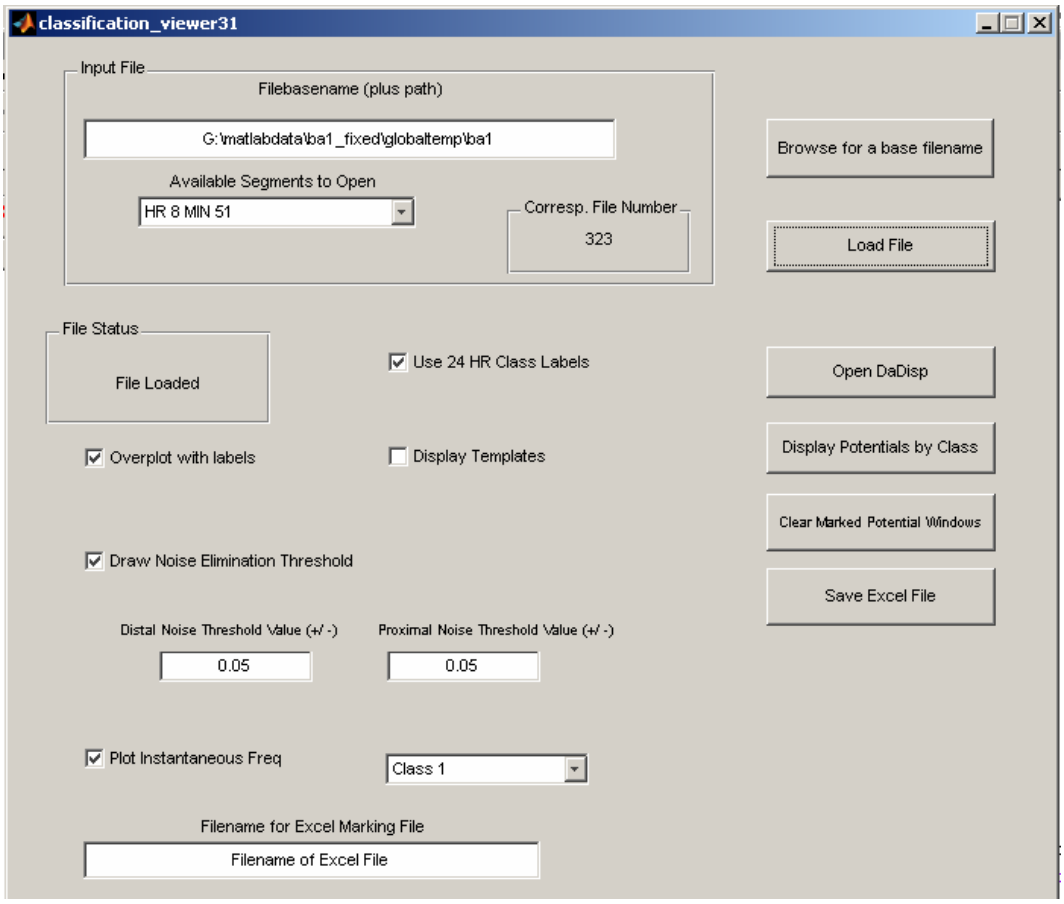

Figure 4.23 Front end of the classification viewing software package. The viewing software allows for the viewing of entire EMG traces through DaDisp 2002, including the annotating of potentials and manual construction of superimposed potentials in order to resolve superpositions into their constituent classes.

Many features were available to the user at the software front end. The user could enter the pathname of a data file or browse for one using the standard windows interface. A drop-down menu allowed the user to select a desired 3-minute EMG portion by its time designation. All 3-minute portions were numbered starting from midnight – 12 am was hour 1, minute zero (HR 1 MIN 0) while 11 pm was hour 24, minute 0 (HR 24 MIN 0). All potentials modified by the user were stored in the excel file whose name is given by the text dialog box at the bottom of Figure 4.23. Lines could be drawn on the distal and proximal EMG

traces denoting a noise threshold to be used in manual classification. Their values can be set through the front end as well.

The viewing program executed DaDisp 2002 to display the EMG traces for a given 3-minutes, plus the instantaneous frequency of the desired local class (set by the drop-down menu). The instantaneous frequency had units of Hz and was simply the reciprocal of the time in seconds between potentials of the same motor unit class. Figure 4.24 shows the DaDisp 2002 display window.

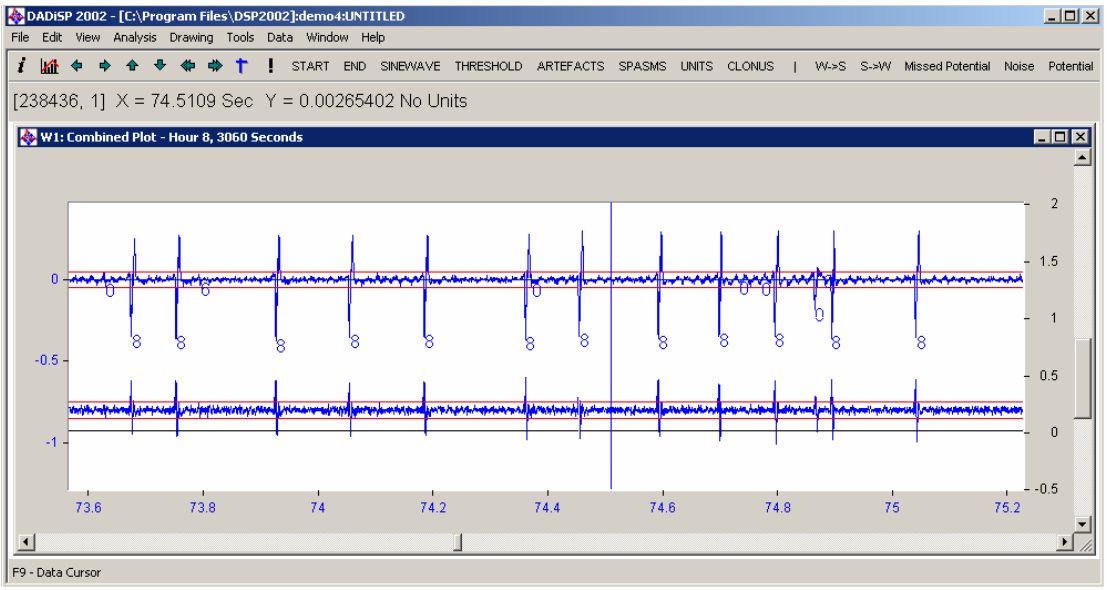

Figure 4.24 EMG traces displayed in DaDisp 2002. DaDisp 2002 was used by the viewing software to display the distal and proximal EMG traces. The classifications for these potentials are directly labeled on the plot. DaDisp also features a cursor function that allows potentials to be marked as noise or missed potentials. The vertical blue line represents the DaDisp cursor.

Within the DaDisp display, potential classifications were annotated directly on the potentials themselves. The user could use DaDisp's cursor feature to select potentials and mark them as noise or missed potentials. These marked potentials could then be saved using the front end of the viewing software package.

More in-depth usage was accessible by clicking on the “Display Potentials by Class” button. Figure 4.25 shows the available features from this submenu.

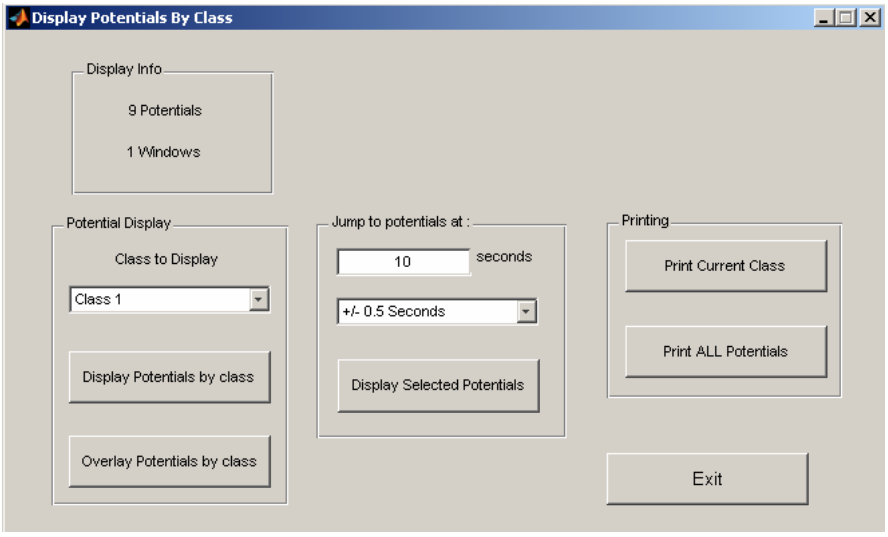

Figure 4.25 Display potentials by class window. This interface featured more operations the user can use to view the classified EMG. This includes viewing potentials individually and by class as well as printing out potentials.

The “Overlay Potentials by Class” button plotted a figure in which all potentials of the class selected by the drop-down menu were overlaid. The potentials of a single class or all potentials could be printed. The display info pane in the upper right corner of the window informs the user of the number of potentials that were classified as the selected class and how many windows it will take to display them individually by clicking on “Display Potentials by Class.” This feature allowed the user to view the potentials of an entire class individually (Figure 4.26).

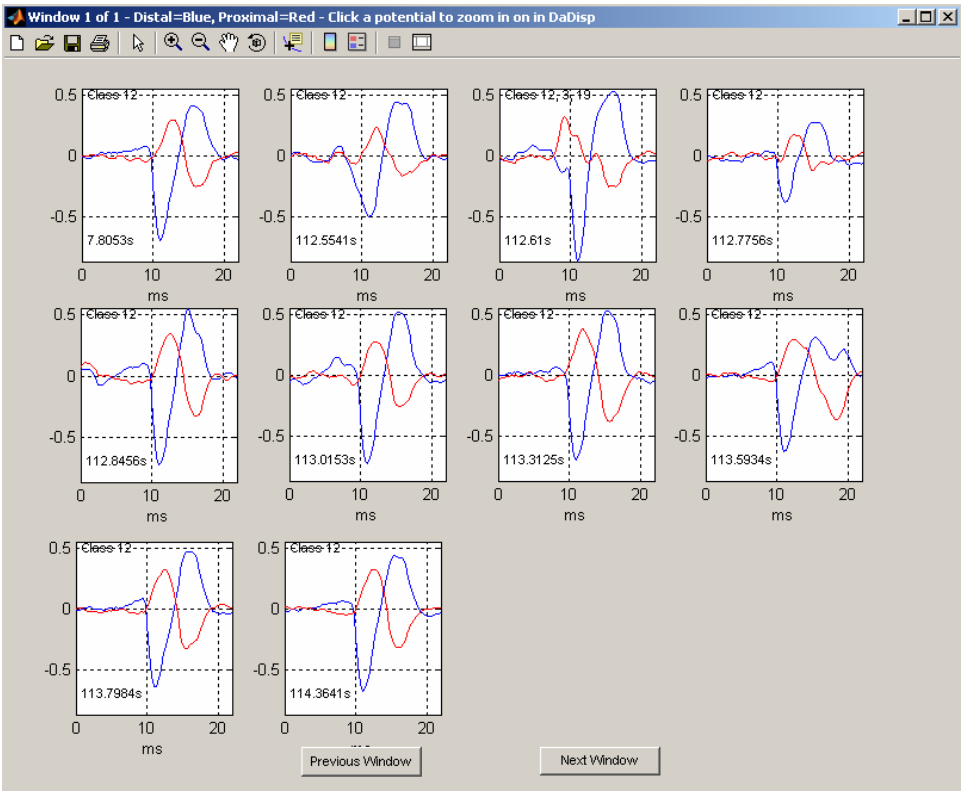

Figure 4.26 Viewing individual potentials window. This display allows a user to view individual potentials, their classes, and the times at which they occurred. Clicking on a window re-scales the x-axis of the EMG displayed in DaDisp so that the potential in the desired window is centered.

From there, the user could view a given potential's class and the time when it occurred. The user could also click within one of the panes to pull up the interface in Figure 4.27.

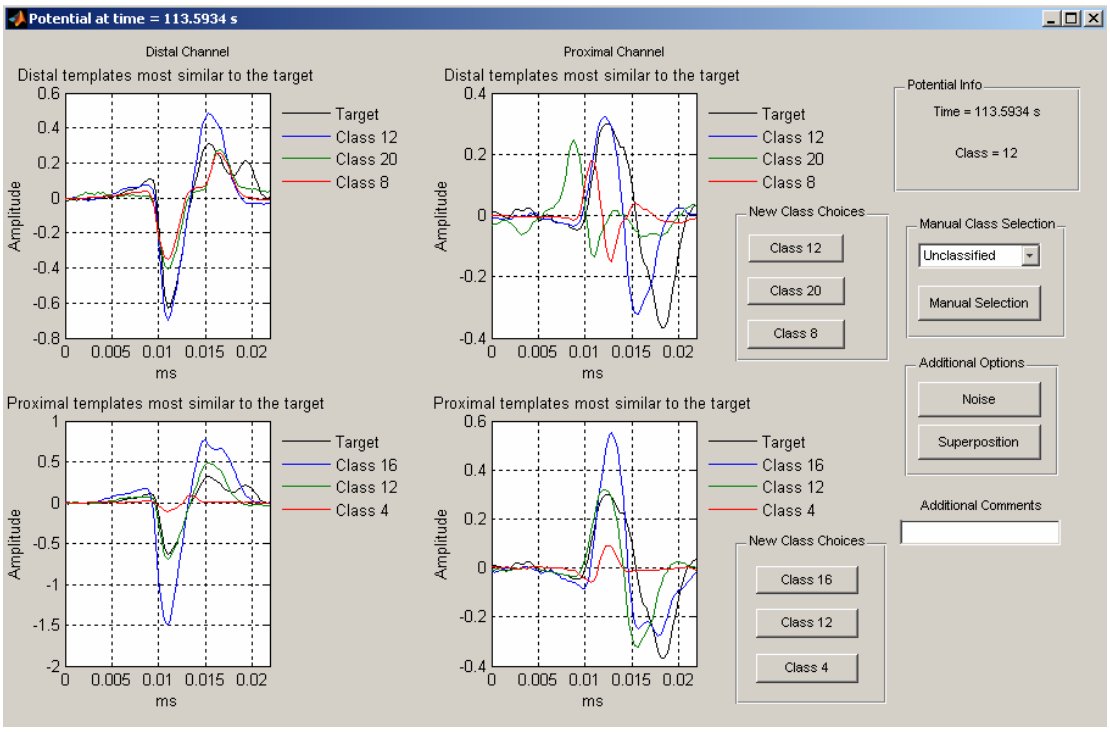

Figure 4.27 Re-classification window. The window displays the currently selected potential as well as the 3 nearest class templates (with respect to either the distal or proximal channel). The user can then classify the potential by clicking on one of the class buttons, or manually selecting the desired class through the drop-down menu on the right side of the window.

In this window, the user had a chance to re-classify the potential as one of the three nearest classes (with respect to either the distal or proximal channel), noise, or any other class using the drop-down menu. The user could also determine if the current potential was a superposition using the applet shown in Figure 4.28.

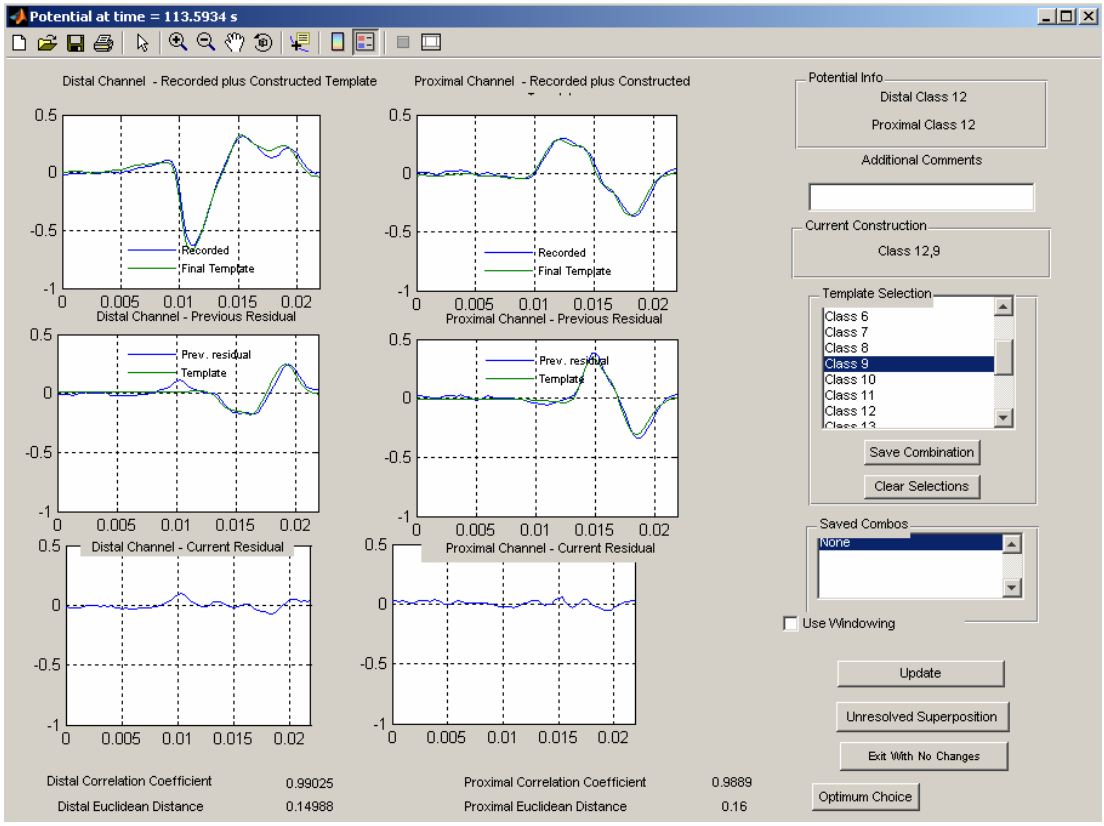

Figure 4.28 Manual superposition building applet. This applet allows the user to select constituent potentials in order to build a superposition to match the target potential. The top panes show the target potential and the constructed superimposed template in each channel. The middle and bottom panes show the residual potential remaining after successive classes have been subtracted from the target potential.

By clicking in the list box on the right side of the window, the user could sequentially select classes to use in building a superposition to match the current potential. The top panes show the representations of the current potential in both channels and the net superimposed potential that was built to match it. The middle panes show the previous residual while the bottom panes show the most current residual obtained from subtracting the most recent class template. The distance measures of correlation and Euclidean distance are shown at the bottom of the window as the superposition is being built. The user could click the "optimum choice" button at the lower right corner of the window to have the

applet select the class template that produces a constructed superposition that most matches the target potential.

If a potential already happens to be classified as a superposition, the following window is displayed (Figure 4.29).

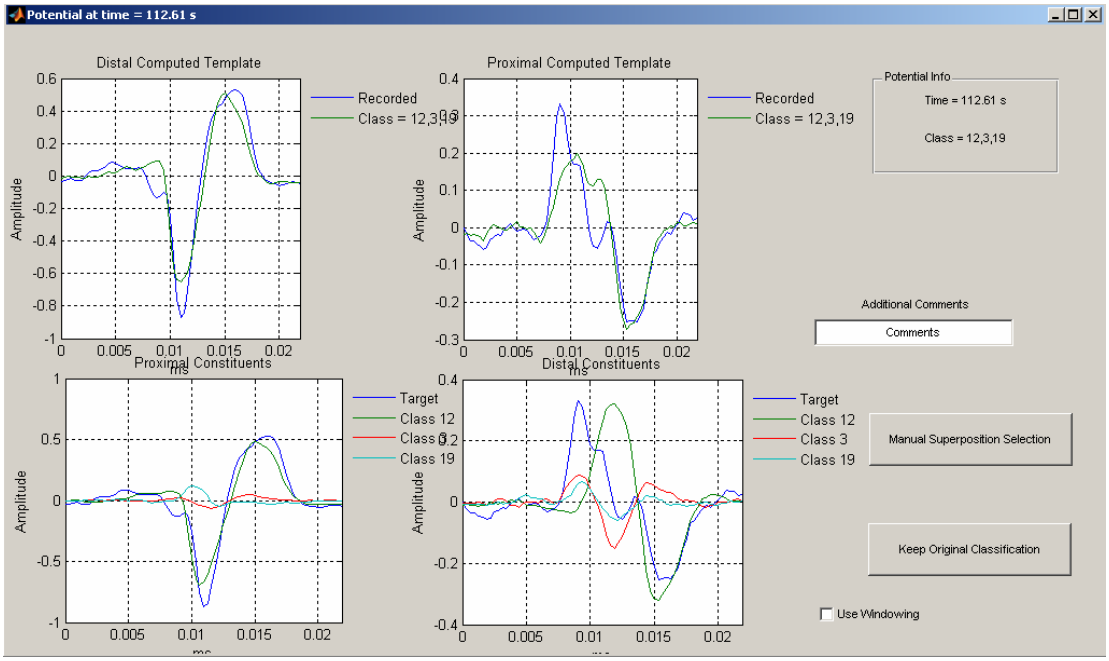

Figure 4.29 Superposition display window. This window shows a potential that has been classified to be a superposition. The bottom panes show the time shifts of the constituent classes required to build the superposition.

In this window, the lower panes show the positions of the constituent class templates as they were shifted to construct the superposition indicated by the classification. All three of the previous windows contain spaces to add user comments which will be added to the excel file containing all classification changes.

4.3.6 Motor Unit Template Uniting

The motor unit template uniting procedure was used to find all of the most active, stable motor units in each 24-hour recording. These most stable motor units constituted the global classes of the recording. This procedure involved three stages. The first stage clustered all the motor unit class templates local to each 3-minute portion to find the global classes. The second stage classified the local classes within each 3-minute EMG portion as global classes, while the final stage searched for global classes that were not initially found in each 3-minute EMG portion.

4.3.6.1 Motor Unit Template Uniting Stage 1

In the first stage of the motor unit template uniting procedure, all motor unit class templates found in each of the 3-minute portion were clustered. Before clustering each pair of templates were aligned in time as described in section 4.3.7 so that any alignment errors using the most negative point of each potential would be minimized. “Composite” template shapes were created by joining the distal channel templates to each corresponding proximal channel template. Where before, each template consisted of 71 data points, each new combined template consisted of 142 data points. Points 1 though 71 were the distal channel template, while points 72 through 142 were the proximal channel template (Figure 4.30).

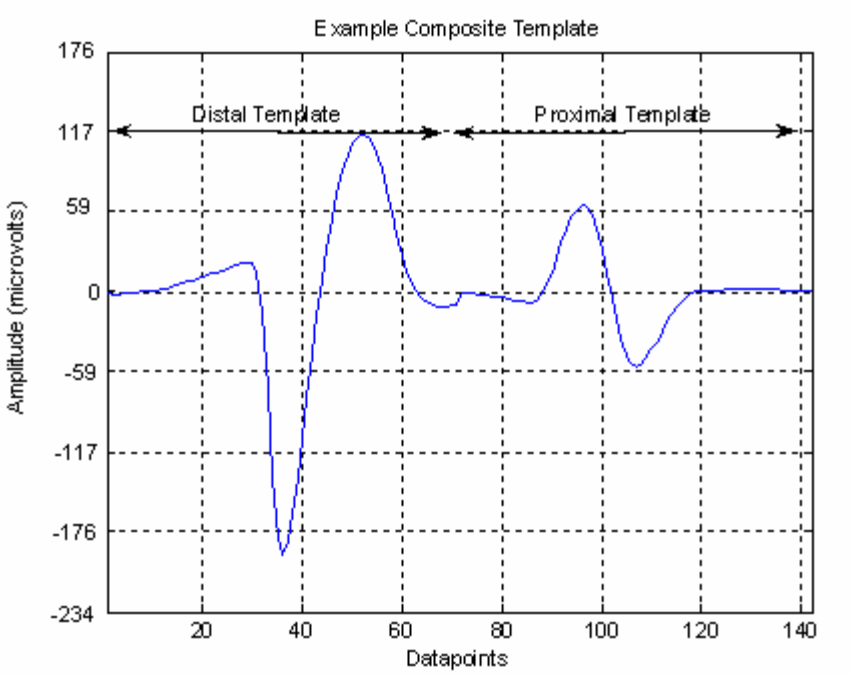

Figure 4.30 Example composite templates. Points 1 through 71 represent the distal template while the remaining points represent the proximal template.

Next, the transitive clustering routine was applied to all the composite templates using high correlation and Euclidean distance thresholds, 0.98 and 0.5, respectively. The high correlation value ensured that only the units with the most stable template shapes were considered for the clustering. The transitive grouping procedure found all matches between pairings over the entire 24-hour recording. All global classes had to have at least five member templates so that only the more commonly occurring templates were retained for further consideration. In other words, a global class had to appear in at least 15 minutes of the 24-hour EMG recording to be retained.

After transitive clustering, there were some resulting global classes that required merging. This was done by giving the user the ability to form new

groups and combine existing ones through a graphical user interface (GUI) program (Figure 4.31).

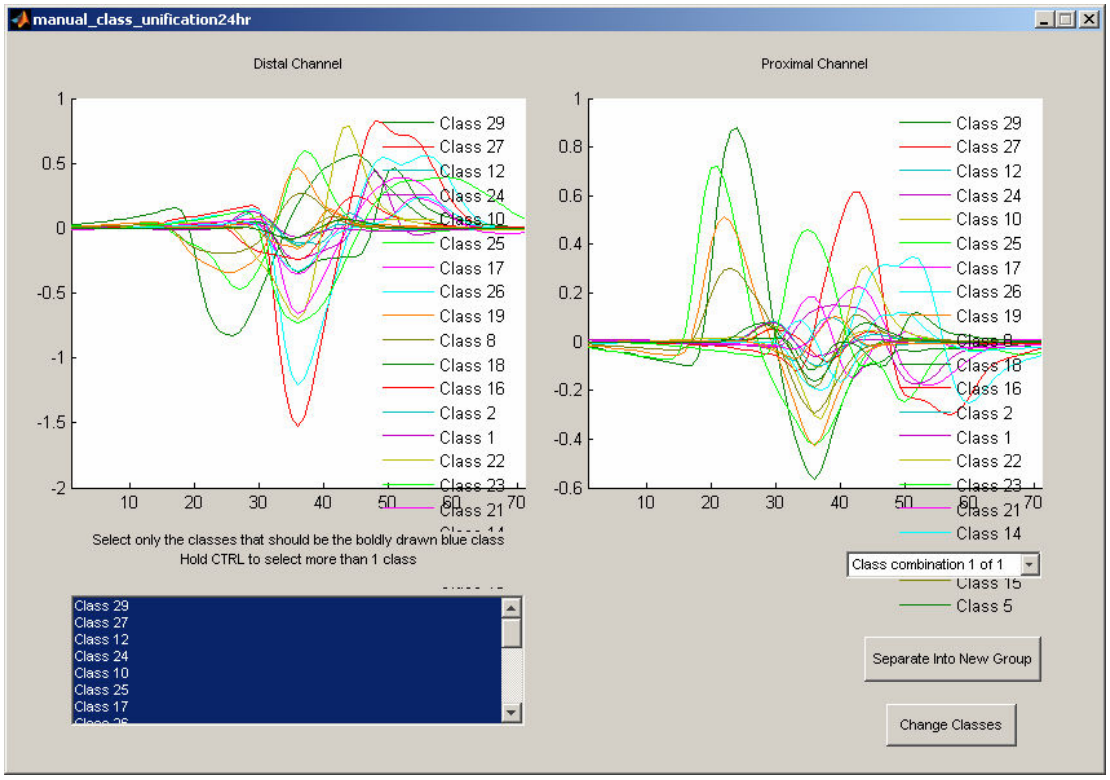

Figure 4.31 GUI program to combine global classes. A user can combine existing global classes using this program.

After being presented with all the most commonly occurring class templates that the program found, the user has the ability to manually select global class templates which should be combined. Figure 4.32 demonstrates a combination.

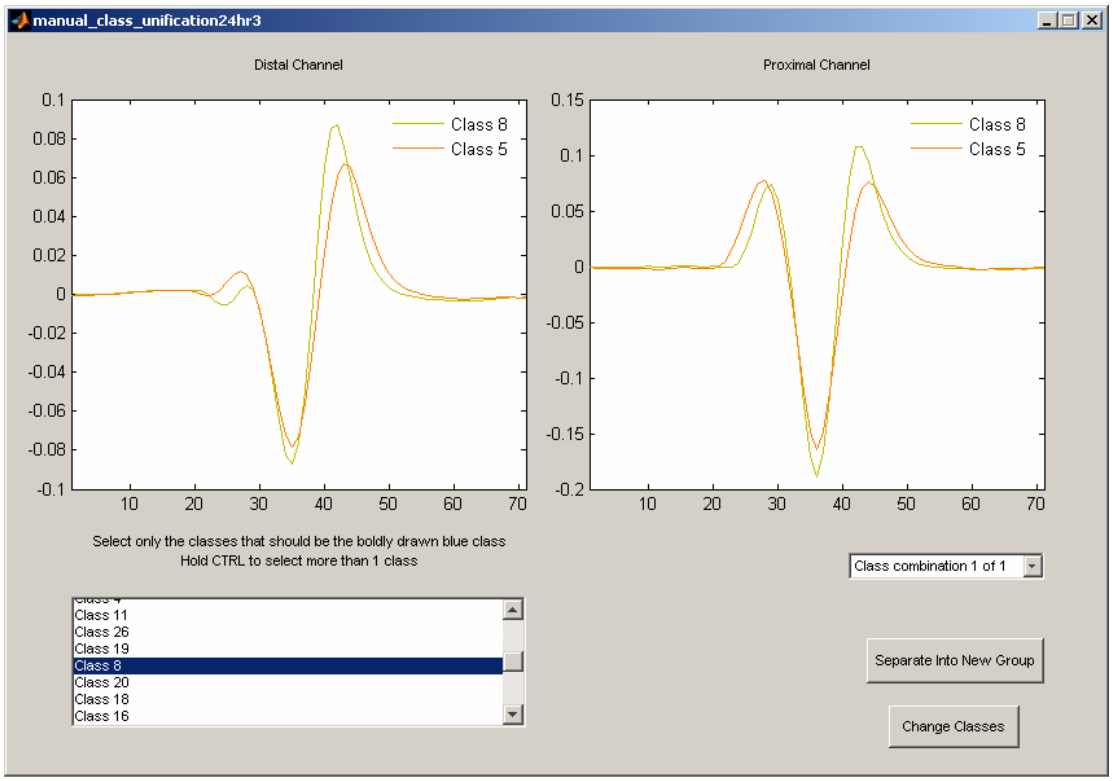

Figure 4.32 An example of combining global classes with the GUI interface.

In Figure 4.32, Global classes 5 and 8 are identical and the user can combine them using the GUI program. After all combinations have been made, another GUI program (Figure 4.33) allows the user to delete a global template group if it happens to be noise or incorrect in some way.

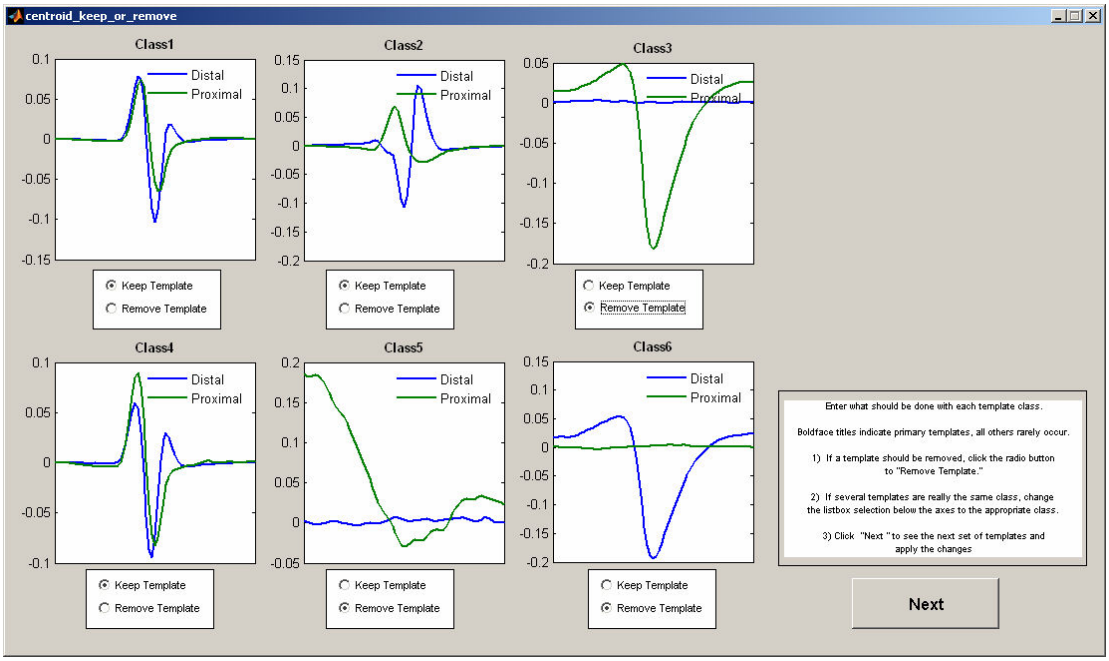

Figure 4.33 GUI interface to remove incorrect global classes.

In Figure 4.33, Global Classes 3, 5 and 6 are noise and can be removed by selecting the “remove template” option on the GUI and clicking the “Next” button to proceed. The output of the first stage of the motor unit template uniting procedure is a collection of global class templates. An example is shown at the beginning of section 5.3.

4.3.6.2 Motor Unit Template Uniting Procedure Stage 2

The second stage of the motor unit template uniting procedure was then used to classify the local templates for every 3-minute portion as global classes. This was accomplished using fuzzy values to compare composite member potentials from each local class to the representative templates from each global class. Fuzzy membership values were computed using equations 3.5 and 3.6.

Pseudocode for the procedure is shown below (Figure 4.34). Variables are in boldface.

```
For n= 1 to 480 3-minute portions
        For k = 1 to the total number of global classes
                Find the closest classified occurrence of global class k to 3-
                minute portion n
                Store this composite class template in Temp_templates
        End For

        For i = 1 to the number of local classes there are in 3-minute portion n
                Store all member potentials of local class i in Temp_candidates
                Use equation 3.5 along with Temp_candidates and
                Temp_templates to compute fuzzy membership values, μwk
                where w is the potential number and k is the global class number
                Find the maximum value of μwk over each potential
                If any 2 maximum values > 0.7 for the same k, then
                        Compute the Euclidean distance and correlation distance
                        between each potential, w and the k from above
                        If the distances meet the threshold then
                                Classify local class i as global class k
                        Otherwise
                                Do not classify local class I as any global class
                        End if
                Otherwise
                        Do not classify local class i as any global class
                End if
        End for
End for
```

Figure 4.34 Pseudocode for the fuzzy membership method that classifies remaining local classes as global classes. Variables are in boldface.

The representative global templates for each global class were those classified composite templates that occur closest to the 3-minute segment in question. In other words, the second stage does comparisons based on nearest neighbor principles. For example, the algorithm will search the hour 15, minute 15 EMG segment for global class 10. Global class 10 wasn't initially found in this 3-minute portion, but was found in hour 15, minute 51 and hour 15, minute 2.

Thus, the class 10 template from hour 15, minute 3 was selected as the class 10 representative template for the hour 15, minute 15 EMG portion.

The matches achieved by stage 2 of the motor unit template uniting algorithm were verified manually for each recording with the help of two GUI programs. Figure 4.28 below shows the main interface for manually verifying the performance of the classification algorithm in the second stage of the motor unit template uniting procedure.

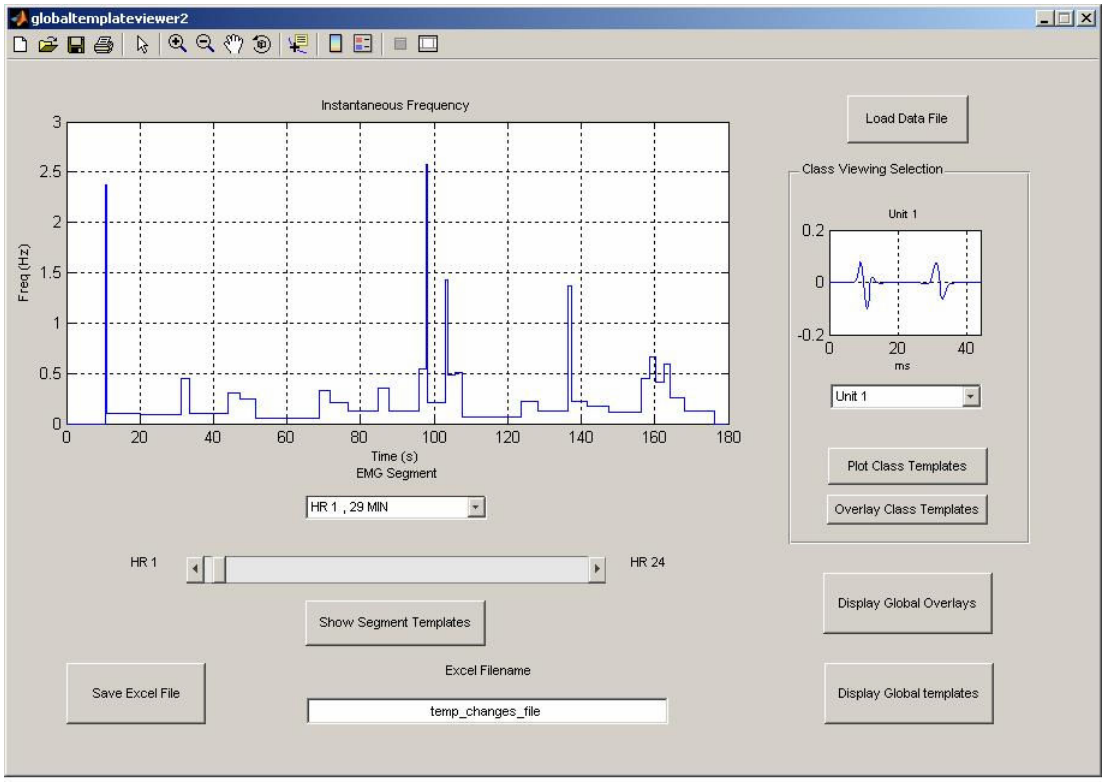

Figure 4.35 GUI interface for verifying the second stage of the motor unit template uniting procedure. This GUI allows the user to inspect the performance of the motor unit template uniting procedure. The user can also view instantaneous frequencies of individual motor unit classes and overlay all global class templates. All global class templates are displayed in the composite form of Figure 4.24. This interface can also save an excel file which contains corrections to the global template matching in order to create a gold standard that can be used to compute performances.

The power of this interface is that it can create gold standards against which to evaluate the second stage of the global template matching procedure.

From this interface, the user can view instantaneous frequency plots of desired global classes in the desired 3-minute EMG segments as indicated by their times in hours and minutes, along with viewing overlays of all templates belonging to a global class. All templates are displayed in the composite form as in Figure 4.36.

Gold standards can be created by selecting the "Show Segment Templates" button for each 3-minute EMG portion selected by the drop down menu and then making classification modifications as described in section 4.3.5. Figure 4.36 shows the window displayed after the "Show Segment Templates" button is clicked.

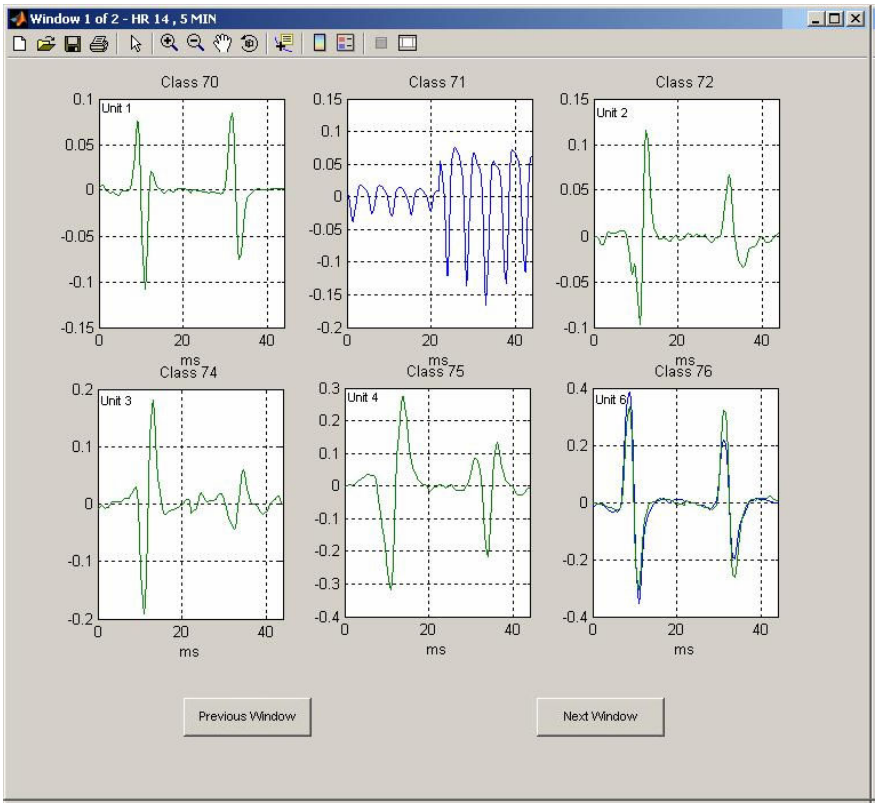

Figure 4.36 Show segment templates window. This window allows the manual inspection of the second stage of the motor unit template uniting procedure. If only a green template is present, the motor unit class label was assigned during the clustering of all templates. If a green template is overlaid on top of a blue template, the green template is the global class whose label appears in the upper left hand corner of the pane (as indicated by the unit number). If only a blue template appears in a pane, then the global template matching routine could not find a global class label for that template. Any window can be clicked to make an adjustment just like in Figure 4.26. The clicking will bring up the interface in Figure 4.27 where changes can be registered.

This window displays the global class labels assigned to each template in the currently selected segment. The presence of only a blue template in a pane (class 71 in Figure 4.36) denotes that the motor unit template uniting procedure could not assign any label to that template and it was left as unclassified. The presence of only a green template in a pane (class 70 in Figure 4.36) denotes that the global class label was assigned during the first stage of the motor unit template uniting procedure (template clustering). A green template overlaid on a blue template (class 76 in Figure 4.36) denotes that the global class label indicated in the upper left hand corner of the pane was assigned to that blue template. The green template is the averaged distal and proximal representations of that global class.

The user has a wide range of options to make the necessary adjustments to the algorithm's results. The user has the ability to assign the correct global class label to a template if it were left unclassified. This results in a missed classification. If a template was assigned the wrong global class, the user has the ability to change it to the correct global class, thereby signaling a misclassification. If a noise template were mistakenly assigned a global class label, generating a false positive, the user can change that label to unclassified. All changes made can then be saved to an excel file by clicking the "Save Excel File" button. This excel file is then later used to build the gold standard for the second stage of the motor unit template uniting procedure. This gold standard can be compared to the algorithm's results to obtain performance percentages

that include those templates that were correctly labeled, those that were misclassified, those that were false positives and those that were missed.

Changes could be made using the GUI in Figure 4.36 by using a mouse. Clicking on the desired pane yields the re-classification window. This window is also a part of the motor unit classification viewing software package. The interface is used as described in section 4.3.5 and can register global class modifications, whether they are noise or misclassifications.

4.3.6.3 Motor Unit Template Uniting Procedure Stage 3

The third and final stage of the procedure found all global classes in each 3-minute EMG portion that were not found by either the first stage of the global template matching procedure or the first pass of the overall classification algorithm. It also combines any classes that were split erroneously. The routine similarly used fuzzy membership values, but this time they were computed for all potentials in each segment. All potentials that had a fuzzy membership value greater than a threshold value of 0.8 for a given global class (and a correlation of at least 0.9 and Euclidean distance less than 0.8) were assigned to that class. All classes at the 3-minute level that were not assigned to any global class were retained for later classification so that superpositions would not be incorrectly labeled.

The third stage of the motor unit template uniting procedure was manually verified in order to produce a gold standard using a similar interface as shown in Figure 4.36. The new interface is shown in Figure 4.37.

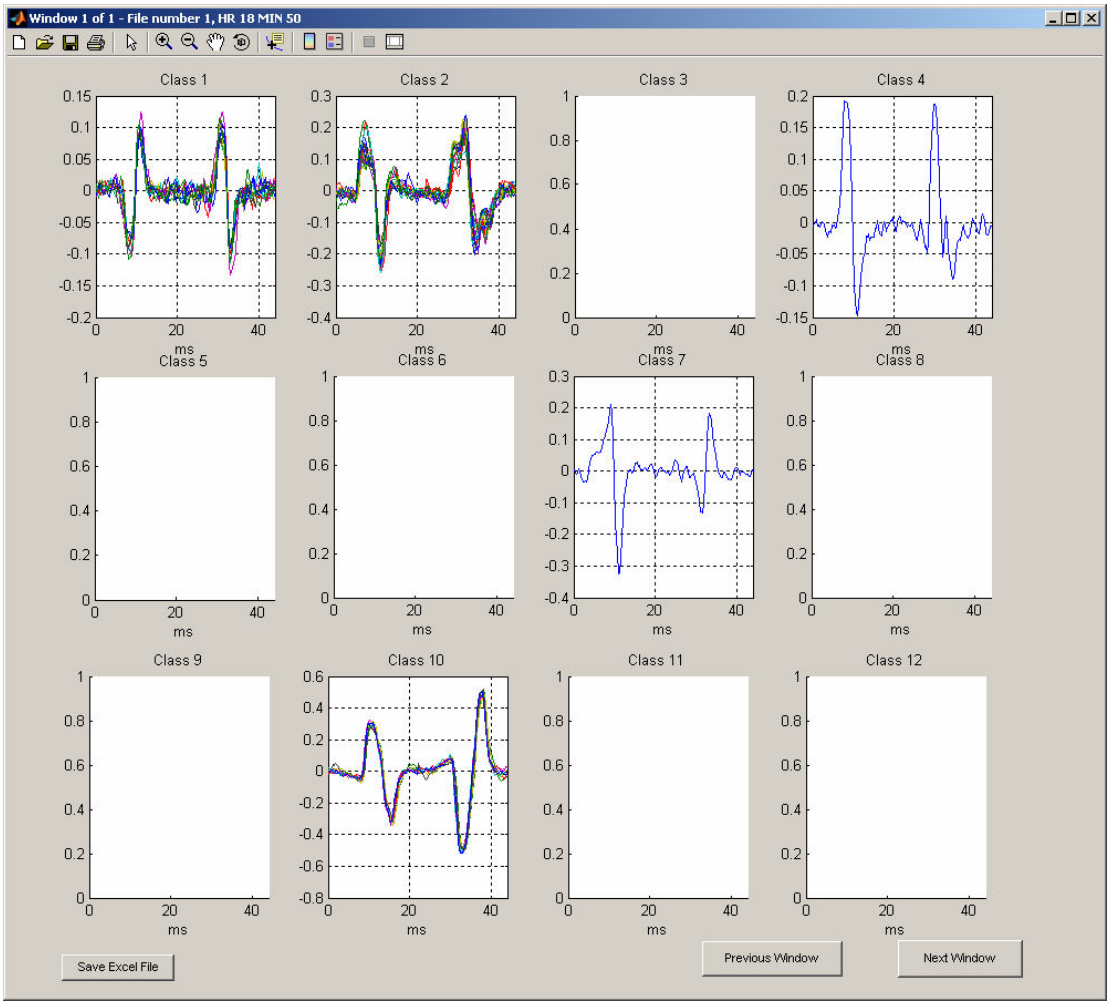

Figure 4.37 GUI interface for manually verifying the third stage of the motor unit template uniting procedure. This window is used to manually verify the third stage of the motor unit template uniting procedure. Each pane displays member potentials found for each global class. Changes can be made by clicking on panes as previously described. Changes must be made if a pane contains potentials that do not belong to a global class, indicating a misclassification, or if a pane belonging to an overflow class contains potentials that in fact belong to a global class, indicating splitting error.

Each pane contains individual potentials that the classification algorithm has found for each global class and each overflow class (those classes that were found in excess of the global classes). Modifications can be made as described previously by clicking on a pane of interest. The “Previous Window” and “Next Window” buttons can be used to navigate through all 480 3-minute segments of each 24-hour recording. Changes can once again be saved by clicking on “Save Excel File” in the lower left corner of the window.

The user's objective is to make sure that each global class correctly contains the appropriate individual potentials that are members of each specific global class. The user must subjectively decide if a majority of overlaid individual potentials (as in Figure 4.37) belong to the assigned class or not. If a pane contains potentials that do not belong to a particular global class, but do belong to a different global class, the user can use the re-classification window to make a change to indicate a misclassification. If a global class' pane contains noise or unclassifiable potentials, the user must label this global class as unclassified, thus making this error a false positive.

A splitting error can result if global classes were not recombined during this third stage of the motor unit template uniting procedure. The net result is potentials that should have been classified are missed. For example in the interface of Figure 4.37, if a global class correctly contains the appropriate member potentials, but a class that is not being tracked (overflow class) also contains the same member potentials, the user must click on the overflow class' pane and record which global class it actually is.

4.3.7 Unsorted Potential Analysis

Unsorted potential analysis was the last stage of the automatic classification algorithm. In this stage, all unclassified potentials in each 3-minute EMG portion were compared with the global class templates found by the global template uniting stage in order to obtain a classification. A potential had to meet

distance criteria when compared with the target class templates in both channels in order to be classified:

1) Correlate to at least 0.94 and have a Euclidean distance of less than 0.5 with the target class template
2) Correlate to at least 0.85 and have a Euclidean distance of less than 0.7 with the target class template of the opposite channel.

If a potential doesn't correspond to a single global class, the superposition resolution algorithm (described in Figure 4.41) attempted to resolve the potential into its constituent global classes. The pseudocode in Figure 4.38 below shows the details of the unsorted potentials analysis.

```
For n =1 to 480 3-minute portions
    For i = 1 to as many unclassified potentials in 3-minute portion n
        For k=1 to as many global classes that there are
            For both the distal and proximal channels
                Cross-correlate the unclassified potential i and global
                class k.
                Slide unclassified potential i to the lag value that
                maximizes the cross-correlation function.
                Compute the correlation coefficient and Euclidean
                distance (normalized to the norm of the global class
                template) between the global class k and shifted version
                of unclassified potential i.
            End For
        End for
        Find the global classes for which the distance measures meet the
        thresholds of 0.94 correlation and 0.5 Euclidean distance.
        If the thresholds are met in both channels,
            If there are multiple global classes that meet the threshold, then
                Label the unclassified potential using the global class of
                the smallest Euclidean distance measure.
            Otherwise,
                Label the unclassified potential as the global class
                whose distance measure meets the threshold.
            End if
        Else if the thresholds are only met in 1 channel for global class k, then
            Check the correlation and Euclidean distances of that
            unclassified potential with global class k in the opposite channel.
            If the thresholds of 0.85 correlation and 0.7 Euclidean distance
            are met, then
                Label the unclassified potential as global class k
            Otherwise,
                Check to see if this unclassified potential is a
                superposition.
            End if
        Else no thresholds are met,
            Check to see if this unclassified potential is a superposition
                .
        End if
        If no classification is found in the first pass, then
            Repeat the above procedure after applying an attenuation
            window to unclassified potential i
        Else if no classification is found in the second pass, then
            Leave unclassified potential i unclassified
        End if
    End For
End for
```

Figure 4.38 Pseudocode for the unclassified potential analysis. The pseudocode in the figure classifies the remaining unclassified potentials throughout each 3-minute portion of a 24-hour recording. Variables are in boldface.

In order to resolve the superimposed potentials into their constituent global classes, a modified dual channel peel-off method [Stashuk, 2001] was employed. Cross-correlation was used to find the correct shifts at which to add the template class potentials in order to best reconstruct the target superimposed potential. This technique could accomplish superposition resolution due to the fact that superpositions are the algebraic summations of motor unit potentials that occur nearly simultaneously [Day SJ and Hulliger M, 2001].

The alignments of all potentials were changed so that timing information could be used in the superposition resolution procedure. The exact times that potentials occur were vital in correctly resolving a superposition. The time shifts required to build a superimposed template must be the same for both channels, so that a superimposed template was constructed in the same manner as it was produced physiologically.

The alignment was changed so that both the distal and proximal representations for a potential were aligned in time (Figure 4.39).

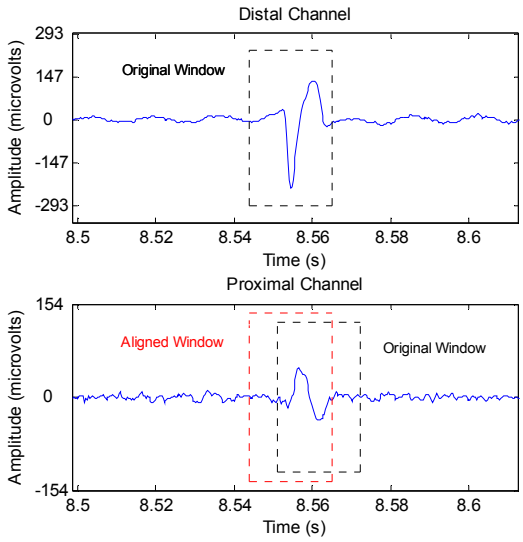

Figure 4.39 Time alignment of potentials. Before the superposition resolution procedure, potentials were aligned in time. In this case, the proximal channel's potential is realigned (red window) because it had a smaller peak to peak value than the distal channel's potential.

The channel whose potential representation had a larger peak to peak value remained unchanged. The other channel's representation was shifted so that its window had the same endpoints in time from the raw EMG as the unchanged representation. Figure 4.40 shows a close-up view of Figure 4.39.

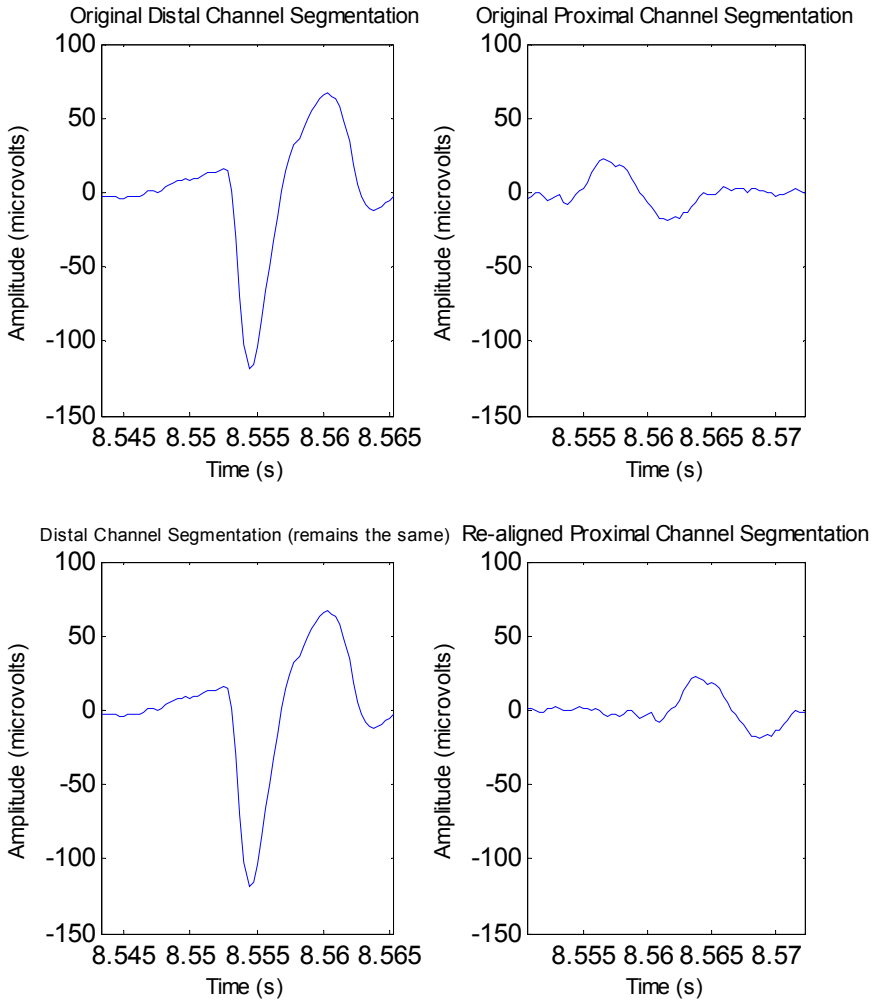

Figure 4.40 Segmentation in time alignment. The top panes show the same originally segmented potential in the distal and proximal channels. The bottom panes show the same potentials with new segmentation based on time alignment. Both bottom pane windows have the same endpoints in time. These endpoints are from the potential in the distal channel because it has a greater peak to peak value.

The original segmentation of the same potential in each channel is shown in the top pane, while the bottom pane contains the re-aligned potentials so that the potentials were segmented in the way they were produced physiologically. Time

aligning in this way can unfortunately produce errors when the distal and proximal channel representations of a potential are similar in peak to peak amplitude (see section 6.4). Figure 4.41 shows pseudocode for the superposition resolution routine. Variables are in boldface.

```
Initialize Peel-off potential(1) = current unsorted candidate, distal channel representation.
Initialize Peel-off potential(2) = current unsorted candidate, proximal channel representation.
Initialize NewTemplate(1) = 0
Initialize NewTemplate(2) = 0
For n = 1 to 3 total global classes to build a superposition
        For k = 1 to as many global classes as there are in the current 3-minute record
                For i = 1 to 2 channels
                        Initialize TemplateBuilder(k,i) to NewTemplate(i)
                        Initialize Residual (k,1) to Peel-off potential (i)
                        Cross-correlate the global class template k with Peel-off potential(i).
                        Find the lag value corresponding to the maximum of the
                        crosscorrelation function.
                        Store in BestLag.
                        Shift global class template potential k, –BestLag points.
                        Store –BestLag in TemplateShifts(k,i)
                        TemplateBuilder(k,i) =TemplateBuilder(k,i) + shifted global class
                        template k.
                        Residual (k,i)=Residual (k,i) – shifted global class template k.
                        Compute the correlation of shifted global class template k with Peel-off
                        potential (i) and store in correlations(k,i)
                End For
        End For
        Find the largest correlation within correlations(k,i) and save K and l as the location of the
        largest value.
        Peel-off Potential(l)=Residual(K,l)
        NewTemplate(l)=TemplateBuilder(K,l)
        Use the shifts from TemplateShifts(K,l) to shift global class K in the opposite channel
        and build NewTemplate(i).
        Peel-off potential (i), where l is the opposite class of l, = Peel-off potential(i)-
        NewTemplate
        Compute the correlation and Euclidean distances between the target potential in both
        channels, and NewTemplate(1) and NewTemplate(2)
        Save K in SuperpositionClassList
        IF n >=2
                IF the correlation in 1 channel is > 0.94 AND euclidean distance<0.5, while the
                other channel is >0.80 in correlation and <0.6 in Euclidean distance then,
                        Label the target potential as a superposition with the classification of
                        SuperpositionClassList
                Else
                        Continue, and try to add a 3rd global class to form a superposition
                End If
        End IF
End For
```

Figure 4.41 Pseudocode for dual channel superposition resolution. The algorithm for dual channel superposition resolution is shown here, with the variables in boldface. This procedure also attempts to find doublets, or superpositions involving the same global class. If no classification is found, the input potential is left unclassified. Variables in the pseudocode are in boldface.

When a second global class was used to build a superposition, the presence of doublets, or superpositions of the same class, were also checked. In order for a potential to be a doublet, each constituent potential involved in the doublet had to be spaced at least 3 ms (9 datapoints) apart. Doublets do not occur at spacings less than this.

Dual channel superposition resolution was limited to find a maximum of 3 constituent global classes within a superimposed potential. This was because any waveform can be constructed with a large number of template shapes and misclassifications could result.

If an unclassified potential still did not obtain a global class label after these comparisons and superposition resolution attempts, the same procedure is repeated after an attenuation window is applied to the unclassified potential. A Kaiser window with a beta value of 5 served as the attenuation window (Figure 4.42).

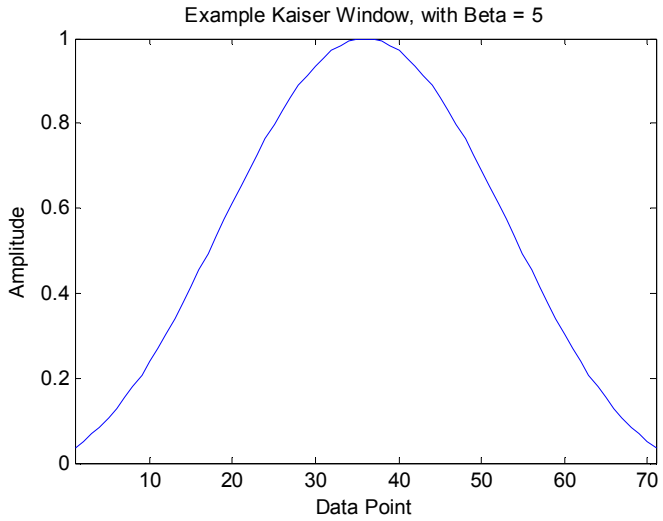

Figure 4.42 Kaiser window. A Kaiser window with a Beta value of 5 served as the attenuation window.

The beta value controls the width of the window. Larger values of beta made wider Kaiser windows and wider sidelobes. The attenuation window preserved the center of the potential while attenuating the potential edges by multiplication. The attenuation operation acts to increase the correlation and reduce the Euclidean distance measures in hopes of achieving a classification. This window was selected because it most optimally helped improve the classification when the algorithm performance was checked against a gold standard classification.

4.3.8 Periodic Motor Unit Classification

Although most of the motor units in these recordings fired erratically, those that fired periodically could be classified by using the inherent timing information in an additional classification stage. The periodic motor unit classification method defined ON regions for periodically firing classes in order to obtain a list of eligible classes that could be assigned to unclassified potentials. All unclassified potentials that occurred at appropriate times with respect to the periodically firing units were then attempted to be classified using less stringent distance thresholds.

The first step in the method was to find the regions in which each motor unit class was ON. The instantaneous frequency (equation 4.5) for a class is simply the frequency representation of the set of interpotential intervals, or the reciprocal of the time between the occurrences of each potential within the motor unit class.

$$IF_k = \{1/IPI_1, 1/IPI_2, \ldots 1/IPI_N\}^k \qquad (4.5)$$

In equation 4.5, IF_k is the instantaneous firing frequency for motor unit class k. IPI_1 is the interpotential interval, or the time in seconds between the first and second potentials in motor unit class k. IPI_N is the interpotential interval between the last pair of potentials in motor unit class k. Figure 4.43 shows a plot of interpotential interval versus its corresponding instantaneous firing frequency.

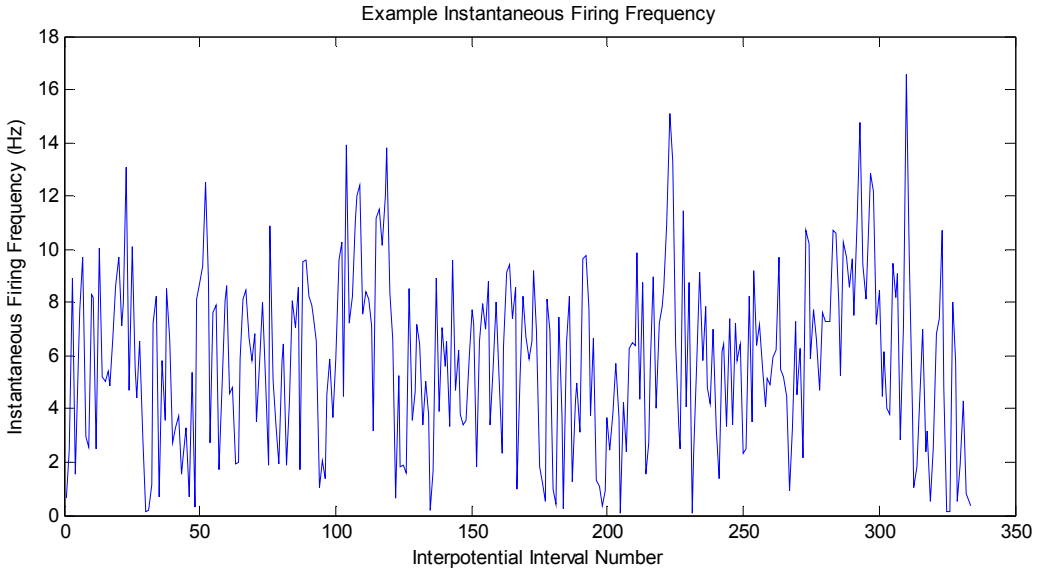

Figure 4.43 Example instantaneous firing frequency vs.interpotential interval number. The instantaneous firing frequency is plotted against the motor unit class potential number.

The ratio of the mean motor unit class firing rate to all of its instantaneous frequency values was utilized to define whether the motor unit class was periodic and determine ON regions (Figure 4.44).

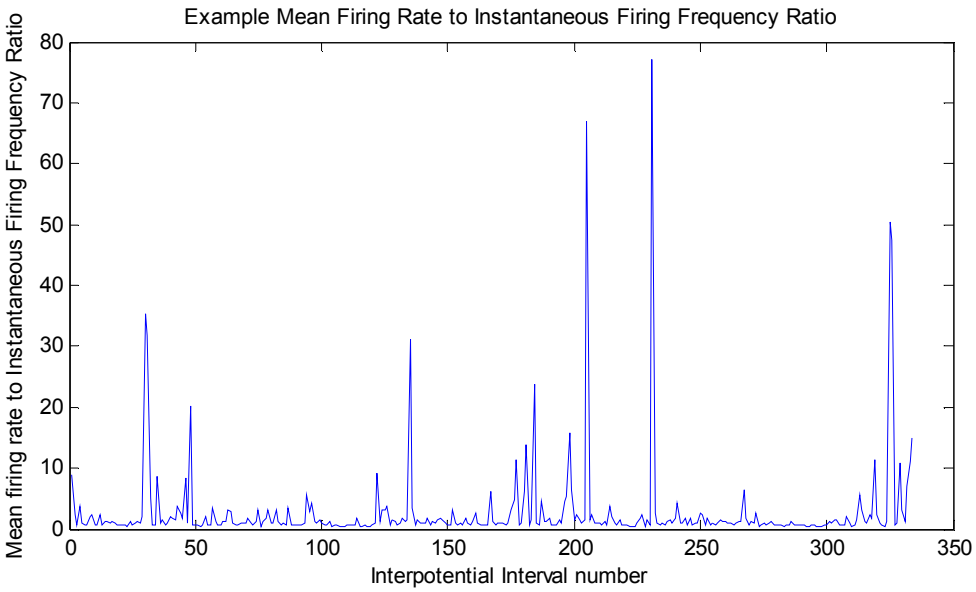

Figure 4.44 Mean firing rate to instantaneous firing frequency ratio.

In Figure 4.44, each point represents the mean firing rate for a motor unit class divided by its corresponding instantaneous frequency value. The periodically firing regions are those where the ratio values are closest to 1 and are easily seen in this representation. The large ratio values represent regions in which the periodic firing stops momentarily.

The mean of the ratio values was then calculated after all ratio values greater than 20 were removed. If this resulting ratio mean were less than 1.8, the motor unit class was considered to be periodic in the local 3-minute EMG portion. The ON regions within that 3-minute portion were defined to be the consecutive potentials whose mean firing rate-to-instantaneous firing frequency ratio values were less than 20. Figure 4.45 shows the instantaneous frequency plot with the ON regions for a motor unit class indicated by the dotted red lines.

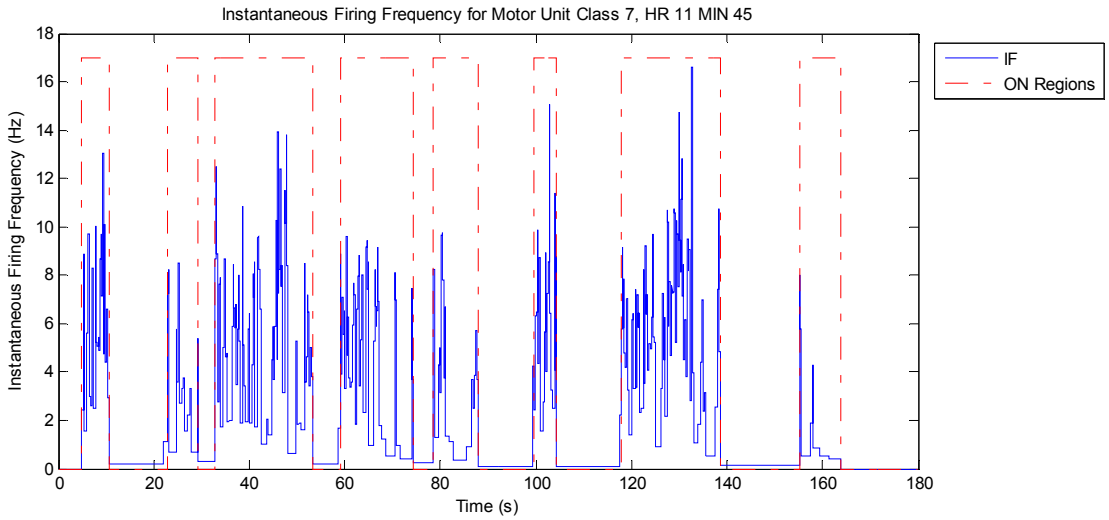

Figure 4.45 ON regions of periodically firing motor unit class. The blue trace is the instantaneous frequency of motor unit class 6 of the subject 1 recording for a 3 minute EMG segment. The dash-dotted red line indicates the ON regions for the motor unit class over the 3 minute segment.

The next stage of the periodic motor unit classification method determined which unclassified potentials were eligible for comparison with periodic motor unit class templates. An unclassified potential was eligible for comparison to a periodic motor unit class if it occurred when the corresponding instantaneous frequency value in that region (extended between the closest relative potentials in the periodic motor unit class) was less than 75 % of the mean firing frequency for that class (Figure 4.46).

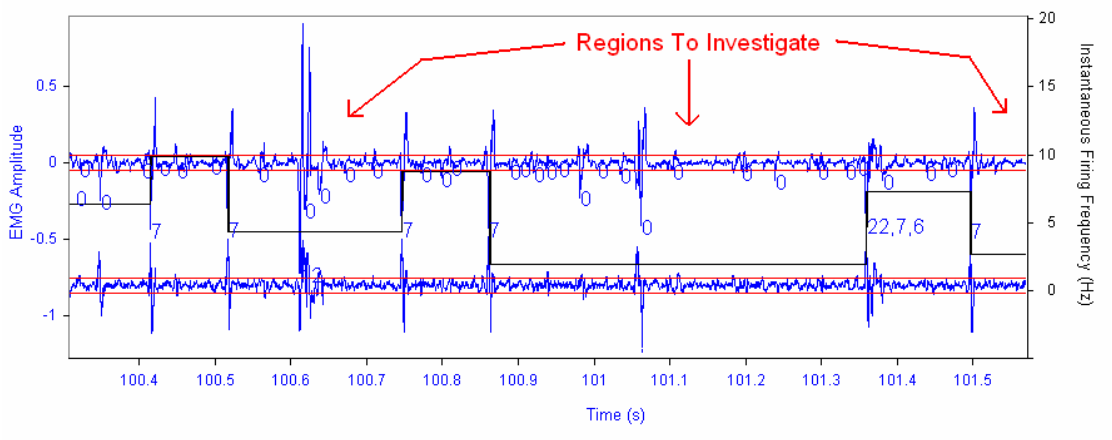

Figure 4.46 Attempting to classify unclassified potentials as a periodically firing motor unit class. The blue trace is EMG while the black trace is the instantaneous firing frequency whose units in Hz are indicated by the scale on the right. The EMG amplitude scale is on the left.

For example in Figure 4.46, class 7 was determined to fire periodically. The times in which the instantaneous firing frequency was less than 75 % of the mean firing rate (5.87 Hz in this case) are indicated by the red arrows on the figure. These are the regions where unclassified potentials (those labeled with a zero) are attempted to be classified as the periodic motor unit class.

If an unclassified potential was within a region where more than one motor unit class was ON, then superpositions were constructed using all eligible periodic motor unit classes. Correlation coefficients were computed between the target unclassified potential and all eligible classes and constructed superpositions.

Two conditions had to be met for a positive match. The correlation between the template potential in at least one channel with the unclassified potential had to be greater than 0.9. The two instantaneous frequency values created from classifying the target potential both had to be less than 1.75 times the mean firing frequency of the class assigned to the unclassified potential.

Chapter 5: Results

5.1 Segmentation Performance

The segmentation routine was evaluated by comparing the potentials that were segmented by the algorithm against those segmented by an expert in EMG recognition. Segmentation of five 3-minute sections from one 24-hour recording shows that 93.7% of the motor unit potentials (n=10,455) were correctly segmented and 6.3% of potentials were missed (n=699). Only 250 potentials were erroneously segmented (false positives; Figure 5.1)

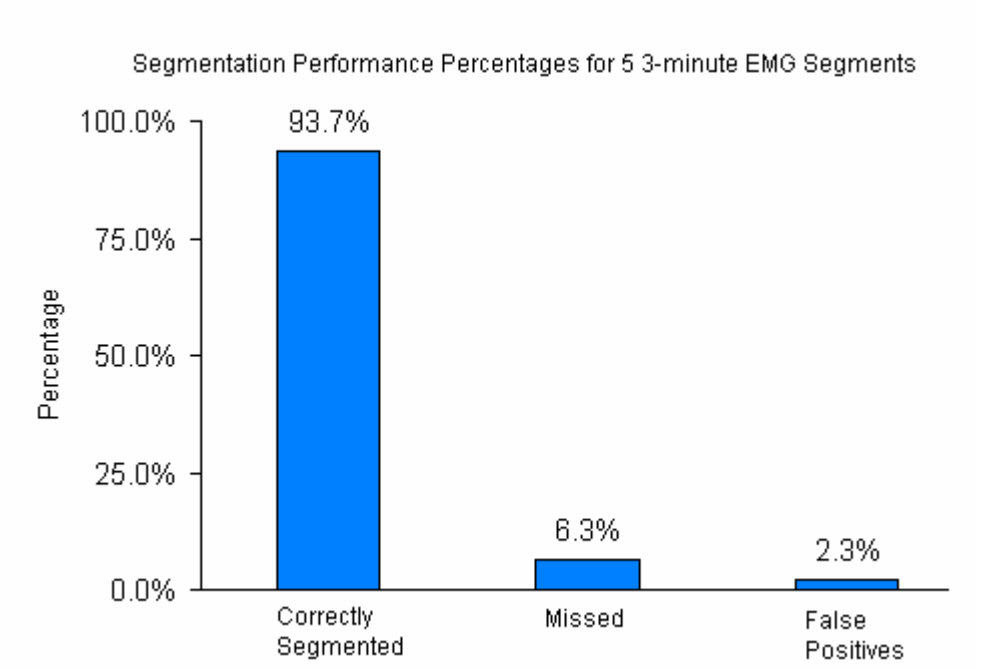

Figure 5.1 Segmentation performance percentages for 5 3-minute EMG portions. The percentages of correctly segmented, missed, and false positive potentials segmented are shown for 5 different 3-minute EMG segments for the subject 1 recording.

Figure 5.2 below shows an overlay of discernible potentials that were not segmented at all because they were eliminated by the frequency based noise elimination method.

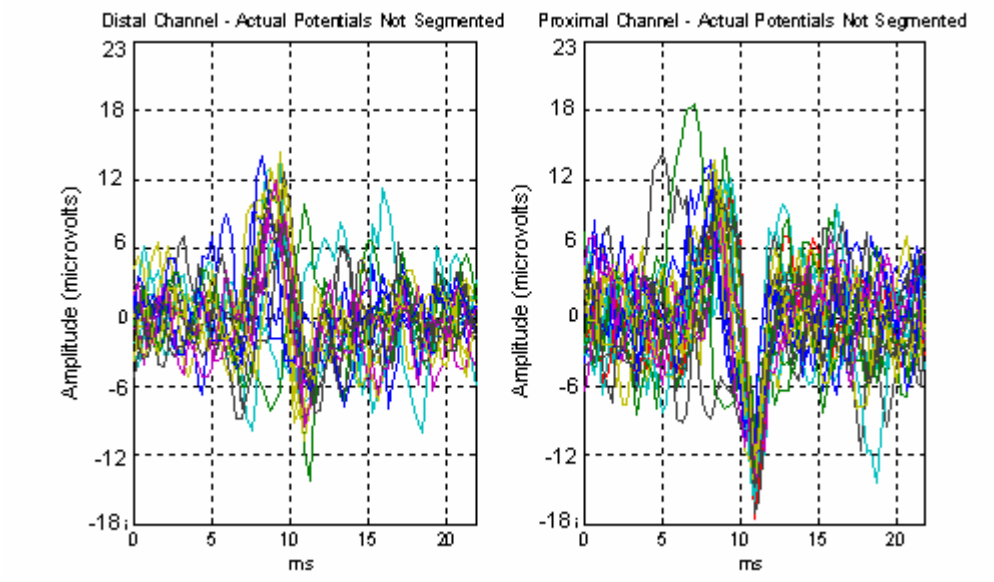

Figure 5.2 Overlays of motor unit potentials not segmented in 3-minute record HR 8 MIN 51 of the subject 1 recording after frequency based noise elimination was applied.

Even though these potentials were visible, their peak to peak amplitude was only 10 μV. They were largely within the baseline noise. With the current amplitude resolution these potentials could not be classified reliably by the algorithm or by an expert classifier.

To further examine the consequence of the noise thresholds on segmentation, the noise thresholds settings were lowered to segment all of the manually identified potentials. A reduced noise threshold increased the number of segmented potentials from 682 to 720, but the number of erroneous noise potentials increased from 40 to 641 (Table 5.1).

Table 5.1 Noise thresholds and noise segmented for 3-minute portion HR 8 MIN 51 of the subject 1 recording. The frequency based noise elimination thresholds were unchanged for the "original" setting (described in section 4.3.1.4). The "lowered thresholds" had the elimination thresholds set so that all 720 actual potentials would be found. The tradeoff for segmented all actual potentials is an increased number of noise potentials segmented. The "Lowered thresholds" setting segments almost as much noise as there are actual potentials.

Noise Threshold Setting	% Found	Actual Potentials Segmented	Actual Potentials Total	Actual Potentials Missed	Noise Potentials	FP % (Noise Potentials)
Original	94.7%	682	720	38	40	5.5%
Lowered thresholds	100.0%	720	720	0	641	47.1%

Thus, the 6% of the total potentials that was gained by lowering the noise elimination thresholds induced a 1600 % increase in the amount of noise segmented and there was almost as much noise as there were motor unit potentials. Given an expert could not manually classify the new potentials with confidence and the large increase in the noise that was segmented, we decided to leave the noise elimination thresholds at the original level to minimize noise segmentation.

5.2 Noise Elimination Procedure Based on Peak to Peak Value

The noise elimination thresholds for all four recordings changed little over the entire 24-hour recording (Figure 5.3).

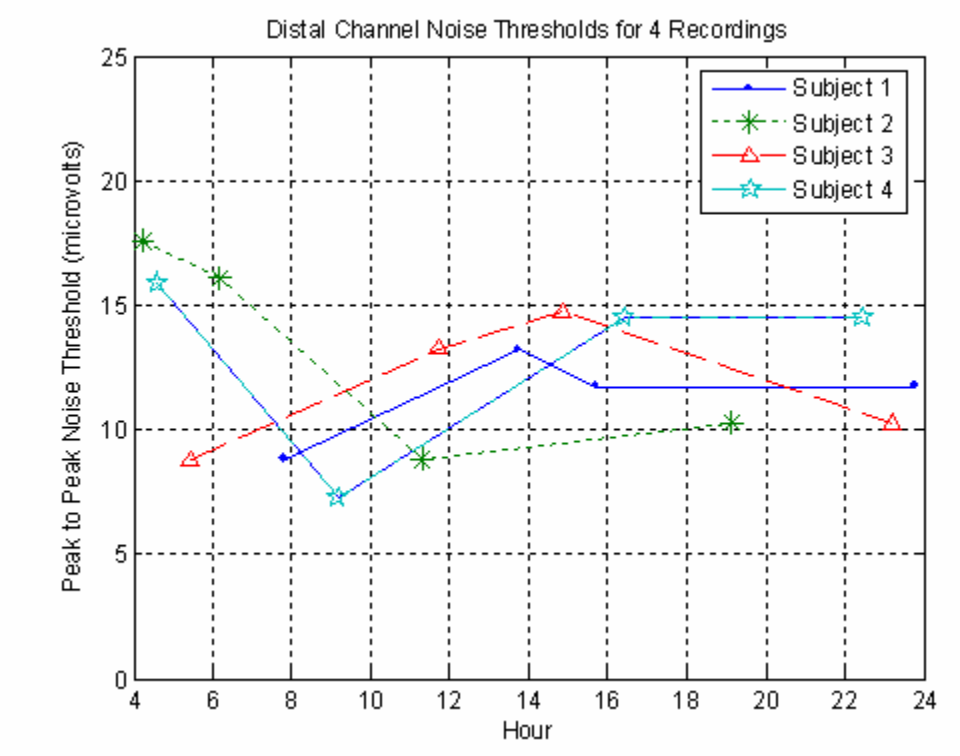

Figure 5.3 Distal channel noise elimination thresholds for four recordings. Noise elimination thresholds in microvolts in the distal channel were computed for four gold standard 3-minute EMG portions in each of four recordings. They were plotted against the time of the segment in which they occurred. These distal channel noise elimination thresholds for the subject 1, subject 2, and subject 3 recordings were on average 4, 3, and 3 microvolts less than that of the proximal channel. The threshold for the subject 4 recording was about 4 microvolts more than that of the proximal channel on average.

The noise elimination thresholds ranged from about 7 μV to17 μV. The distal channel noise elimination thresholds for the subject 1, subject 2, and subject 3 recordings were on average 4, 3, and 3 μV less than that of the proximal channel. The threshold for the subject 4 recording was about 4 μV more than that of the proximal channel on average. This illustrates that the proximal channel generally had more noise than the distal channel.

For all 4 subjects (16 manually classified 3-minute EMG portions), the number of potentials segmented ranged from 307 – 5385 (mean =2727, standard error = 360). Of these potentials, 1-4639 (mean 1102, standard error = 293) were eliminated based on the comparative peak to peak noise elimination method. The potentials that were eliminated were further categorized into those that were labeled as noise (0-3131, mean = 434, standard error = 208), labeled as unclassified (0-4637, mean =646, standard error = 227), or actually assigned a class (0-123, mean = 21.5, standard error = 7.7). Thus very few potentials that were assigned a class were actually eliminated, while much greater numbers of unclassifiable potentials were eliminated.

Figure 5.4 shows the percentage of segmented potentials eliminated per subject and the percentage of classified potentials that were eliminated (with respect to all eliminated potentials).

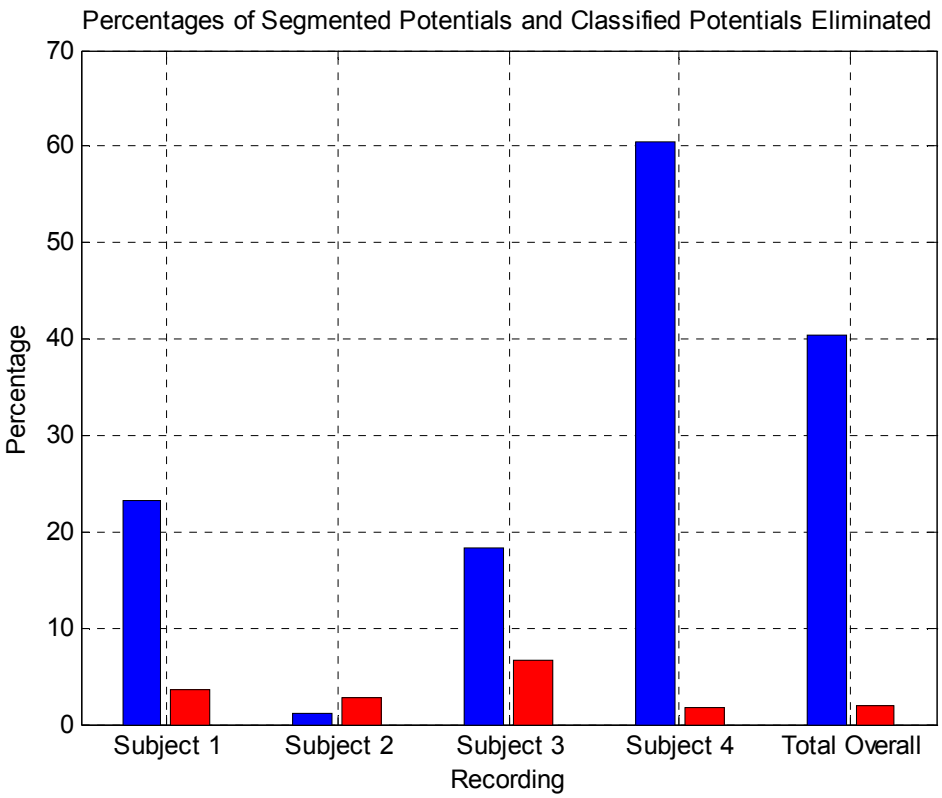

Figure 5.4 Percentages of potentials eliminated during the noise elimination routine. Results of potential elimination for 16 manually classified segments throughout the 4 recordings on a per recording basis. The percentages of segmented potentials that were eliminated per recording are shown in blue. The percentages of classified potentials that were eliminated with respect to all potentials eliminated are shown in red.

The mean and standard errors (mean, standard error) for the percentages of overall potentials eliminated for the subject 1, subject 2, subject 3, and subject 4 recordings were (23.3%, 7.1%), (1.4%, 1.1%), (17.5%, 6.8%), and (59.5%,16.3%), respectively. Similarly, the mean and standard errors (mean, standard error) for the percentages of classified potentials eliminated the subject 1, subject 2, subject 3, and subject 4 recordings were (2.5, 2.3%), (12.5%, 25%), (17.5%, 26.4%), and (4.1%,5.3%), respectively. The small percentages of classified potentials eliminated illustrate the success of the noise elimination routine based on comparative peak to peak value in eliminating very few

potentials that could actually be classified. Further, the classified potentials that were eliminated were not global classes.

5.3 Motor Unit classes Tracked Over 24-hours

Global classes, or the motor unit classes tracked over 24 hours, were found for each recording. Figure 5.5 shows the templates in both the distal and proximal channels that represent the global classes found for the subject 3 recording.

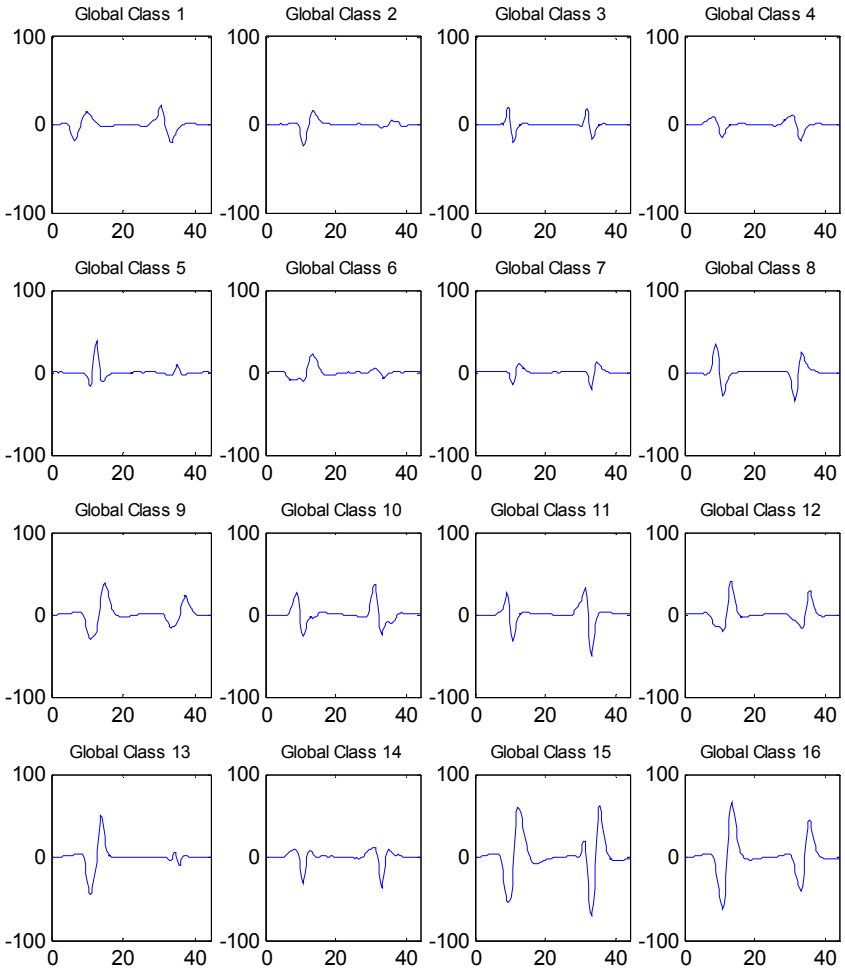

Figure 5.5 Global class templates found for the subject 3 recording. When transitive grouping was applied to the templates found in each of the 480 3-minute segments for the subject 3 recording, these 16 classes of potentials were found to be the most stable and commonly occurring. The left side of each pane shows distal channel templates while the right side shows proximal channel templates. Amplitude units are in microvolts on the y-axis and the time units on the x-axis are in milliseconds.

The templates varied in duration, polarity, amplitude and shape, thus providing many features to aid in classifying individual potentials. There were a total of 22, 7, and 8 global classes found for the subject 1, 2 and 4 recordings, respectively for a total of 53 global classes overall. Figure 5.6 shows a cumulative distribution for the peak to peak amplitudes for the templates of all global classes found and sorted in order of the distal template peak to peak values from least to greatest.

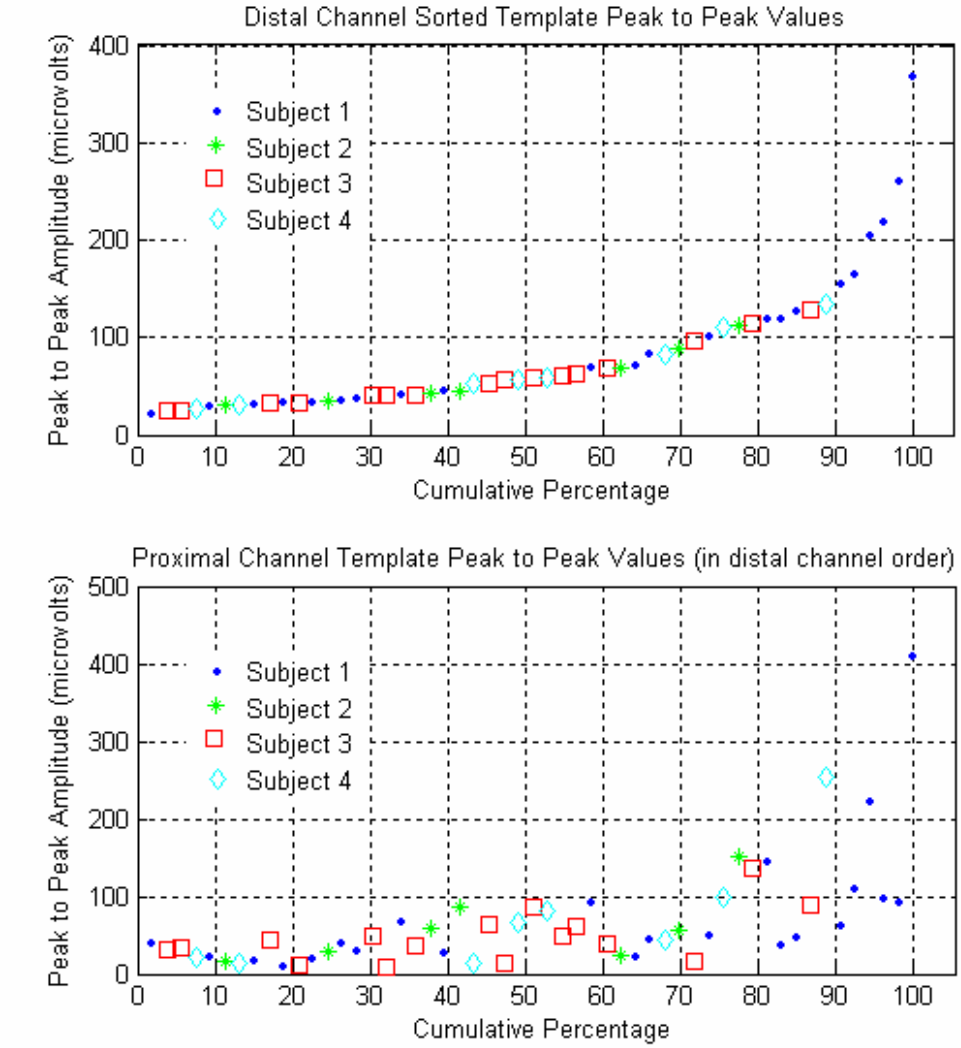

Figure 5.6 Sorted global class template peak to peak amplitudes. The peak to peak values of all global class templates were sorted from least to greatest according to the amplitudes of the distal channel's templates. The top pane shows the distal channel global class template amplitudes. The lower pane shows the peak to peak amplitudes of the proximal channel's global class amplitudes also sorted according to the amplitudes of the distal channel's templates.

The global class template peak to peak amplitudes varied from 22 to 368 μV (mean = 81 μV, standard error = 9 μV) in the distal channel and from 9 to 408 μV (mean = 66 μV, standard error = 10 μV) in the proximal channel. Global classes from each subject included both small and larger amplitude potentials suggesting that the algorithm was able to select a wide range of potentials for classification across recordings.

Figure 5.7 shows a similar plot of the signal to noise ratios for all global class templates. The peak to peak noise amplitudes were taken to be double the global thresholds computed at the end of the segmentation procedure.

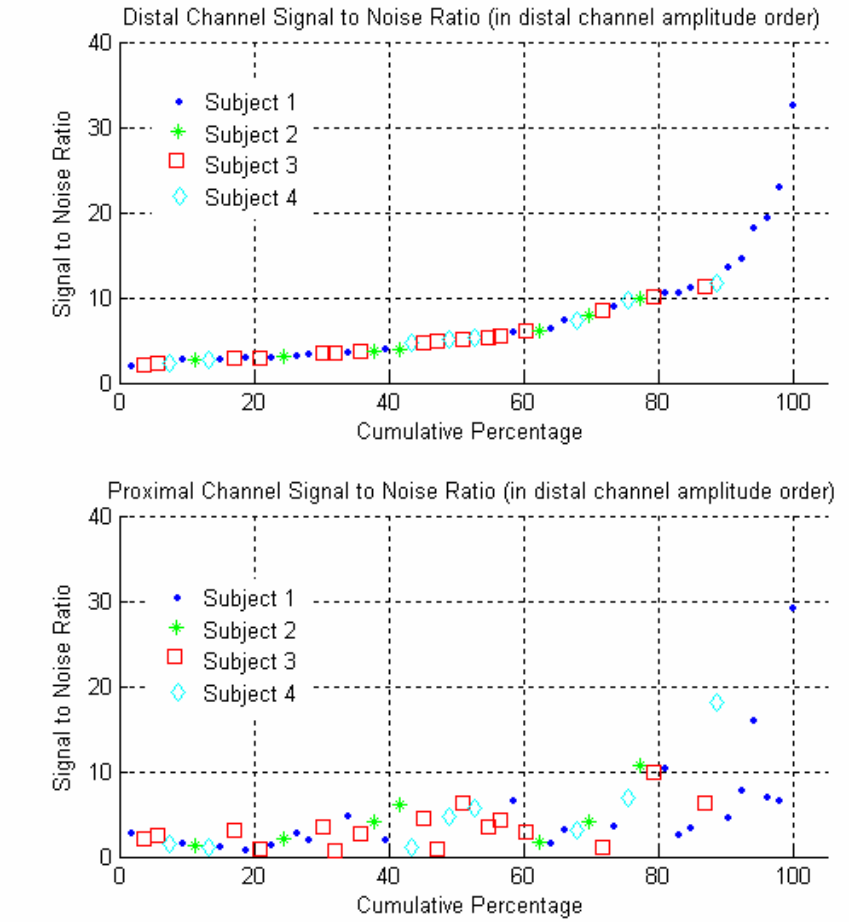

Figure 5.7 Sorted global class template signal to noise ratios. The signal to noise ratios of all global class templates were sorted from least to greatest according to the amplitudes of the distal channel's templates. The top pane shows the distal channel template signal to noise ratios. The lower pane shows the signal to noise ratios of the proximal channel's global class templates also sorted according to the amplitudes of the distal channel's templates.

Since the plots in Figure 5.7 are scaled versions of those in Figure 5.6, the baseline noise is similar across recordings. The global class signal to noise ratios varied from about 1.8 to 31.2 (mean = 6.9, standard error = 0.77) in the distal channel and from 0.64 to 31.6 (mean = 4.95, standard error = 0.73) in the proximal channel.

5.4 Classification Performances

An EMG expert classified 12 minutes of data from each 24-hour recording by using the GUI-based viewing tools described in section 4.3.5. Some global classes were only occasionally active so there is less confidence in their analysis. When there were less than 10 member potentials for a given global class in the 12 minutes of data, additional 3-minute records were analyzed to provide additional potentials belonging to those given global classes.

The classification performance was based on 5 parameters. The percentage correct was the percentage of manually classified potentials that were correctly labeled by the classification algorithm. The missed percentage was the percentage of the manually classified potentials that were left unclassified. The misclassified percentage is the percentage of potentials that were assigned an incorrect global class label, and the false positive percentage was the percent of potentials that were assigned a global class label when they instead should have been left unclassified. Finally, the percent accuracy for a given global class was the percentage of potentials that were correctly classified with respect to all potentials assigned that given global class label (equation 5.1).

$$\%Accuracy = \frac{N^c_{correct}}{(N^c_{correct} + N^c_{missed} + N^c_{Misclassified} + N^c_{FalsePositives})} \quad (5.1)$$

In equation 5.1 $N^c_{correct}$ is the number of correct classifications of potentials for a given class "c." N^c_{missed} is the number of classifications missed, $N^c_{Misclassified}$ is the number of misclassified potentials, and $N^c_{FalsePositives}$ is the number of false positives for that given class "c." Figure 5.8 shows a cumulative percentage plot of the percent correct, false positive percentage (FP %), percent misclassified, and percent accuracy.

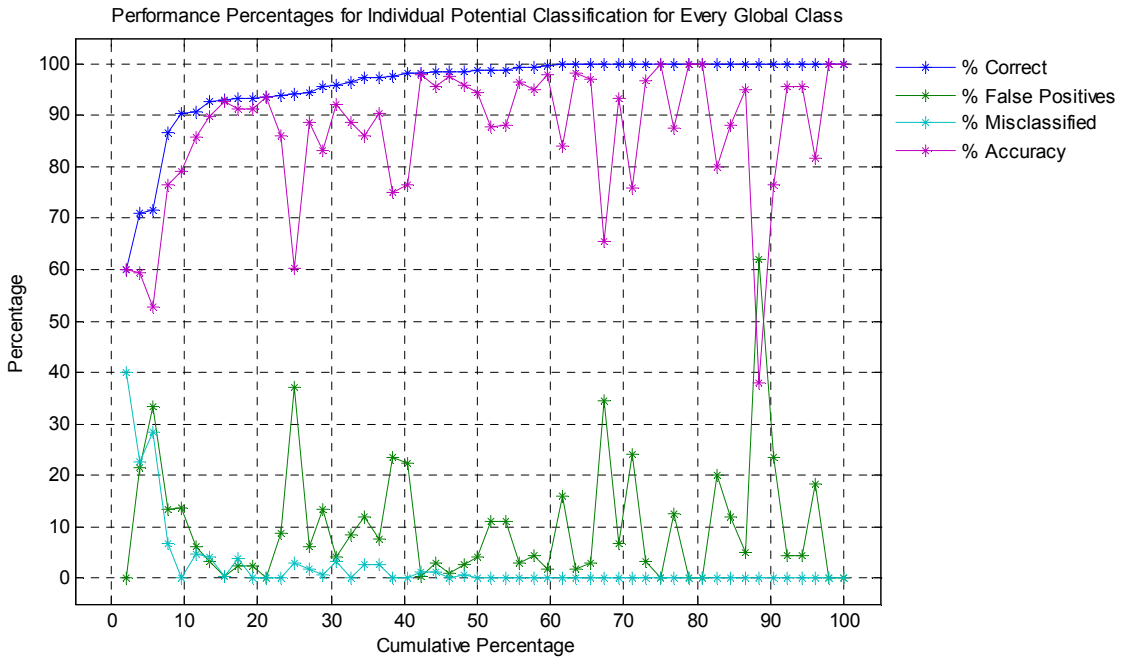

Figure 5.8 Sorted individual potential classification performances. The percentage correct for all global classes for all recordings were sorted then plotted. This order was then applied when plotting the false positive percentage, percent misclassified, and the percent accuracy.

Over all global classes for each recording, the percent correct ranged from 60.0 to 100.0% (mean = 96.0%, standard error = 1.1 %), the false positive percentage ranged from 0 to 61.9% (mean = 10.3%, standard error = 1.7%), the percentage

missed ranged from 0.0 to 10.5 % (mean = 1.8 %, standard error = 0.4 %), and the percentage misclassified ranged from 0.0 to 40.0 % (mean = 2.5 %, standard error = 1.0 %). The percent accuracy ranged from 38.1 to 100.0 % (mean = 86.4%, standard error = 1.9%).

Figure 5.8 shows that the accuracy is primarily determined by the false positive percentage. The percent correct was plotted against the false positive percentage in order to investigate their relationship (Figure 5.9).

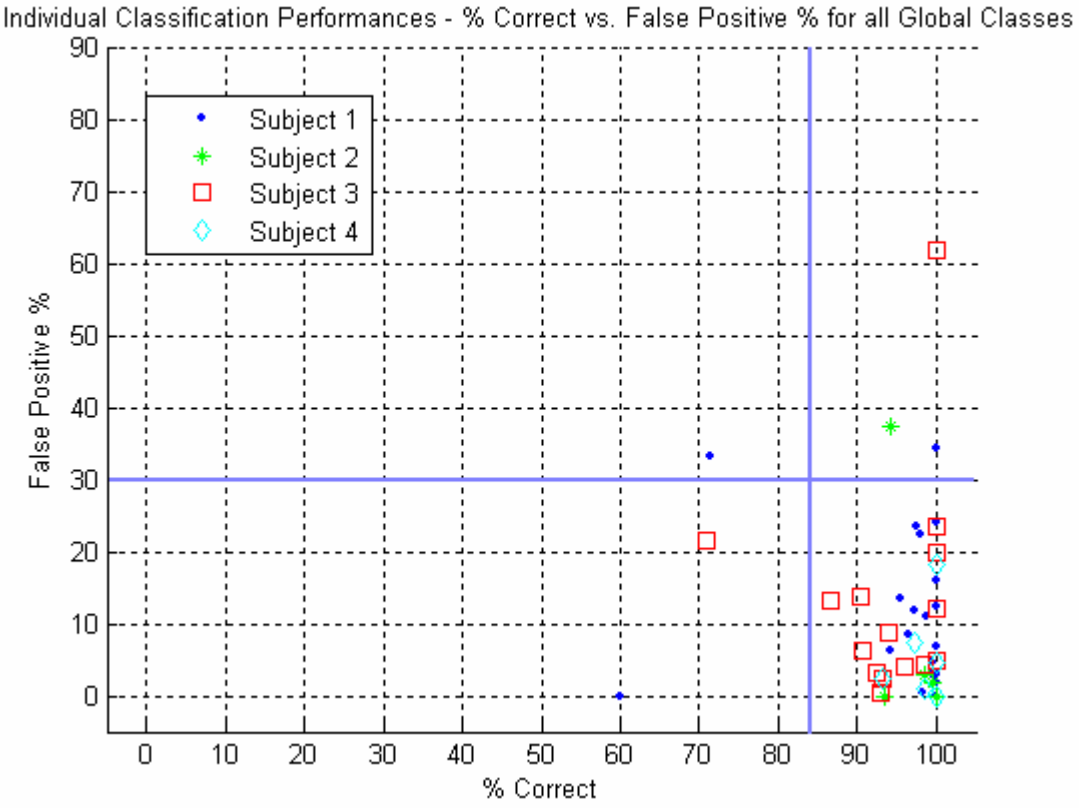

Figure 5.9 Individual potential classification performances of % correct versus false positive %. The % correct in individual classification performance was plotted against the false positive % for all global classes in all recordings. The lavender line divides the figure into 4 quadrants that represent low false positives with low percent correct, low false positives with high percent correct, high false positives with low percent correct, and high false positives with high percent correct. The dividing lines for these quadrants are 85 % correct and 30 % false positives.

Figure 5.9 was divided into 4 quadrants representing the possible combinations of low and high percent correct coupled with a low and high false positive percentage. The dividing lines for the quadrants were about 85% correct and 30% false positive. The individual classification performances for a majority of global classes across all recordings existed in the high percent correct, low false positive percent quadrant (47 out of 53 or 88.7 %). Only 1 individual class (1 out of 53, 1.9%) had a classification performance that fell into the low percent correct and high false positive percentage quadrant, but 2 fell into the low percent correct, low false positive percentage quadrant (2 out of 53, or 3.8 %). Finally, the high percent correct, high false positive percentage quadrant contained 3 individual classification performances (5 out of 53, or 5.7%).

Across all the recordings, the individual classification performances for the global classes were similar. Two performances for the global classes of the subject 3 recording fell outside the high percent correct, low false positive quadrant (2 out of 15, or 13.3 %). Only 3 global classes for the subject 1 recording (3 out of 23, or 13.0 %) and only 1 global class from the subject 2 recording (1 out of 8, or 12.5 %) fell outside the quadrant with the best performance. The performances of all 7 classes for subject 4 were within the high performance group. Overall, these results revealed that the automatic classification algorithm can classify more than 88 % of the global classes over all recordings with a performance of at least 85% correct with a false positive percentage of less than 30 %.

The signal to noise ratios of each global class template over all recordings were plotted against the percent accuracy of the individual classification performance (Figure 5.10).

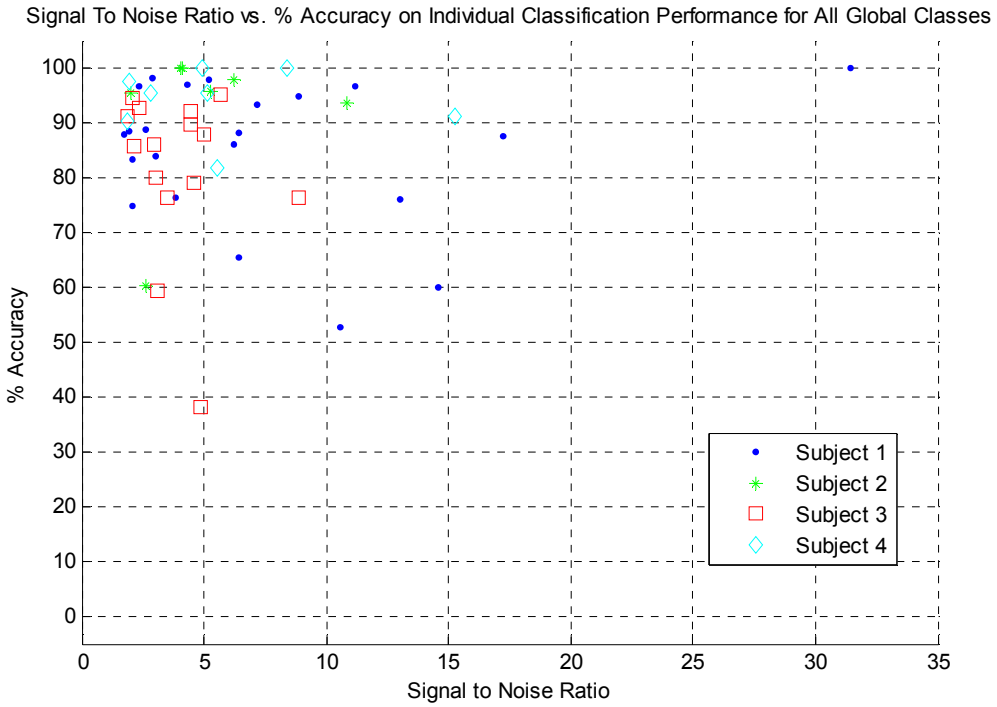

Figure 5.10 Signal to noise ratio vs % accuracy in individual potential classification performance. The signal to noise ratio for each global class template was plotted against its respective % accuracy in individual potential classification.

According to Figure 5.10, the signal to noise ratio has no obvious relationship to the percent accuracy. The accuracy seems to be independent of the signal to noise ratio for each recording

Potentials that are superpositions were more difficult for the automated classification to accurately classify. The percent accuracies were compared when superpositions were included in the performance calculation and when they were excluded (Figure 5.11).

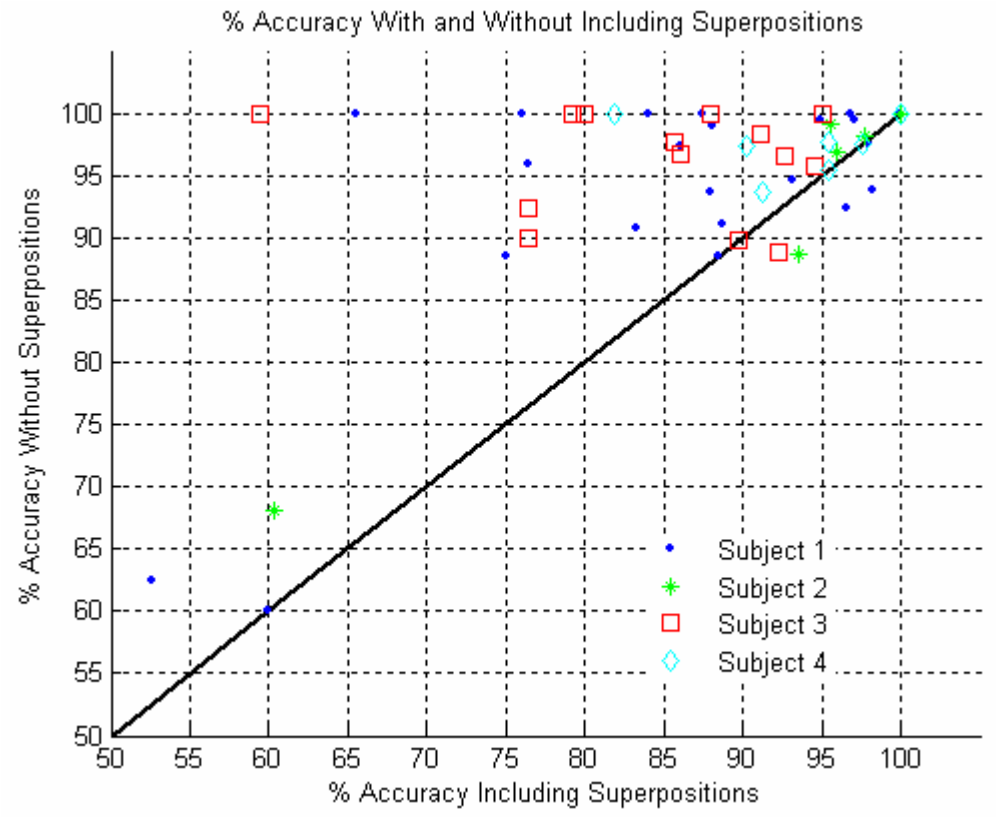

Figure 5.11 Percent accuracy including superpositions versus without superpositions. The % accuracies for each global class of each recording including superimposed potentials were plotted against the corresponding % accuracies excluding all superimposed potentials. The unity line (black line) was included for comparison.

In Figure 5.11, the upper half of the triangle (above the black unity line) represents the region in which the percent accuracies were greater with the superpositions excluded. The accuracies for almost all global classes were better when superpositions were excluded. Superpositions were harder to correctly classify, thus explaining the reduction in accuracy. Overall, the average reduction in accuracy when superpositions were included was 7.4%, ranging in-between -4.9% to 40.5% (standard error = 1.3%). In general, recordings with a higher number of global classes (Subjects 1 and 3), and thus the opportunity for more superpositions, showed greater increases in accuracy when superpositions were removed.

5.5 Global Class Tracking

The final output of the motor unit potential classification algorithm consisted of the times during which each was active. An ON time for a global class was defined to be a 3-minute region in which there was at least one member potential. Figure 5.12 below shows a graph of ON times for each globally tracked class in the subject 3 recording. Hour 0 is midnight to 1 am while hour 23 is from 11 pm to midnight. Subject 3 took no medications during the recording. The gray shaded regions indicate the times when the subject was sleeping. An expert manually labeled spasm regions in all four recordings and these regions were excluded from further analysis.

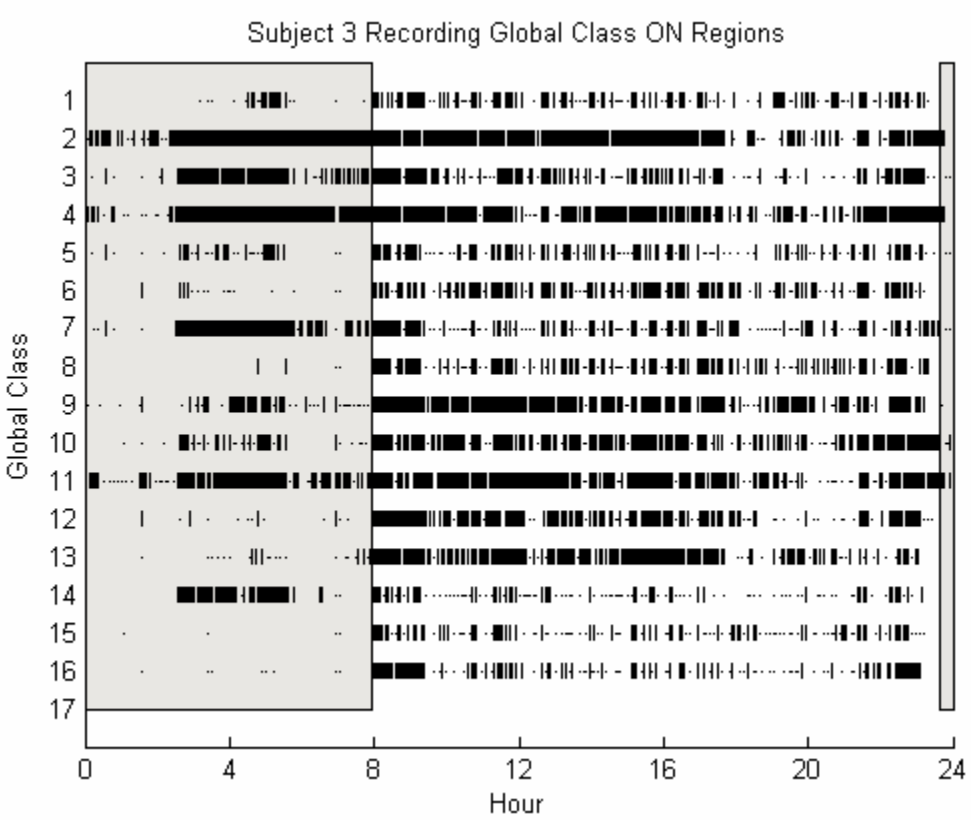

Figure 5.12 ON regions for the subject 3 recording. The classes are labeled on the y-axis while the time is labeled on the x-axis in hours. According to the timing standard, hour 0 is midnight to 1 am and hour 23 is 11 pm to midnight. A solid line represents an ON region for a particular class, or a 3 minute span of time when there is at least one firing of that motor unit. The absence of a solid line shows that that particular unit was OFF. Spasm times that were manually labeled by an expert classifier were removed before compiling this graph.

The global classes were labeled on the y-axis while the time in hours is labeled on the x-axis. A solid line for a class represents an ON region and the absence of a solid line indicates that a class was off. Dots in the figure signify ON regions that are approximately 3 minutes in length.

In the subject 3 recording, global classes 2, 4, and 11 were almost always active, where as global classes 1, 5, and 15 were sporadically active overall. About 7 global classes (1, 6, 8, 12, 13, 15, and 17) were primarily not active during sleep, but active during the time awake. Of these 7 global classes, two global classes (12 and 13) were constantly active during the time awake, while the remaining five global classes fired more sporadically during the time awake.

5.5.1 Motor Unit Template Uniting Stage 2

The first stage of the motor unit template uniting stage found the most stable, commonly occurring motor unit classes to form global classes (as described in section 4.3.6.1). This encompassed the clustering of all class templates local to 3-minute records and global class labels were assigned to these class templates. In the second stage, all unlabeled local class templates were attempted to be classified as global classes. The performances of the second stage over all global classes over all recordings were evaluated using a gold standard manually produced by an expert classifier using the GUI-based tools described in section 4.4.6.2.

The second stage of the motor unit template uniting stage can be viewed as a new classification problem, but this time local class templates over the entire

24 hours must be assigned a global class label. The percent correct, false positive percentages, misclassified percentages, and the percent accuracy have the same definitions as before, but this time with respect to the global classes found during stage one. The performance results of the second stage of the motor unit template uniting stage are shown in a cumulative distribution in Figure 5.13.

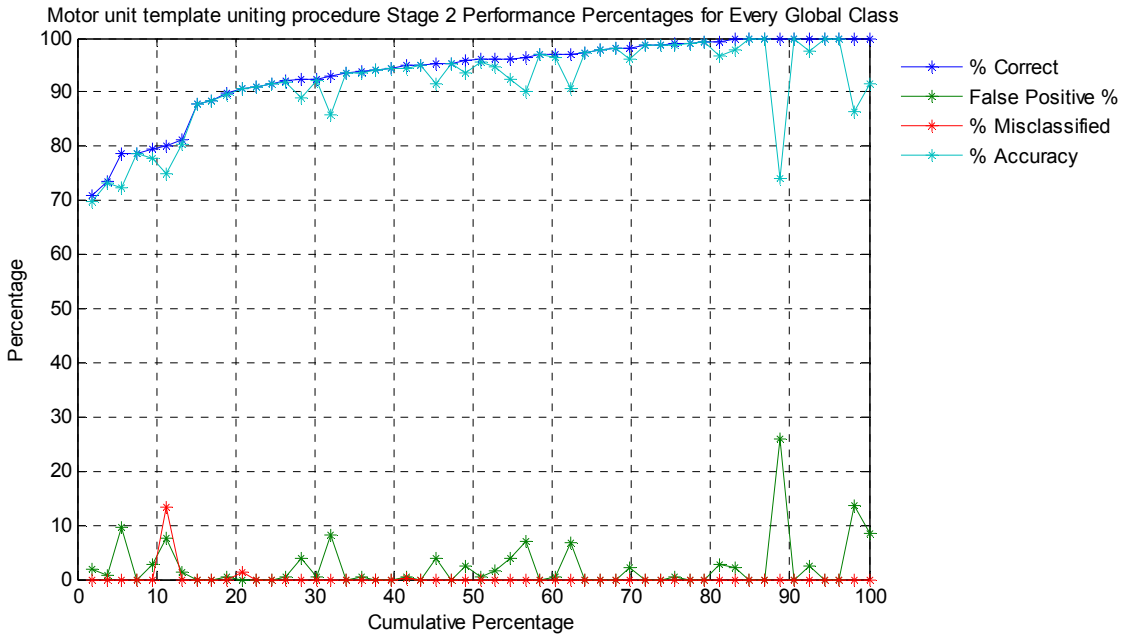

Figure 5.13 Motor unit template uniting procedure stage 2 performance percentages. The percentage correct for tracking all global classes in stage 2 of the motor unit template uniting procedure for all recordings were sorted then plotted. This order was then applied when plotting the false positive %, % misclassified, and the % accuracy.

The performances for the second stage of the motor unit template uniting procedure were outstanding. There were no tracking accuracies that were less than 69%, but there were 39 global classes out of 53 (73.6%) that had accuracies greater than 90%. The percentage correct ranged from 70.8 to 100% (mean = 93.6%, standard error = 1.0%), the false positive percentage ranged from 0 to 25.8% (mean = 2.3%, standard error = 0.62%), and the percent misclassified ranged from 0 to 13.3% (mean = 0.28%, standard error = 0.25%).

Finally, the percent accuracies ranged from 69.9 to 100% (mean = 91.6%, standard error = 1.1%).

Since the accuracy of the second stage of the motor unit template uniting procedure was primarily determined by the false positive percentage, the percent correct was plotted against the false positive percentage (Figure 5.14).

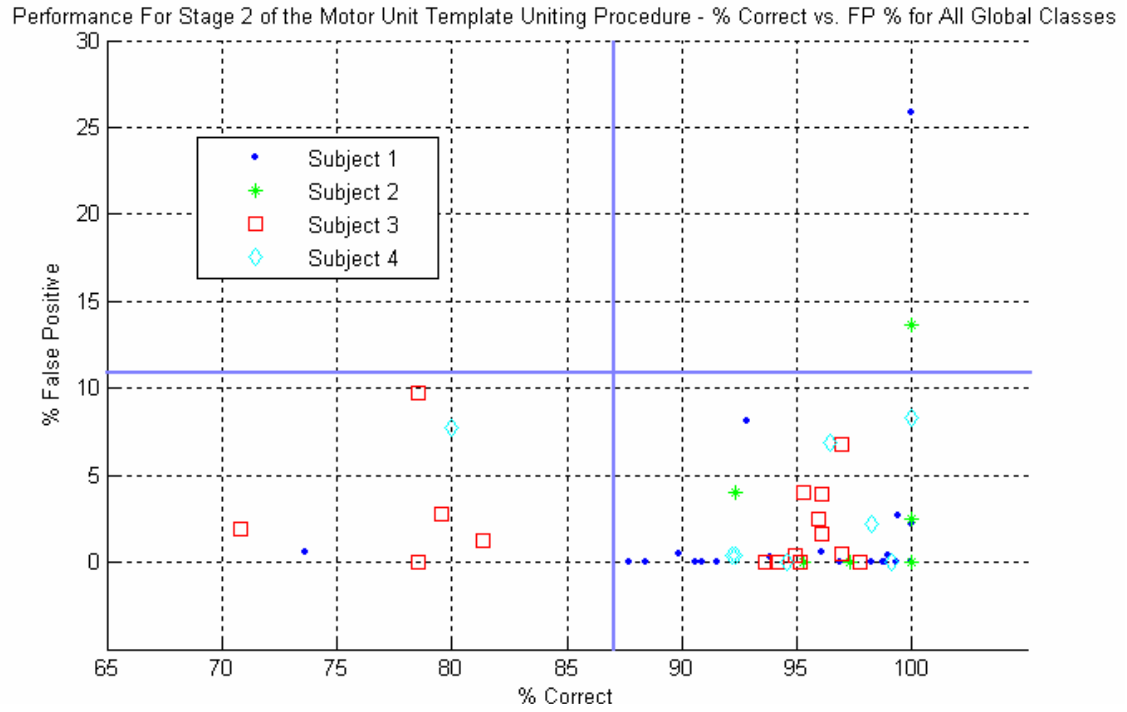

Figure 5.14 Motor unit template uniting procedure stage 2 performances of % correct versus false positive %. The % correct in tracking was plotted against the false positive % for all global classes in all recordings. The lavender line divides the figure into 4 quadrants that represent low false positives with low percent correct, lo false positives with high percent correct, high false positives with low percent correct, and high false positives with high percent correct. The dividing lines for these quadrants are 86 % correct and 11 % false positives.

Like Figure 5.8, Figure 5.14 was divided into four quadrants representing the four different combinations of high and low percent correct and high and low false positive percentages. The quadrant boundaries in this case were 86 % correct and 11% false positives. The performances for most of the global classes fall into the high percent correct, low false positive percentage quadrant (45 out of

53, or 84.9%). All but one of the global class performances for the subject 2 recording and all but two global class performances for the subject 1 recording were in this quadrant. There were only 2 global class performances that fell into the high percent correct, high false positive category (3.8%). The remaining global class performances fell into the low percent correct, low false positive category (6 out of 53, or 11.3%). Most global class performances in this quadrant were from the subject 3 recording. There were no global class performances in the low percent correct, high false positive quadrant. In summary, the global classes of the subject 1, 2, and 4 recordings achieved very good performances while almost a third of those of the subject 3 recording had a low percent correct coupled with low false positives.

The initial number of local templates classified as global classes after stage one of the motor unit template uniting procedure was compared to the overall accuracy in global class tracking (Figure 5.15).

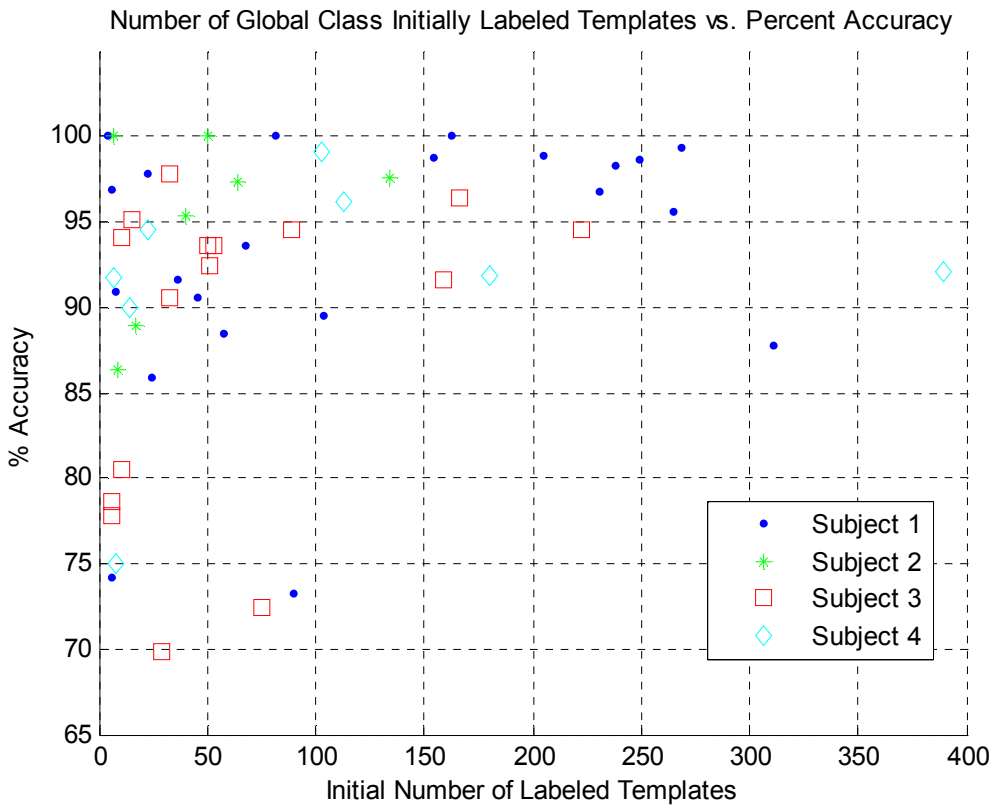

Figure 5.15 Number of global class templates versus the accuracy of stage 2 of the motor unit template uniting procedure. The total number of templates for each global class throughout the entire recording was plotted against the percent accuracy for the second stage of the motor unit template uniting procedure.

As described in section 4.3.6.2, a nearest neighbor procedure was utilized in conjunction with fuzzy membership values for individual potentials in order to classify local class templates as global classes. The global classes that have more local templates already assigned global class labels after the first stage of the motor unit template uniting procedure have more optimal nearest neighbors to be used in stage two. Thus, they have the ability to perform better. In other words, having more initially labeled local templates to use as representative global class templates, allows us to select nearest neighbor templates that occur closer in time to the local templates of a 3-minute record that we are trying to classify. We would expect those global classes that have a larger number of

labeled local templates to perform better, i.e. have a high accuracy. Figure 5.15 shows that this is not necessarily the case. In fact, there is no such relationship for any recording and the two parameters are largely independent. This suggests that the local templates are mostly stable over time and do not change appreciably to cause performances to decrease.

5.5.2 M-wave Results

M-waves were obtained from each subject both before and after each 24-hour recording for cross-subject data comparisons in addition to determining electrode stability. The M-waves were obtained for cross-subject comparison because the peak to peak values of each global class template can be normalized to the M-wave. The M-wave represents the maximal EMG response from the muscle being studied. Table 5.2 shows the M-waves obtained from each subject from each of the distal and proximal channels.

Table 5.2 M-wave amplitudes for all subjects. M-wave values were obtained for the thenar muscle in each channel both before and after each recording. The table also shows the mean peak to peak values between pre-recording and post-recording. The differences in amplitude between the pre-recording and post-recording values are expressed as a percentage of the pre-recording peak to peak value.

Recording	Distal PTP Val (mV) Pre-recording	Distal PTP Val (mV) Post-recording	Distal PTP Val Mean (mV)	Distal PTP Val % of Pre-recording	Proximal PTP Val (mV) Pre-recording	Proximal PTP Val (mV) Post-recording	Proximal PTP Val Mean (mV)	Proximal PTP Val % of Pre-recording
Subject 1	10.94	10.78	10.86	98.53	10.71	10.13	10.42	94.64
Subject 2	6.01	6.80	6.41	113.17	6.94	7.88	7.41	113.58
Subject 3	5.45	6.70	6.07	122.97	6.22	7.35	6.79	118.18
Subject 4	3.41	3.54	3.47	103.82	4.19	4.22	4.21	100.88

In theory, obtaining identical M-wave amplitudes before and after the recording should reveal that the recording electrodes did not move at all during the 24-hour recording. Table 5.2 shows that the M-wave amplitudes increased

from the pre-recording to post-recording values in all but one subject. The increases in M-wave amplitudes may stem from the fact that the properties of the recording electrodes change after 24 hours of use. Since the electrodes were taped into position with numerous wrappings, the electrode/skin interface may have become more conductive due to sweat and increased adherence of the electrodes to the skin. This increased conductance may have yielded the increased M-wave amplitudes.

5.5.3 Motor Unit Template Uniting Stage 3

While the second stage of the motor unit template uniting procedure performed most of the global class tracking, the third stage was also important. The third stage of the motor unit template uniting procedure found all global classes in each segment that were not found by either the first stage of the motor unit template uniting procedure or the clustering pass of the overall classification algorithm. It also combined any classes that were erroneously split. Splitting error means that a global class correctly had the correct members, but some members of that global class were incorrectly categorized as a class that was not tracked over the entire recording. Splitting error did not contribute negatively to the tracking accuracy, but did produce more missed potentials in the individual classification results.

The performances of the third and final stage over all global classes over all recordings were evaluated using a gold standard manually produced by an expert classifier using the GUI-based tools described in section 4.3.6.3. These

performances rated the ability of the classification algorithm to associate the correct individual member potentials with each global class at the 3-minute record level. The performance percentages have the same definitions as those in section 5.4. The performance results of the third stage of the motor unit template uniting stage are shown in a cumulative distribution in Figure 5.16.

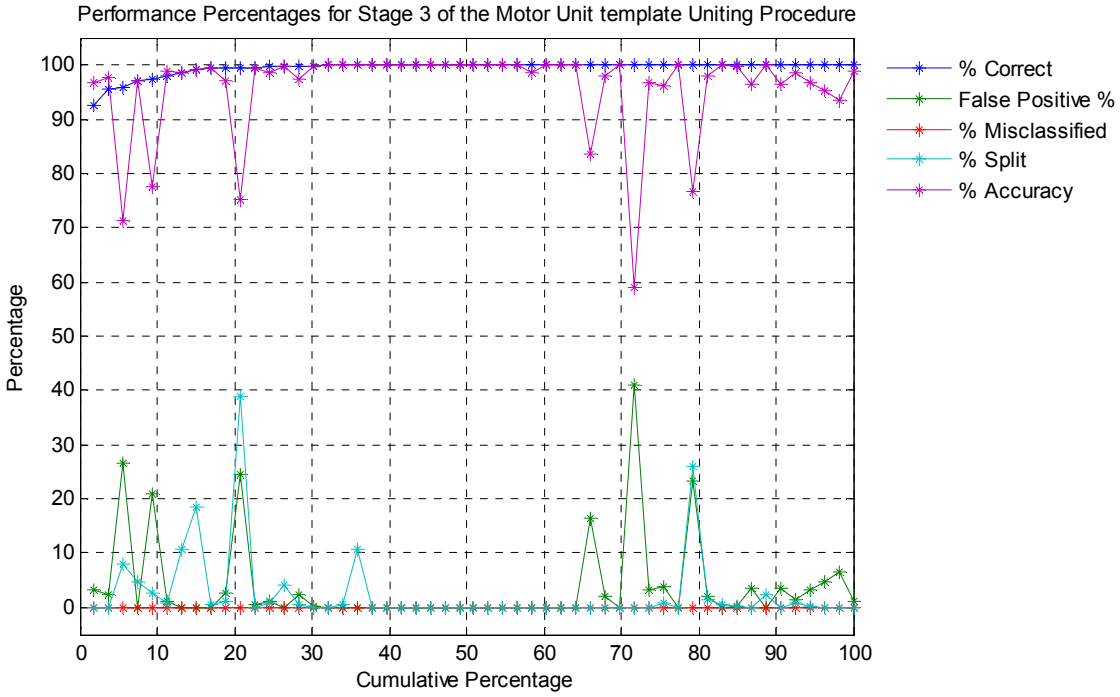

Figure 5.16 Motor unit template uniting procedure stage 3 performance percentages. The percentage correct for tracking all global classes in stage 3 of the motor unit template uniting procedure for all recordings were sorted then plotted. This order was then applied when plotting the false positive %, % misclassified, and the % accuracy.

The performances for the third stage of the motor unit template uniting procedure were outstanding. The percentages correct ranged from 92.7 to 100% (mean = 99.5%, standard error = 0.19%), the false positive percentages ranged from 0 to 40.9% (mean = 3.8%, standard error = 1.2%), the percent split ranged from 0 to 38.9% (mean = 2.6%, standard error = 0.96%), and the percent accuracy ranged from 59.0 to 100 % (mean = 96.0%, standard error =1.2%). There were no misclassifications. The false positive percentage was again responsible for

lowering the accuracy of the third stage of the motor unit template uniting procedure. The percentage correct was plotted against the false positive percentage for the third stage of the motor unit class uniting procedure (Figure 5.17).

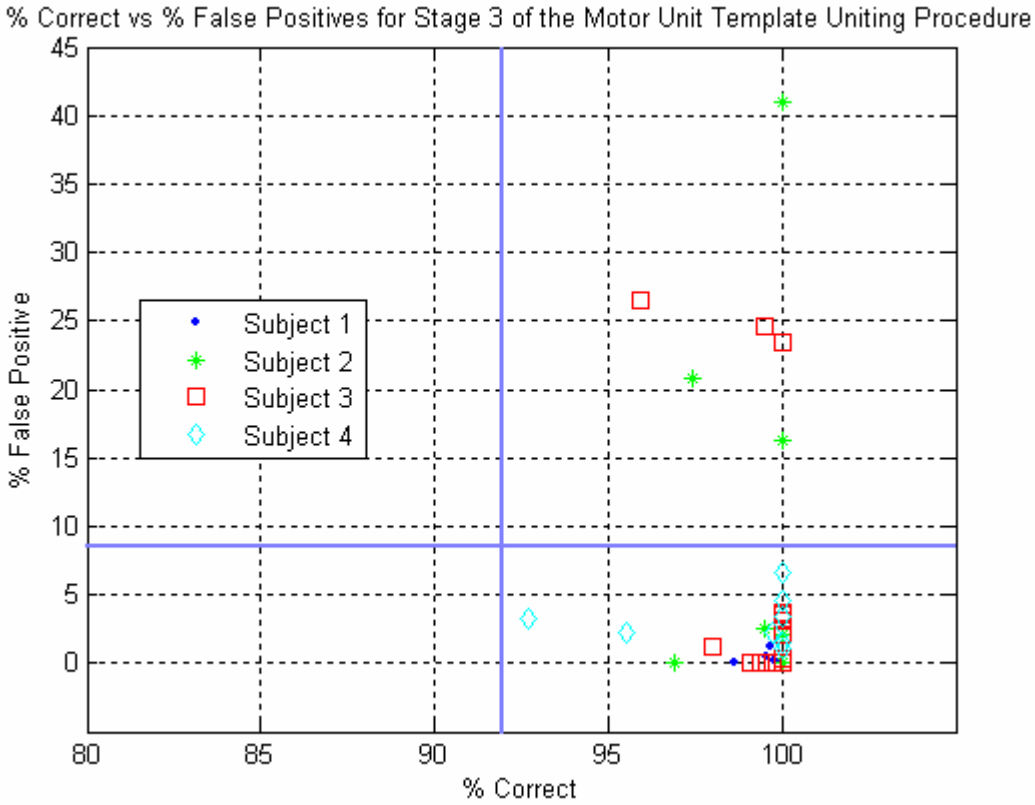

Figure 5.17 Motor unit template uniting procedure stage 3 performances of % correct versus false positive %. The % correct in tracking was plotted against the false positive % for all global classes in all recordings. The lavender line divides the figure into 4 quadrants that represent low false positives with low percent correct, lo false positives with high percent correct, high false positives with low percent correct, and high false positives with high percent correct. The dividing lines for these quadrants are 92 % correct and 9 % false positives.

The four quadrant method was similarly applied in this case. The dividing lines were drawn at approximately 92% correct and 9% false positives. The majority of global classes fell into the high percent correct, low false positive quadrant (47 out of 53, or 88.6%). The remaining global classes fell into the high percent correct, high false positive quadrant (6 out of 53, or 11.4%). All of the

percentages correct were very high and unrelated to the false positive percentage, much like stage 2 of the motor unit template uniting procedure.

Since the splitting percentage affects the percentage missed in individual classification, the percentage missed was plotted against the splitting percentage for all global classes in each recording (Figure 5.18).

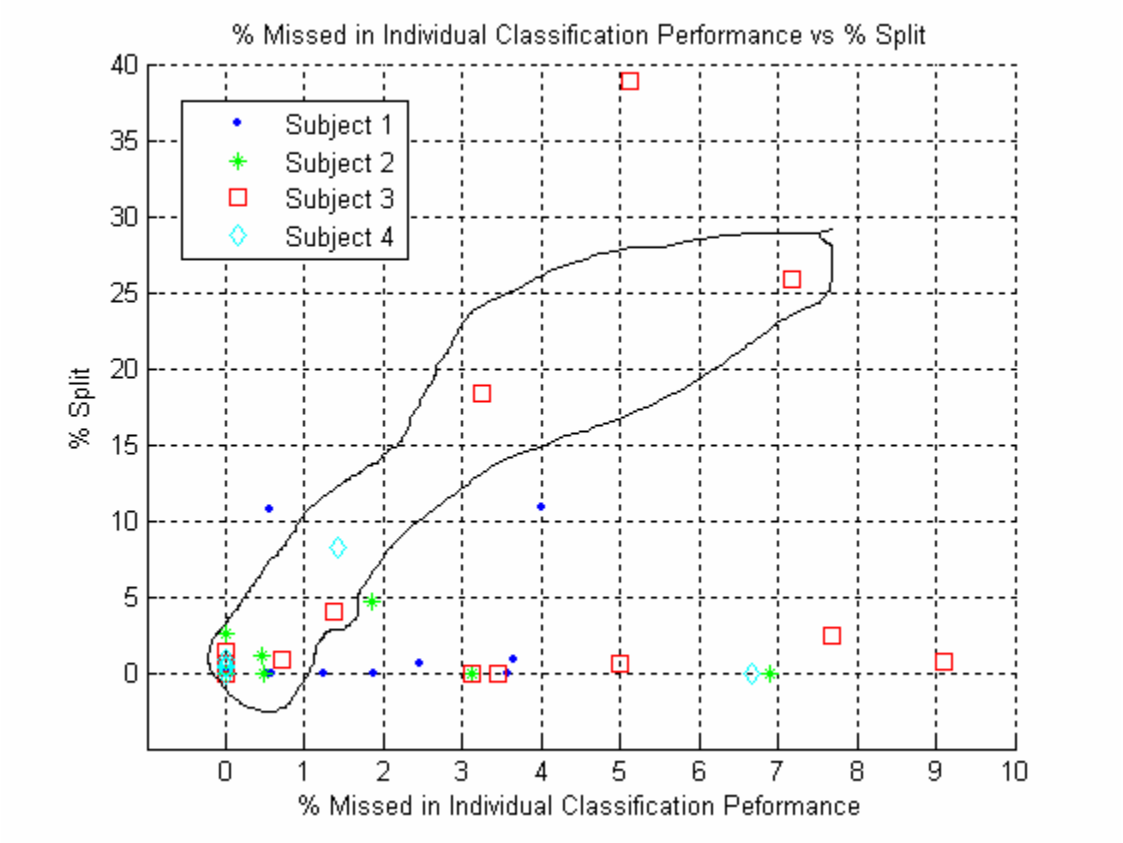

Figure 5.18 Percent missed in individual classification performance versus the splitting percentage. The percent missed in the individual classification performance was plotted against the splitting percentage. The splitting error represents potentials that are missed during the individual classification. The circled global class points of the subject 3 recording seem to demonstrate a directly proportional relationship.

Although there are no trends in Figure 5.18, several global classes in the subject 3 recording appear to form a directly proportional relationship between the percent missed and the percent split. A clearer relationship could be seen between the percent missed and the percent split if more 3-minute records were manually evaluated. Unfortunately, manually classifying more 3-minute records

is exceedingly time consuming, so it is not feasible to form a more comprehensive set of gold standards for performance evaluation.

5.6 Performance Comparison

The outcome measures for the classification algorithm were the performances for the individual potential classification, plus the two tracking performances. They were compared to see if the tracking measures impacted the classification performances. Figure 5.19 shows the individual classification percentage correct plotted against the percentage correct for the second stage of the motor unit template uniting procedure.

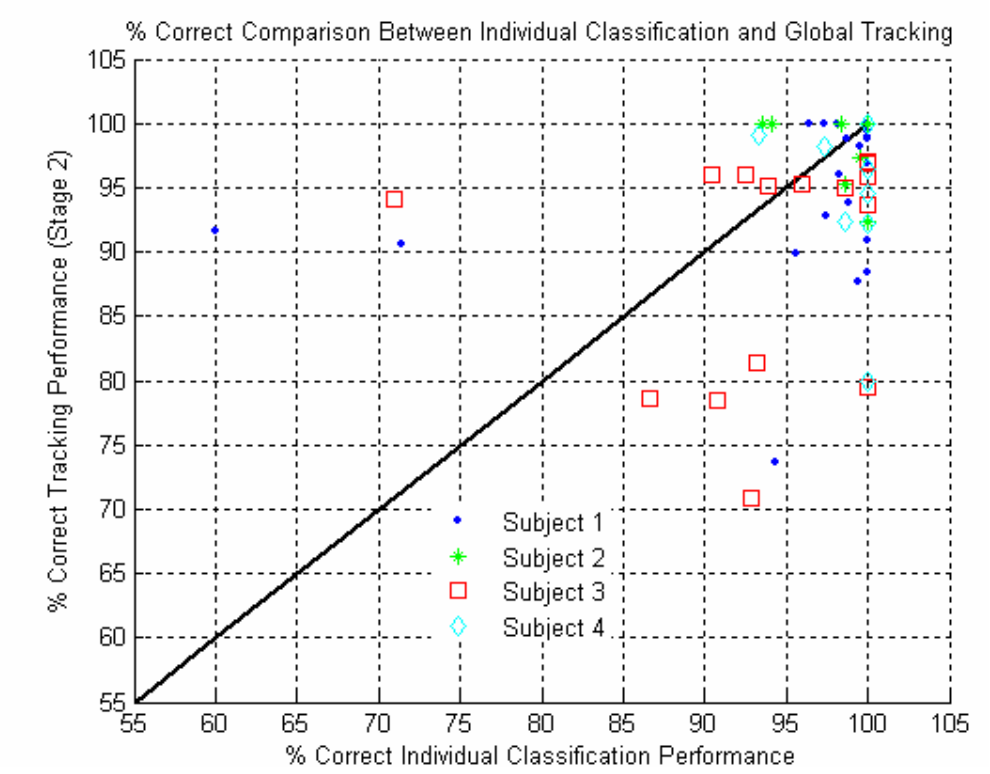

Figure 5.19 Percent correct comparison between individual classification and tracking (stage 2 of the motor unit template uniting procedure). The percent correct for the individual classification global class was plotted against the percent correct for each global classes tracking (stage 2 of the motor unit template uniting procedure. The unity line (black line) was included for comparison.

Most of the global classes lie below the unity line, indicating that the percentages correct for the individual classification performance are greater than their corresponding percentages correct with respect to tracking. This was especially the case for 7 classes where classification performance exceeded 85 % correct but tracking performance was less than 85 % correct. In contrast, tracking performance exceeded 90 % for another three classes whereas the correct classification was less than 75 %. These results suggest that it is not a requirement for a global class to be well tracked if it is to be well classified. This relationship is further explored by plotting the accuracy with respect to individual classification performance versus accuracy with respect to tracking (Figure 5.20).

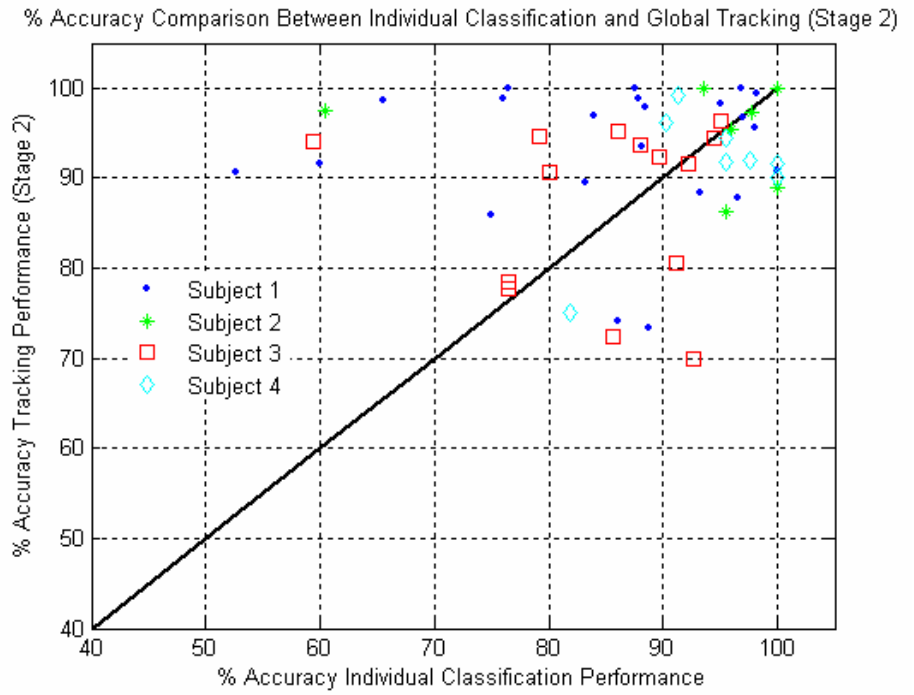

Figure 5.20 Percent accuracy comparison between individual classification and tracking (stage 2 of the motor unit template uniting procedure). The percent accuracy for the individual classification global class was plotted against the percent accuracy for each global classes tracking (stage 2 of the motor unit template uniting procedure. The unity line (black line) was included for comparison.

Figure 5.20 shows that most of the global class accuracies lie above the unity line, meaning that the tracking accuracies for the global classes are higher than

those of the individual classifications, with all having tracking accuracies greater than 70%. This reveals that all global classes were tracked accurately, but their classification accuracies were more variable and unrelated to the tracking accuracies. Global class tracking and the individual classification of the global classes seem to be independent.

False positives dominated the decline in accuracy, so the relationship of tracking accuracy and the false positive percentage was investigated (Figure 5.21).

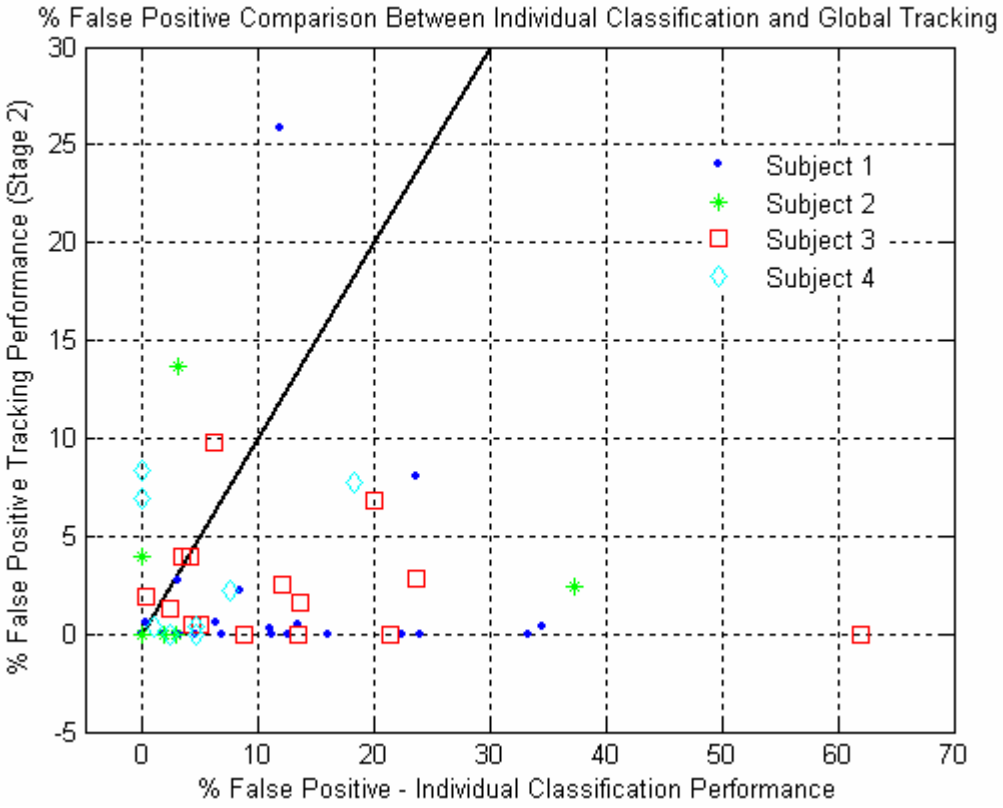

Figure 5.21 Percent false positive comparison between individual classification and tracking (stage 2 of the motor unit template uniting procedure). The percent false positives for the individual classification global class was plotted against the percent false positives for each global classes tracking (stage 2 of the motor unit template uniting procedure. The unity line (black line) was included for comparison.

The majority of global classes lie beneath the unity line in Figure 5.21, meaning that the false positive percentages for the individual classification performance are generally greater than the false positive percentages for global class tracking (approximately 8 out of 53, or 15.1%, had greater false positive percentage for global class tracking). This majority of global classes had less than 10% false positive percentages with respect to global class tracking, but wide ranging false positive percentages with respect to individual classification (0 to 62%). It seems that the false positives in individual classification are unrelated to the false positives in global class tracking. The factors that may contribute to these differences in false positives are addressed in the Discussion.

The individual classification performance was also compared to that of the tracking performance in stage 3 of the motor unit template uniting procedure. Figure 5.22 shows the percent accuracy of the individual classification performance plotted against the percent accuracy of the tracking performance of stage 3 of the motor unit template uniting procedure.

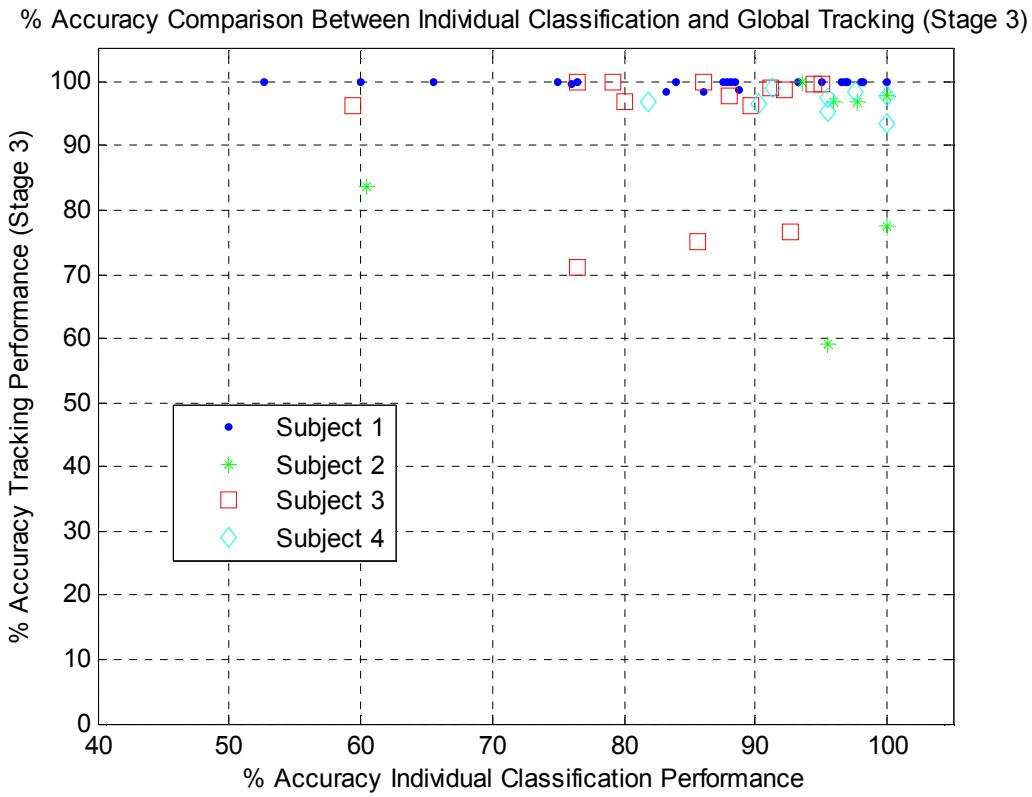

Figure 5.22 Percent accuracy comparison between individual classification and tracking (stage 3 of the motor unit template uniting procedure). The percent accuracy for the individual classification global class was plotted against the percent accuracy for each global classes tracking (stage 3 of the motor unit template uniting procedure).

The global classes were tracked in stage 3 with a high accuracy (47 out of 53, or 89%, performed better than 90% accuracy), where as the corresponding individual classification performance accuracies were more wide ranging (between 52 and 100 %). The percent accuracy for stage 3 seems to be completely unrelated to the percent accuracy of the individual classification performance. A similar comparison was made between the percent accuracies of stage 2 and stage 3 of the motor unit template uniting procedure (Figure 5.23).

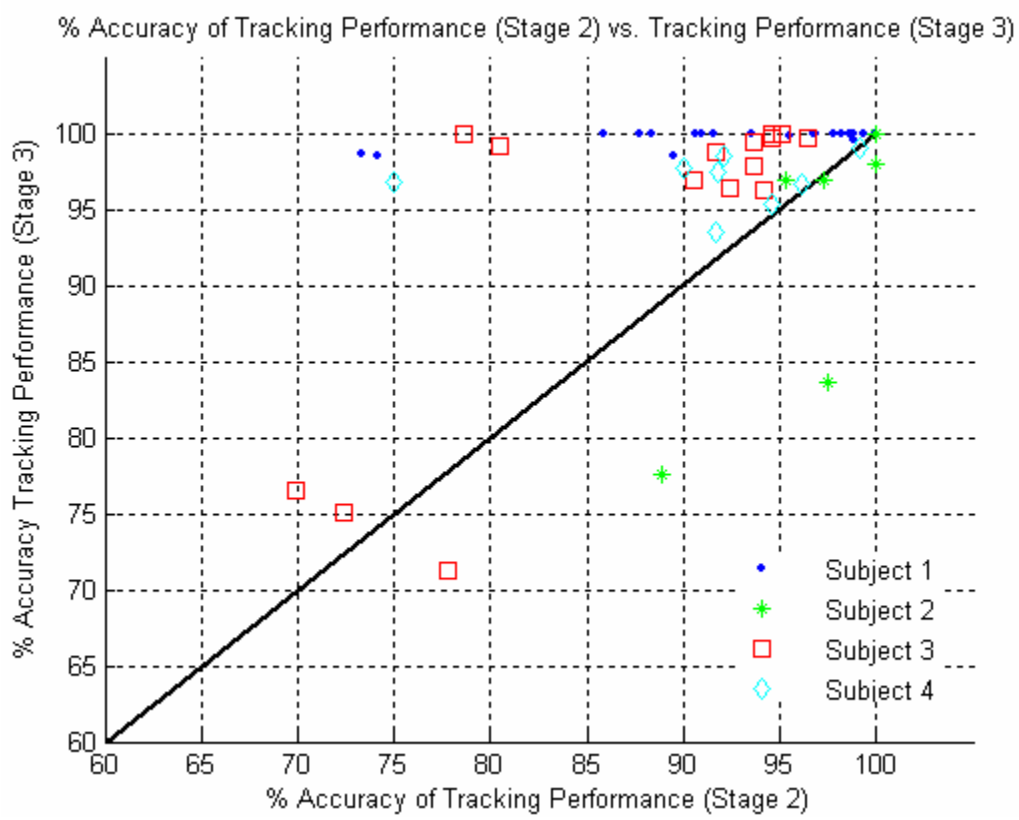

Figure 5.23 Percent accuracy comparison between the tracking performances of stages 2 and 3 of the motor unit template uniting procedure. The percent accuracy for the tracking performance of stage 2 was plotted against the percent accuracy for stage 3 of the motor unit template uniting procedure for each global class. The unity line (black line) was included for comparison.

Most of the data falls above the unity line indicating that the accuracy of the tracking performance was greater for stage 3 than for stage 2.

The numbers of firings for each global class for the entire recording were compared to the overall accuracies in tracking (Figure 5.24).

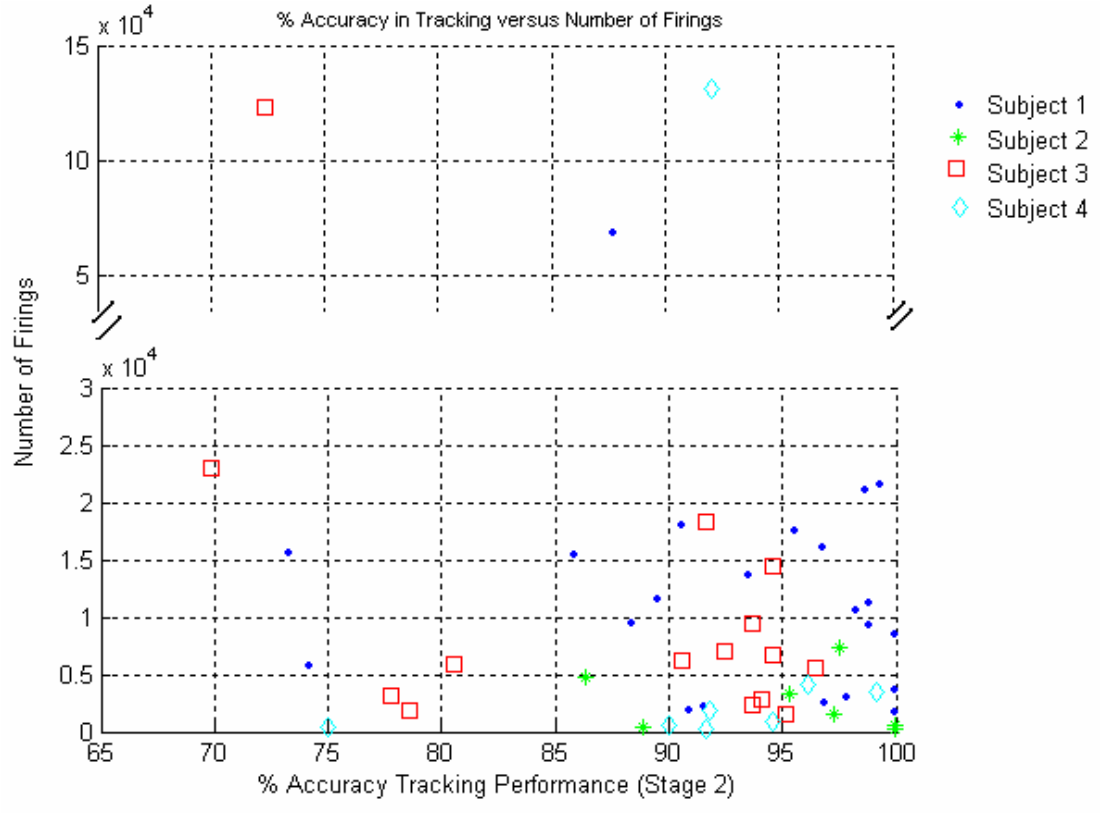

Figure 5.24 Percent false positive comparison between individual classification and tracking (stage 2 of the motor unit template uniting procedure). The percent false positives for the individual classification global class was plotted against the percent false positives for each global classes tracking (stage 2 of the motor unit template uniting procedure. The unity line (black line) was included for comparison.

We can theorize that those global classes with more firings should be more trackable. Since local templates were derived by averaging individual member potentials, having more member potentials should produce better representative local templates. Better local templates should make the trackability better. According to Figure 5.24, this relationship is not apparent. It seems that the trackability was not affected by the number of firings for each global class.

5.7 Performances Between Classifiers

A non-expert classifier and two expert classifiers derived gold standard classifications for individual potential classification. The gold standards for individual potential classifications of the non-expert classifier were evaluated with respect to those of one expert classifier for three of the four recordings over 23 global classes (Table 5.3).

Table 5.3 Evaluation of non-expert gold standards for individual potential classification with respect to those of an expert. Only three of the four recordings were compared for a total of 23 global classes.

Recording	Number of Global Classes Compared	% Correct	% FP	%Missed	%Misclassified	% Accuracy
Subject 2	6	77.6%	30.9%	17.4%	5.0%	63.7%
Subject 3	12	88.4%	56.0%	5.6%	6.0%	40.9%
Subject 4	5	96.4%	24.7%	1.6%	2.0%	73.6%
Total	23	87.5%	37.2%	8.2%	4.3%	59.4%

Overall, the non-expert's classifications agreed with those of the expert with a about a 59% accuracy.

The gold standards for individual potential classifications of the two expert classifiers were compared for 10 global classes from two recordings (Table 5.4).

Table 5.4 Comparison of two expert gold standards for individual potential classification over 10 global classes. Only 2 of the 4 recordings were compared.

Recording	Global Class	% Correct	% False Positives	%Missed	%Misclassified	% Accuracy
Subject 2	5	94.0%	1.6%	0.0%	6.0%	92.6%
Subject 2	6	92.9%	0.0%	7.1%	0.0%	92.9%
Subject 2	7	86.5%	4.0%	12.0%	1.6%	83.4%
Subject 3	1	57.1%	0.0%	28.6%	14.3%	57.1%
Subject 3	2	98.7%	3.6%	0.7%	0.7%	95.1%
Subject 3	3	84.0%	8.7%	4.0%	12.0%	77.8%
Subject 3	7	97.3%	1.1%	2.1%	0.6%	96.3%
Subject 3	8	66.7%	33.3%	33.3%	0.0%	50.0%
Subject 3	10	72.7%	20.0%	27.3%	0.0%	61.5%
Subject 3	11	88.3%	6.8%	7.8%	3.9%	82.9%
-	Total	83.8%	7.9%	12.3%	3.9%	79.0%

On average, the 2 classifiers agreed on classification 79% of the time. For three of these classes, only 4, 7 and 13 potentials were examined and agreement was low for these classes (50%, 57% and 62%, respectively). When these infrequently firing classes were excluded, classification agreement increased to 89 %, on average (n=7 classes).

Tables 5.2 and 5.3 shows that when using the software classification tools to manually classify individual portions of EMG, all users can produce different results. The degree to which the manual results differ can depend on the expertise of the classifiers. The expert classifiers agree within 79% accuracy, while the agreement of the non-expert classifier when compared to an expert classifier was substantially less (about 59%).

Since two experts were able to classify individual potentials at an accuracy of 79%, an automatic classification algorithm should be expected to perform just as well. In the case of the automatic classification algorithm described here, individual potentials are classified with an accuracy of better than 79% for 49 of 53 global classes (92.5%). After performing intra-class correlation statistical tests, it was found that the performance differences between expert raters were not significantly different. It was also found that the performance differences between an expert rater and the algorithm were not significantly different as well. Thus, the hypothesis that automatic (software-based) classification of motor unit potentials is as accurate as manual (user-based) analysis of motor unit potentials was met.

The non-expert classifier and one expert classifier also derived gold standards for global class tracking (both stage 2 and 3 of the motor unit template uniting procedure). The outcome evaluation of the non-expert's performance at tracking during stage 2 of the motor unit template uniting procedure with respect to that of an expert was even better for classification of individual potentials (Table 5.5).

Table 5.5 Comparison of non-expert gold standards for global class tracking (stage 2 of the motor unit template uniting procedure) to those of an expert. A total of 31 global classes over 4 recordings were compared.

Recording	Number of Global Classes Compared	% correct	% False Positives	% Misclassified	% Accuracy
Subject 1	17	92.6%	9.0%	7.4%	85.2%
Subject 2	4	93.5%	2.4%	6.5%	91.4%
Subject 3	8	95.4%	5.1%	3.1%	92.1%
Subject 4	2	98.5%	0.0%	1.5%	98.5%
Total	31	95.0%	4.1%	4.6%	91.8%

The evaluations in Table 5.5 were computed by checking which global classes were present in which 3-minute EMG portions in the second stage of the motor unit template uniting procedure of both the gold standards of the non-expert and the expert. Both gold standards agree with 92% accuracy and 95% correct.

The gold standard tracking results for stage 3 of the motor unit template uniting procedure were compared between those of the non-expert and those of the expert (Table 5.6).

Table 5.6 Comparison of non-expert gold standards for global class tracking (stage 3 of the motor unit template uniting procedure) to those of an expert.

Recording	Non Expert Results				Expert Results			
	% Correct	%FP	%Missed	% Accuracy	% Correct	%FP	%Missed	% Accuracy
Subject 1	99.6%	3.0%	0.4%	96.7%	94.4%	0.8%	5.9%	93.4%
Subject 2	99.7%	8.7%	0.3%	91.7%	99.5%	5.8%	0.4%	94.2%
Subject 3	98.2%	7.5%	1.8%	91.3%	99.5%	5.8%	0.4%	94.2%
Subject 4	100.0%	10.8%	0.0%	90.3%	94.1%	1.0%	6.1%	93.0%
Total	99.4%	7.5%	0.6%	92.5%	93.5%	1.4%	6.9%	91.8%

These gold standard results are similar, with both the non-expert and expert achieving tracking performances with accuracies of 92%.

5.8 Processing and Manual Classification Times

The automated EMG classification program required about two weeks on average to process a 24-hour recording, but manual classification times were much longer. Table 5.7 shows the approximate execution times for each stage of the automated EMG classification program (including the stages that must be manually accomplished by a human operator) on a 2.8 GHz Intel processor based machine.

Table 5.7 Automated EMG classification program approximate execution times. The approximate execution times for each stage plus the entire execution time of the entire algorithm on a 2.8 GHz Intel processor based machine are listed below. These times are compared with those required to manually accomplish the same amount of processing.

Stage	Program Execution Time	Time To Manually Complete (12 minutes of EMG)	Time to Manually Complete 24 hours of Processing (Extrapolated)
Segmentation	5 Hours	5 days	2.5 Years
Clustering	1 Day		
Template Matching	30 minutes	-	30 minutes
Manual Tracking Verification	10 Days	-	10 Days
Final Unsorted Analysis	5 Days		-
TOTAL	*~ 19 days*	5 days	>2.53 years

Table 5.2 also shows the time required for an expert to manually classify a recording with the help of the classification algorithm. It took an expert a complete 40 hour week to manually classify 12 minutes of EMG. If extrapolated to the entire 24-hour recording, the time required skyrockets to about 2 and a half years. This extraordinary amount of time makes the manual classification of an entire 24-hour recording virtually impossible. The proportion of time spent processing data (99 % for algorithm analysis, 1 % for manual analysis) versus human intervention time (1 % for the algorithm and 99 % for manual analysis) also differs significantly ($p<0.001$, Chi square test). Thus, the hypothesis that the automatic (software-based) classification of motor unit potentials is faster than manual (user-based) analysis of motor unit potentials was met.

5.9 Involuntary Motor Unit Behavior

To illustrate some of the biological importance of developing an algorithm to classify long term EMG recordings at the motor unit level, examples of motor unit firing behavior will be given, including the common motor unit firing patterns, the potential relationship between the global class excitability and size, how motor unit activity changes during awake and sleep time, and possible effects of anti-spasm medication.

There were two main types of firing behavior during the 24-hour recordings – tonic and sporadic (Figures 5.25 and 5.26, respectively).

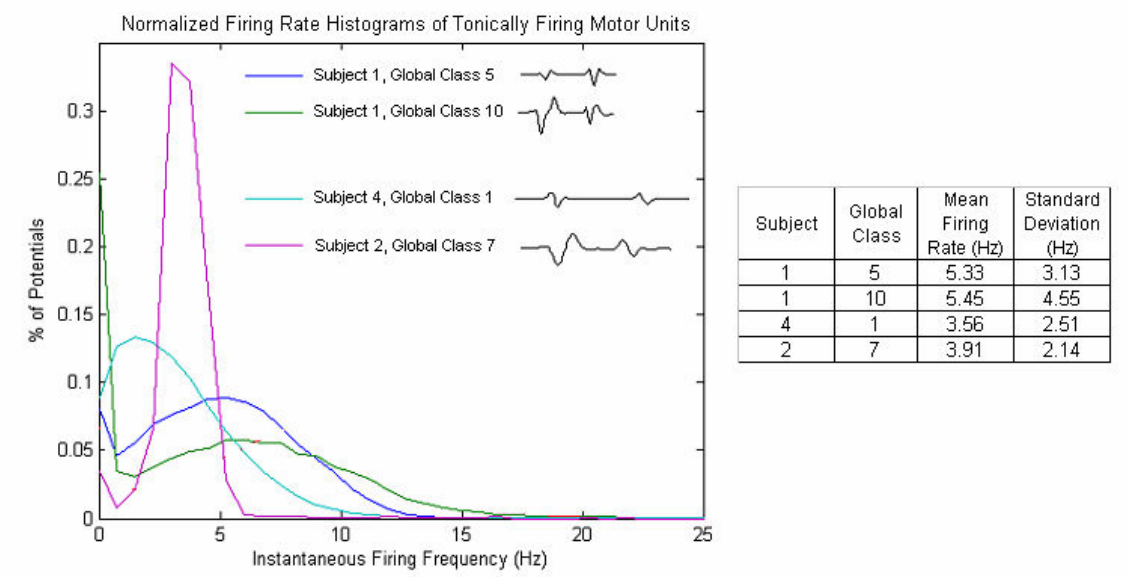

Subject	Global Class	Mean Firing Rate (Hz)	Standard Deviation (Hz)
1	5	5.33	3.13
1	10	5.45	4.55
4	1	3.56	2.51
2	7	3.91	2.14

Figure 5.25 Tonic firing global class example. Four global classes over 3 recordings are shown whose firing patterns are mostly periodic. The histograms were normalized to the number of potentials in each respective global class over the entire recording. The firing rate statistics are also shown.

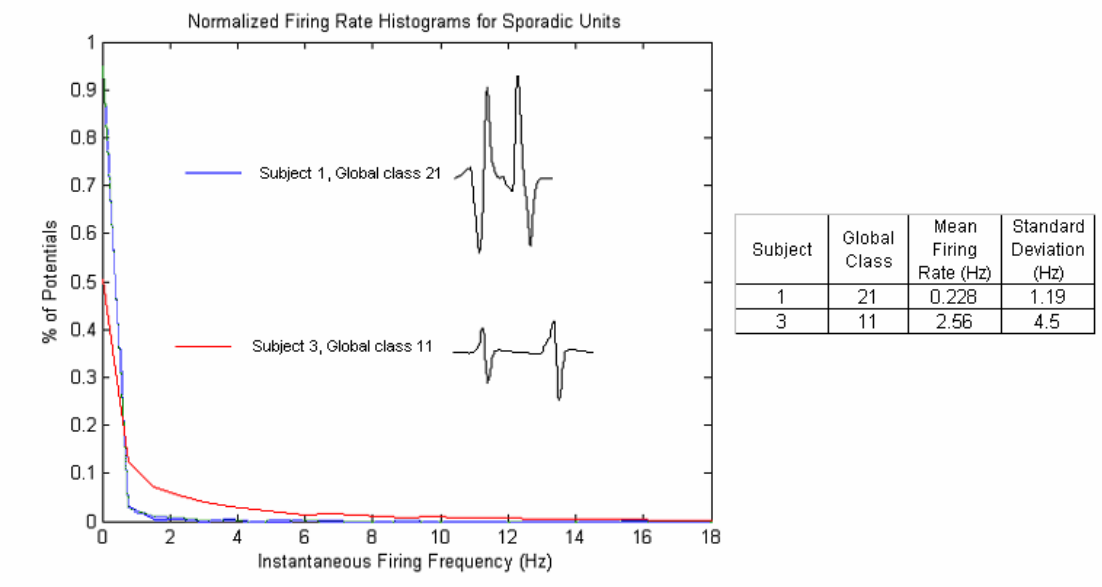

Subject	Global Class	Mean Firing Rate (Hz)	Standard Deviation (Hz)
1	21	0.228	1.19
3	11	2.56	4.5

Figure 5.26 Sporadically firing global class example. Two global classes in two recordings are shown whose firing patterns are sporadic. The firing rate statistics are also shown.

Global classes 5 and 10 of the subject 1 recording, global class 1 of the subject 4 recording, and global class 7 of the subject 2 recording, all showed some tonic firing at frequencies less than 6 Hz. Global classes 21 and 11 of the subject 1 and 3 recordings, respectively, fired mostly sporadically. The global classes with the smaller amplitude templates seemed to fire most often and sometimes periodically, while global classes with larger templates fired more sporadically. Global classes could also exhibit both firing patterns (e.g. global class 10 in Figure 5.25).

To examine which kinds of motor units may fire spontaneously, the number of potentials over the entire recording was plotted against the peak to

peak values of the global class templates normalized by their respective M-wave amplitudes (Figure 5.27).

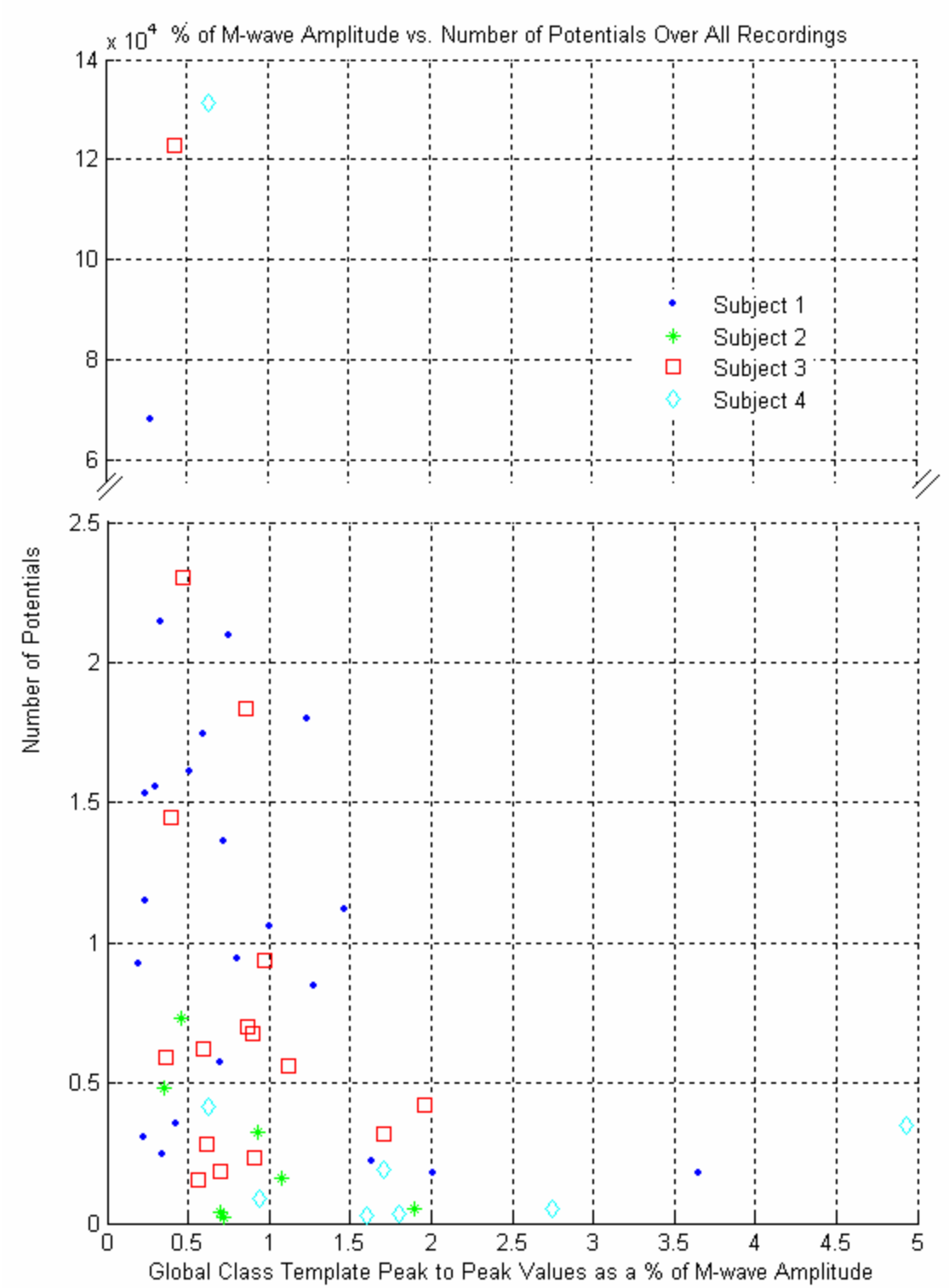

Figure 5.27 Peak to peak value versus the number of potentials for each global class. The number of potentials over the entire 24 hour recording is plotted for each global class in each recording.

The global classes with the smaller amplitude templates seemed to fire most often and sometimes tonically suggesting that these classes were more excitable, while global classes with larger templates fired more sporadically. These global classes may have higher thresholds for activation. Figure 5.27 shows a general trend of an inverse relationship between the number of potentials over 24 hours and the peak to peak value of each global class template. This trend is clearer when viewed on a per subject basis, particularly when only the global classes with individual classification accuracies of greater than 90% are compared (Figure 5.28).

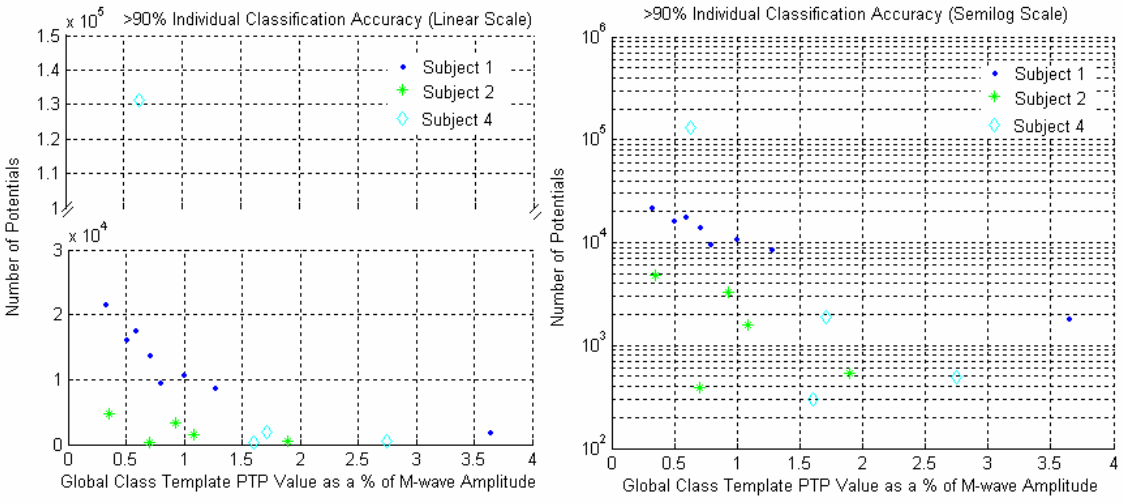

Figure 5.28 Peak to peak value versus the number of potentials for each global class (only those with greater than 90% accuracy in individual classification performance). The number of potentials over the entire 24 hour recording is plotted for the global class in each recording whose individual classification accuracy is greater than 90%. Both panes have identical data, but the left pane has a linear scale while the right pane has a semilog scale.

The semilog plot in Figure 5.28 shows that the global class points of the subject 1 recording form a line, revealing that the relationship is exponential between the number of potentials over the entire recording and the global

class template peak to peak value. The same is true for four of the five global class points of the subject 2 recording (excluding the point at 0.69 on the x-axis).

Another more global approach to examine the amount of motor unit activity present during a 24-hour period is to plot motor unit duty times. The duty times for all 16 global classes of the subject 3 recording are plotted in ascending order in Figure 5.29. Displayed are the ON times as a percentage of 24 hours in which the global classes were ON.

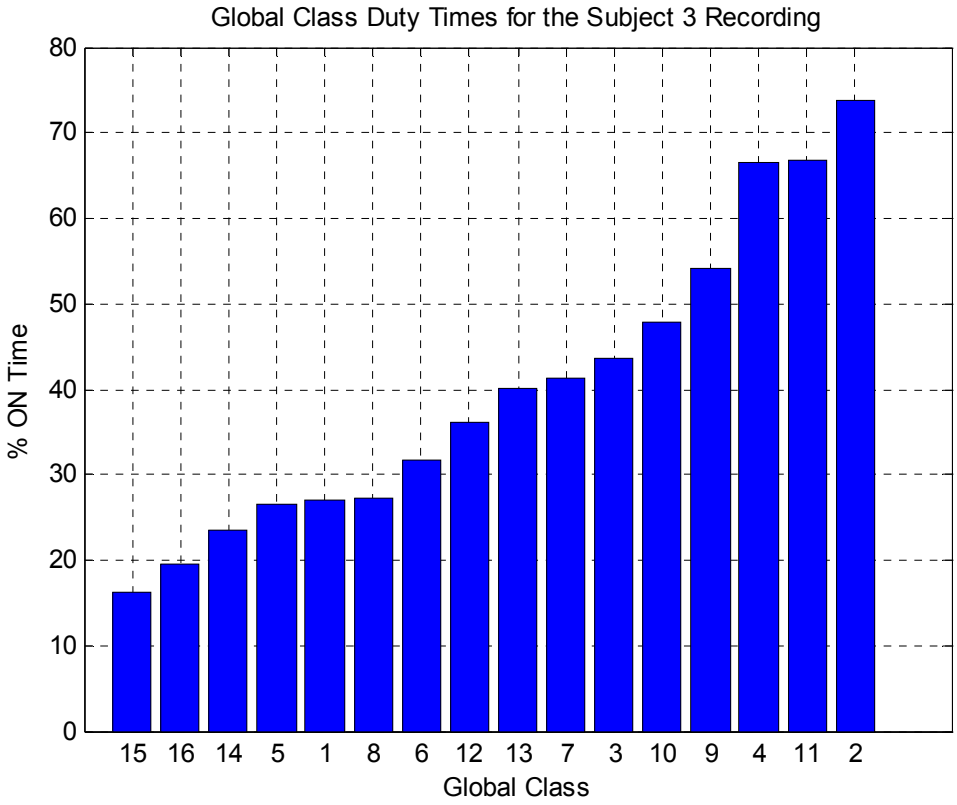

Figure 5.29 Global class duty times for the subject 3 recording. The duty times for all 16 global classes in the subject 3 recording were plotted in ascending order. The duty times represented the percentage of time that each global motor unit class was ON over the entire 24 hour recording.

For a global motor unit class to be considered ON, there had to be at least one firing in a 3-minute span. The global classes were active between about 17 and 75% of the recording.

To illustrate the importance of subject state, duty times were also plotted with respect to the percentage of the overall ON times that subject 3 was awake (Figure 5.30).

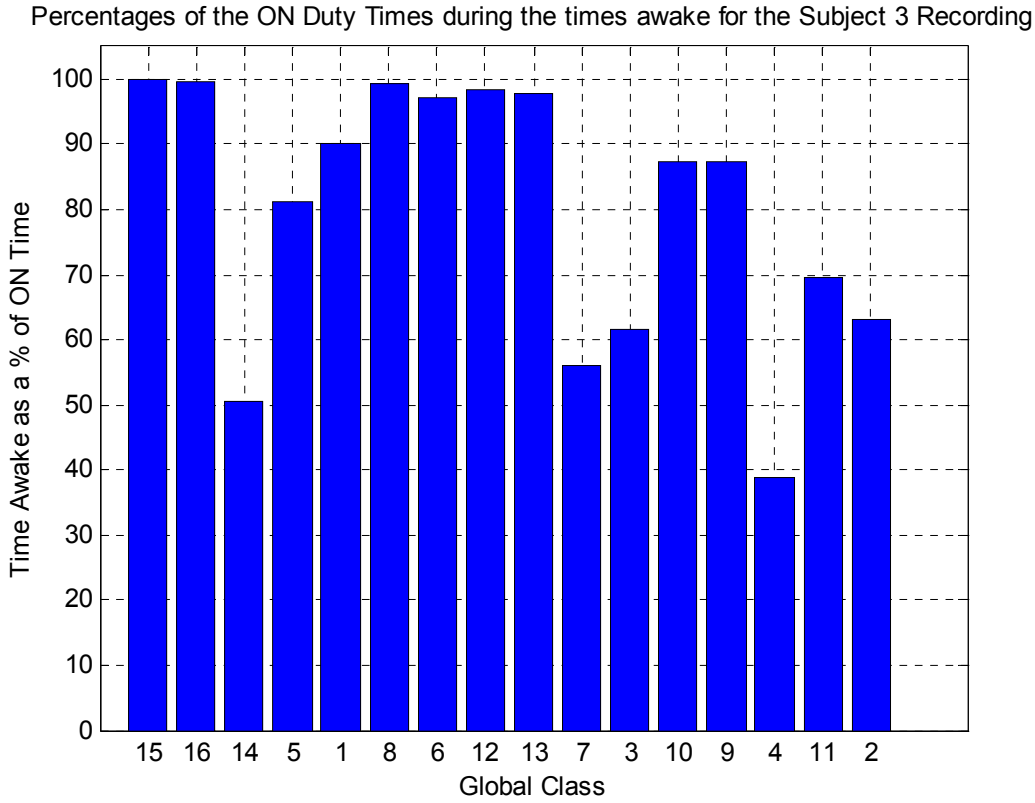

Figure 5.30 Global class awake duty times with respect to the overall duty times for the subject 3 recording. The times that the global motor unit classes were ON during the awake time were plotted as percentages with respect to the total ON time for each global motor unit class.

A majority of the global motor unit classes in the subject 3 recording were active mostly during the time the subject was awake. Only global motor unit classes 3, 4, 7, and 14 were just as active during the time asleep as the time awake.

The output of the classification algorithm can be used to determine the effects of anti-spasm medications. Three of the four subjects took anti-spasm medication. The activity of these drugs may influence the results by suppressing the activity of some motor units. As an example, Subject 2 administered a

baclofen/klonopin dosage at 3 different times during the 24 hour recording. The approximate times of the drug administration are shown with red lines along with the dose number (as in number of administrations) in Figure 5.31.

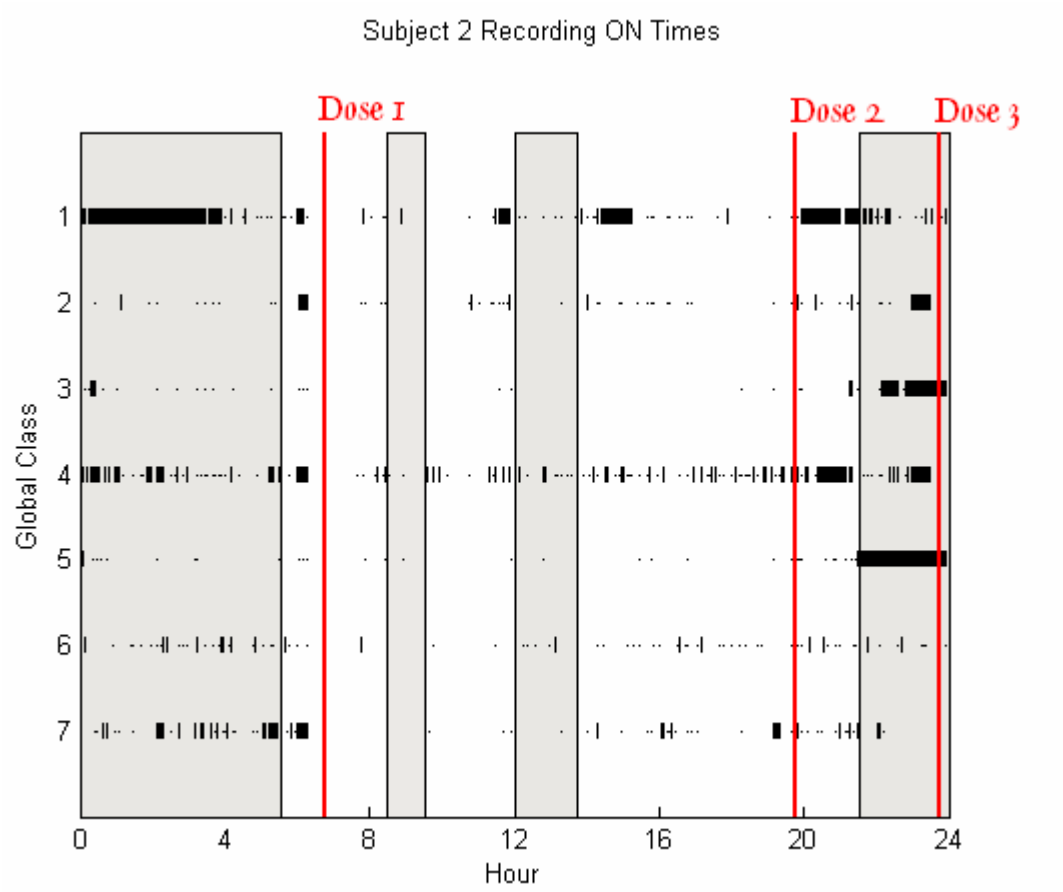

Figure 5.31 ON regions for the subject 2 recording. The classes are labeled on the y-axis while the time is labeled on the x-axis in hours. According to the timing standard, hour 0 is midnight to 1 am and hour 23 is 11 pm to midnight. The red lines indicate the approximate times of the administering of anti-spasm medications. The shaded areas show sleep time.

After the first dose of medication, the activity in all 7 global classes decreases, with global class1 becoming active again about 4 hours later. The second application of the medications seem to coincide with an increase of activity in global classes 1 and 4. Global class 1 appears to become very active after the third medication application, whereas the activity of global classes 3 and 5 are dramatically reduced.

Chapter 6: Discussion

The algorithm developed in this study was designed to classify motor unit potentials automatically in 24-hour recordings of surface EMG. Thenar muscles of SCI subjects were chosen for study because previous investigations have shown that spontaneous single motor unit activity is common [Zjdewind and Thomas, 2001]. The performance of the algorithm was assessed two ways: By comparing its tracking of global classes over the entire 24 hour range to that of a human operator and by examining its ability to correctly classify individual motor unit potentials as to belonging to particular global classes relative to an EMG expert. The algorithm was able to track 53 global classes in four 24-hour recordings and achieve 92% accuracy for 58% of the global classes (n = 31), the level of agreement between a non-expert and an expert rater. For 77% of the global classes (n=41), the algorithm was able to achieve a classification performance of greater than 79 % accuracy over two recordings, the level of agreement between two expert raters. This performance represented an average of 96% correct with a false positive rate of about 10.2 %. The algorithm required up to three weeks on average to produce results for each recording, about the same time as a person took to classify only 12 minutes of data and to track the unit templates over 24 hours. Thus, the goal of accurately and automatically following the long term activity of spontaneously firing motor units in muscles paralyzed by spinal cord injury was accomplished.

While these overall performance statistics are good, it is important to keep in mind that these statistics only estimate the ability of the algorithm to correctly

classify potentials. There is no feasible way to ascertain the entire performance of the algorithm over a full 24-hour EMG recording. This is due to the inherent need for an algorithm of this type in the first place – it would be take a human operator more than 118 months (2.5 years) to manually classify an entire 24-hour EMG recording, more than 157 times that (three weeks) needed by the algorithm to accomplish the same feat.

A number of issues ranging from noise removal to the limitations and impediments of the automatic motor unit potential classification algorithm will be discussed in the subsequent sections.

6.1 Segmentation and Noise Removal

The goals of segmentation were to extract as many motor unit potentials as possible and to minimize the noise that was mistakenly segmented. Noise elimination thresholds determined the balance between the elimination of motor unit potentials and the elimination of noise. The frequency based noise elimination thresholds were set based on the gold standard classification of HR 16 MIN 45 of the subject 1 recording, while the noise elimination thresholds were based on comparative peak to peak values adapted for each 3-minute portion of a 24-hour recording.

The segmentation procedure was extremely successful, finding a large percentage of actual motor unit potentials (93.7%) with a small false positive rate (2.3%). Of the actual motor unit potentials that either were missed by the segmentation procedure or eliminated mistakenly as noise, their amplitudes were

small relative to the baseline noise. Almost none of them were discernible enough at the current amplitude resolution to be accurately classified and tracked over 24-hours by an expert classifier (Figure 5.2).

Adaptive noise elimination thresholds were a major strength in minimizing the noise segmented. These thresholds gave the segmentation procedure the leeway to eliminate considerable noise when it was prevalent while eliminating much less in cleaner, noise-free recordings. In comparison, fixed thresholds are not able to change based on the noise level of recordings, like those thresholds for the frequency based noise elimination method, but specifically target repeatable noise. The value of fixed thresholds is that they can remove noise that similarly manifests itself from recording to recording. Thus, an adaptive noise elimination procedure was the best way to reduce the noise level.

Extensive noise removal is a beneficial tool for the automatic classification algorithm. If there are less potentials to classify, the algorithm's execution speed increases. Similarly, the removal of noise-like potentials reduces the algorithm's ability to make incorrect classifications. Some classifiable potentials may be lost when extensively removing noise, causing the resulting firing patterns to be incorrectly skewed. If noise elimination thresholds were reduced in order to retain these classifiable potentials, erroneous classifications made for the preserved noise-like potentials would do the same firing pattern skewing that was meant to be prevented.

6.2 Algorithm Classification Performance

The automatic global classification algorithm was able to achieve a mean accuracy of 86% similar to the performance of two human raters. Only 17 global classes (32%) had a lower accuracy than the mean and these classes occurred in 3 of the 4 recordings. Human operators, both non-expert and expert, can reach different results using the EMG viewing software in manual classification for a number of reasons. Some human operators may have more experience at manually classifying motor unit potentials than others, especially in the case presented here (non-expert versus expert classifiers). Classifications can also be subjective in nature and differ from operator to operator. The length of time required to classify a portion of EMG is also a factor. Over time, subjective judgments can change either due to operator fatigue or increased experience working with a given portion of EMG. Several other factors could contribute towards the reduced classification performance of the algorithm, as described below.

6.2.1 Signal to Noise Ratios

Global classes with wide ranging signal to noise ratios (from 0.64 to were able to be followed accurately over 24 hours, but the performances for the various global classes varied over all the recordings. The plot of signal to noise ratios of the individual global classes from all recordings to the overall accuracy of classification shows no clear relationship between these parameters (Figure 5.10). Large signal to noise ratios yield high classification accuracies, but lower

signal to noise ratio motor unit templates still have good results as well. The global class with the lowest accuracy (38%) had global class templates with signal to noise ratios (8.5 distal, 1.2 proximal). This average signal to noise ratio of 4.85 was close to the overall signal to noise ratio mean of 5.9. Thus, a low signal to noise ratio alone could not explain why some classes could not be classified reliably.

It was possible for one channel to have a template with a large signal to noise ratio template while the other channel template had a small signal to noise ratio template. As described in section 4.3.4, the classification algorithm only used distance metrics in one channel to make judgments if the peak to peak value of one channel's template was too small. While this did allow the tracking of more motor unit classes, it also could be problematic in resolving the differences between motor unit classes that are similar in one channel, but different in another. For example, global classes 9 and 13 in the subject 3 recording fit these criteria (Figure 5.5, section 5.3), resulting in false positives and the lowest accuracy reported (38%). They are similar in the distal channel, but differ markedly in the proximal channel. Some global class 9 potentials were confused for global class 13 potentials because distance metrics weren't used for the proximal channel in this case. This situation could be remedied by always applying distance metrics to every channel, but this would limit the number of global classes that could be tracked.

6.2.2 Amplitude Resolution

Another consideration is amplitude resolution. The average global class potential only occupied about 25% of the full scale range of the data logger. Figure 6.1 shows an example of some raw data as it was recorded by the data logger.

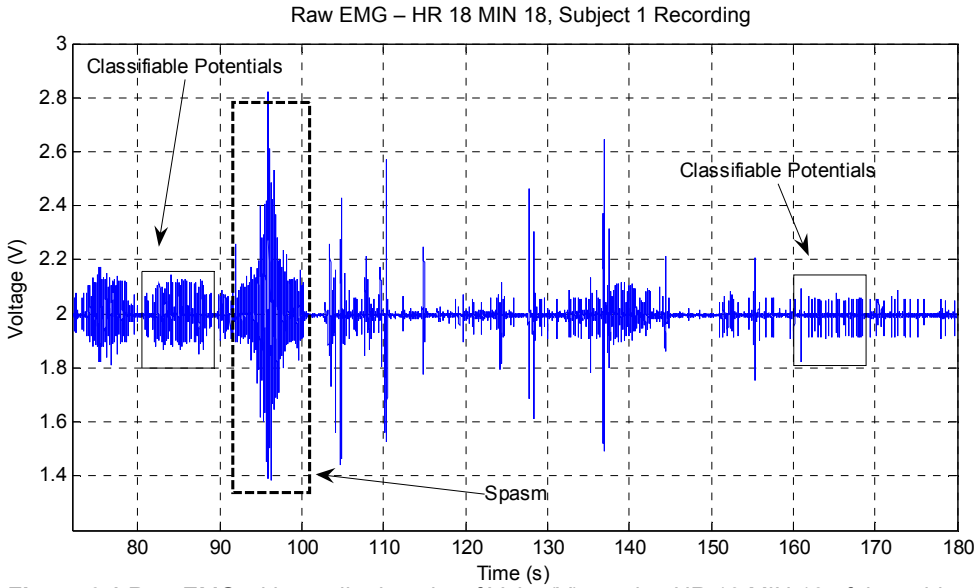

Figure 6.1 Raw EMG with amplitude units of Volts (V), portion HR 18 MIN 18 of the subject 1 recording. The EMG here appears just as it was recorded by the data logger. The available voltage range of the data logger was 0-4 V and the voltage resolution was 1 mV. The potentials that could be classified, as shown by the rectangles with solid lines, only have a peak to peak value of approximately 200 mV. Potentials with peak to peak values of about 100 mV are about the size of an average potential across all recordings. Some potentials with even smaller peak to peak values could still be tracked, but those with peak to peak values of less than 12 mV could not be tracked. Spasms, like that in the rectangle with the broken line, were much larger and filled up more of the total logger's input range.

Accurately classifiable potentials are shown in the boxes with solid lines and used only about 5% of the data logger's input range. Only those potentials with peak to peak values of less than 12 mV (0.3% of the logger's range) could not be classified accurately. After smoothing and filtering, these motor unit potentials appeared to be discernible and legitimate potentials, but when recorded with low amplitude resolution, these smaller potentials did not always assume the same waveform shape, making their classification unreliable. If the gain were

increased, the EMG would have been recorded with a higher amplitude resolution and smaller motor unit potential waveforms would have been more stable. Increased gain would mean that the baseline noise would have also been increased and more noise may have been segmented as a result. This segmented noise also may have been misconstrued as superimposed potentials, possibly reducing classification accuracy.

Figure 6.1 also shows a spasm, (rectangle with the broken line) that produced much more EMG and filled up more of the total logger's input range (about 70%) in this case. If the gain had been higher, any spasm like this one would simply cause the amplifiers to saturate, leaving the logger to record a constant value of 0 V or 4 V. This would be beneficial because any large amplitude spasms would not appear as waveforms that resemble EMG in the first place. The gain was set at a level to capture both the spasms and the motor unit potentials to characterize involuntary EMG in thenar muscles paralyzed by SCI.

The exclusion of spasm data from the classification was important. EMG from different potentials interferes with each other, making resolution of these superimposed potentials almost impossible to classify and the algorithm was not designed for spasm analysis. The motor unit firing behavior during spasms is different than the spontaneous motor unit activity characterized here. Spasms are responsive to specific inputs, tend to be stronger contractions, and fire at higher rates [Thomas and Ross, 1997].

6.2.3 Superposition Resolution Difficulties

When two or more motor unit potentials fired close together, their potentials could superimpose. Figure 6.2 shows a superposition correctly resolved by the classification algorithm.

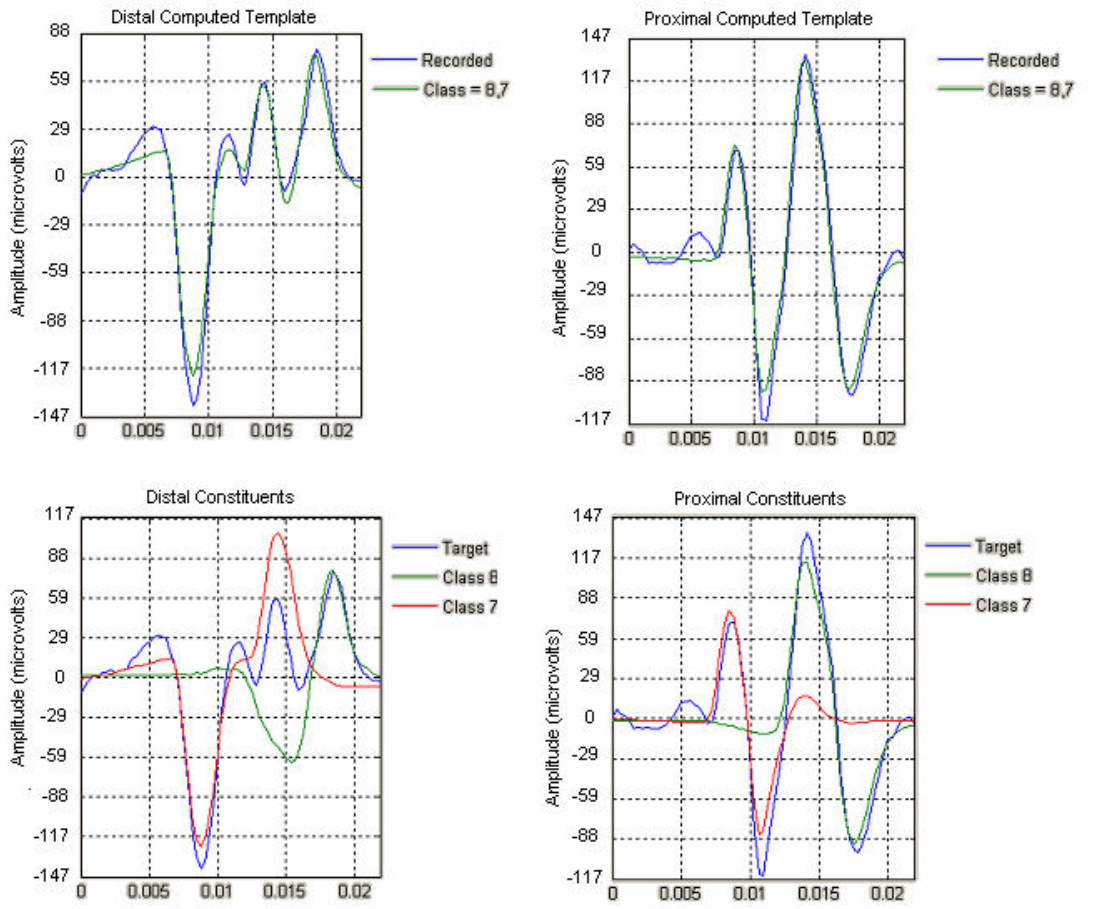

Figure 6.2 Example superposition. The left panes show the superimposed potential in the distal channel while the right panes show the same superimposed potential in the proximal channel. The x-axes have units in seconds.

In the bottom panes of Figure 6.2, the constituent templates of the superimposed potential (red and green potentials) are shown at the appropriate phase shifts required to build the target superimposed potential (blue trace). In the top panes, the sum of the constituent potentials in the bottom panes produce the green traces in each channel. The green traces match the target blue traces in these top panes.

Superpositions were not always resolved by human operators or the classification algorithm. An inability to resolve superimposed potentials reduced the overall success of the classification for the 53 classes by an average of 7.4% in accuracy. The only way for a superposition to be resolved was for each of the constituent classes in that superposition to exist independently as a global class. If one of these global classes has a very small peak to peak amplitude, it most likely was not found due to the aforementioned limitations of the classification algorithm. A person will see this potential as classifiable, but for the algorithm it will go unclassified.

The poorer performance of the superposition resolution routine compared to the overall classification algorithm could be attributed to the distance metrics used within the algorithm. The correct global class template to use at each level of superposition resolution was determined by computing the correlation coefficient after a cross-correlation method was used to slide the global class template into its optimal position. A problem using the correlation coefficient is illustrated in Figure 6.3.

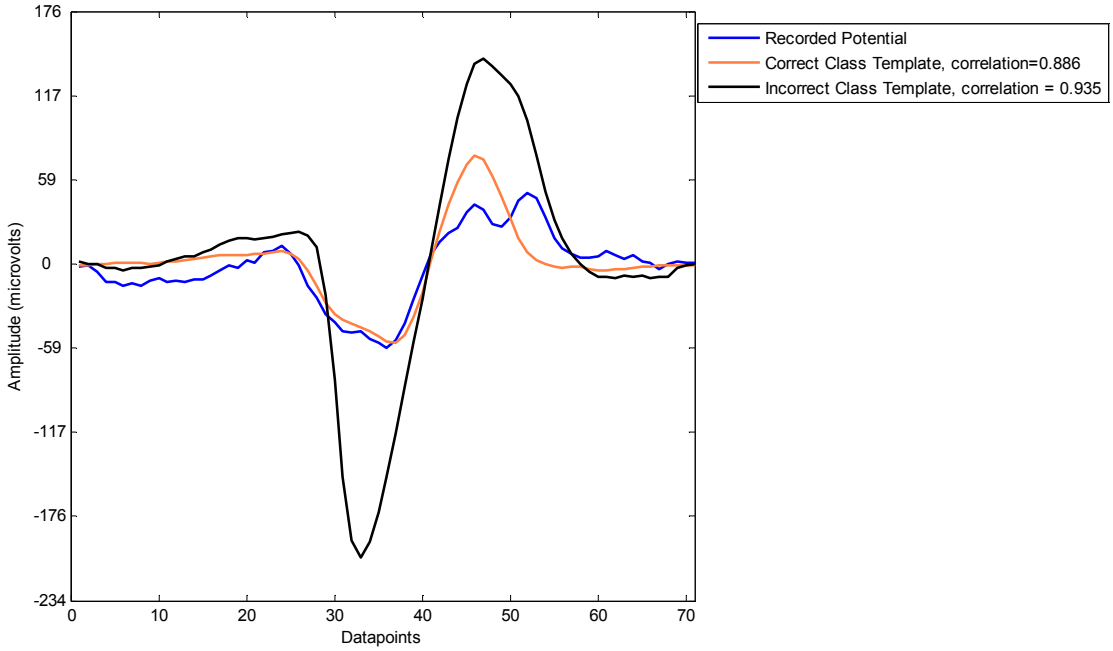

Figure 6.3 Correlation coefficient errors in selecting constituent classes in superpositions. The blue potential is the recorded superposition that must be resolved. The orange potential is the class template for the correct constituent potential within the superimposed blue potential.

The blue potential is the superimposed potential to be resolved. The first correct constituent class template of this superimposed potential is the orange one, but the correlation between the orange and blue potentials is only 0.88. Unfortunately, the black class template potential is selected as the first constituent in this situation because it correlates highest with the target superimposed potential (0.94) because it varies the same way as the blue superimposed class along the whole extent of both potentials. The orange class template ceases to vary along with the blue superimposed template at about data point 50, thus resulting in the lower correlation value.

It is possible that this issue could be corrected by employing a Euclidean distance metric along with the correlation coefficient. The black class template

would then be rejected as it would have a much larger Euclidean distance from the superimposed potential than that of the orange class template. In order to be successful and effective in resolving superpositions while keeping misclassifications low, correct thresholds for both metrics and a suitable way of using them across both channels of would need to be found.

Another issue is that superpositions of small unknown classes prove problematic for automatic classification. Occasionally, a potential that visually could be classified as belonging to a certain global class by a person would not be classified as such by the algorithm because it was not mathematically similar enough to the target global class template for a class. The potential could actually be a superposition whose constituent potentials belong to the class in question and some small unknown class. Figure 6.4 shows an example of this situation.

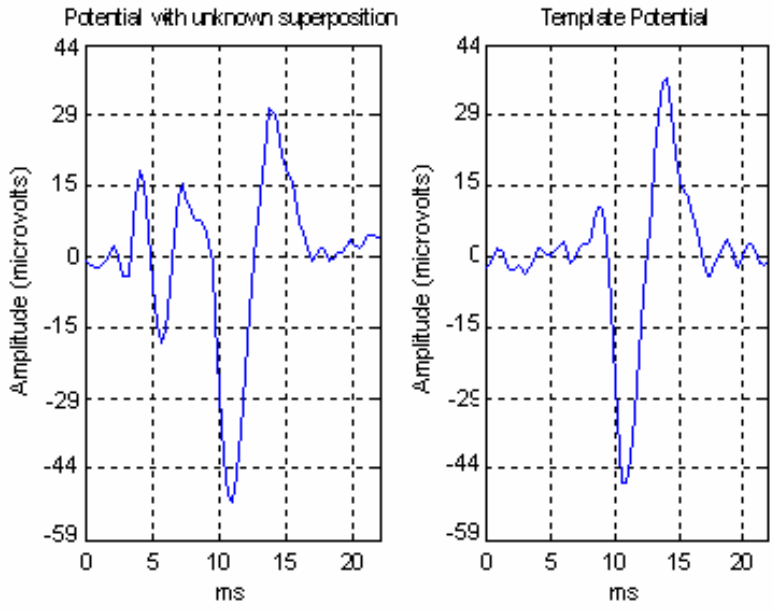

Figure 6.4 Potential superimposed with an unknown class. The right pane shows a motor unit class template while the left pane shows a potential that should be a member of the class indicated by the left pane. Unfortunately, it was superimposed with an unknown motor unit class and the algorithm let it go unclassified. Since it has a small peak to peak value it is likely that this class was not clustered. In order for a superposition to be correctly resolved, all of its constituent classes must have superposition-free potentials elsewhere in the record.

The right pane shows a global class template in the distal channel in the subject 3 recording. The left pane shows a potential that belongs to the global class in the right pane. The left pane potential remained unclassified because it is superimposed with an unknown class.

This superposition problem has a solution at the classification level of individual potentials. The attenuation window described in section 4.3.7 has the ability of attenuating the unknown potentials so that a proper classification can be made. If the unknown class has been attenuated enough, a correct classification could be made. Unfortunately, it would not work for this example (Figure 6.5), but this method was effective elsewhere.

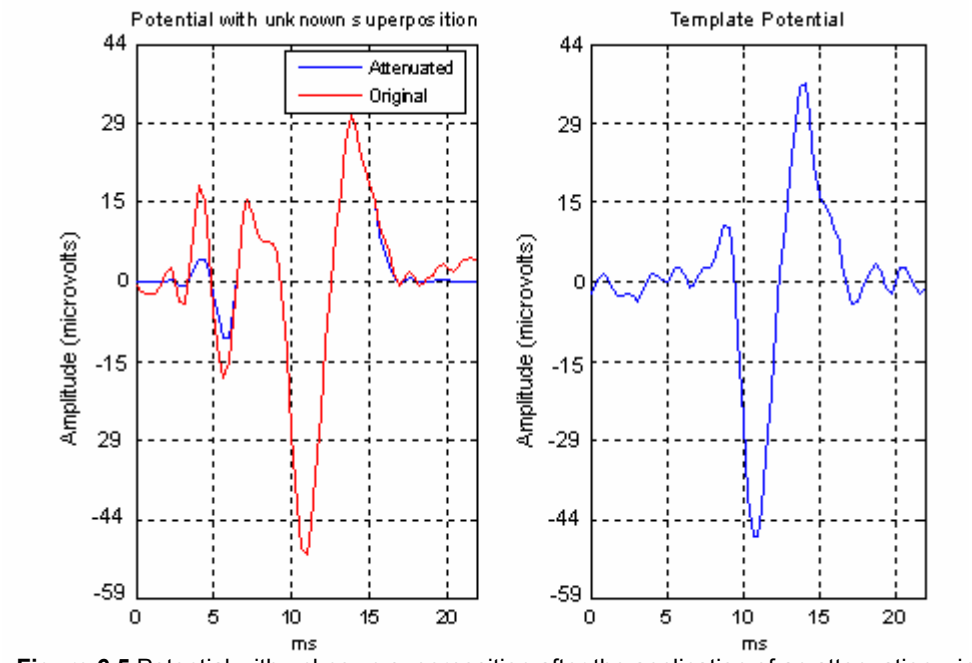

Figure 6.5 Potential with unknown superposition after the application of an attenuation window. The red potential in the left pane is the original one while the blue one results after the original potential is multiplied by an attenuation window (section 4.3.6). A proper classification still cannot be made because not enough of the unknown class potential has been attenuated.

6.3 Global Class Tracking

Algorithm-based classification of motor unit potentials was accurate over a few minutes, but to be useful for long term recordings, algorithm performance must remain reliable over time. The motor unit template uniting routine could track an average of 13 different global classes per 24-hour recording.

Unfortunately, the global class number can be erroneously increased if there are a frequent number of superpositions or a rapidly firing motor unit class. If an identical superposition occurs at least 3 times in a 3-minute EMG portion, then that superposition will be incorrectly assigned to a local class. If this incorrect superposition class appears identically in at least five different 3-minute EMG portions, then it will be an erroneous global class as well. The same situation can result if a motor unit class is firing so rapidly that multiple instances of the same motor unit class appear in the same segmented window (Figure 6.6).

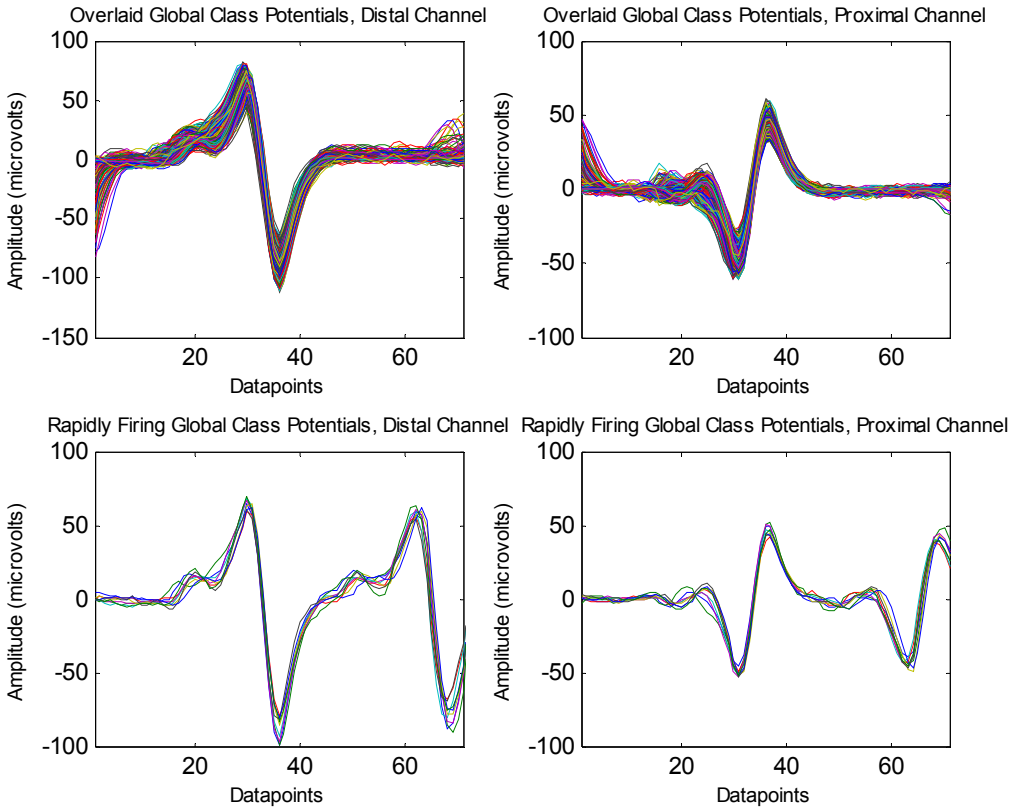

Figure 6.6 Example of rapidly firing global class that is erroneously labeled as a new class. The top panes show the distal and proximal representations of overlaid potentials of a global class. The bottom panes show overlaid potentials of the same class that is rapidly firing. There is more than one occurrence of the same class in each of the distal and proximal segmented windows. These waveforms are repeatable, thereby causing the formation of a new class.

In Figure 6.6, the top panes show the proximal and distal representations of overlaid potentials belonging to a given global class. In the bottom panes are more overlaid potentials where that global class was firing so rapidly that there was more than one occurrence of the same global class potential in the same segmented window.

Factors that may contribute to the exclusion of potentials from the global class list include sampling errors, changes in template shapes, alterations in electrode properties and position, and periodic noise. These same factors can also reduce tracking performance and ultimately classification accuracy

Sampling error contributed to the inability to track some motor unit potential classes. For example, global classes that had waveforms like those shown in Figure 6.7 were difficult to track.

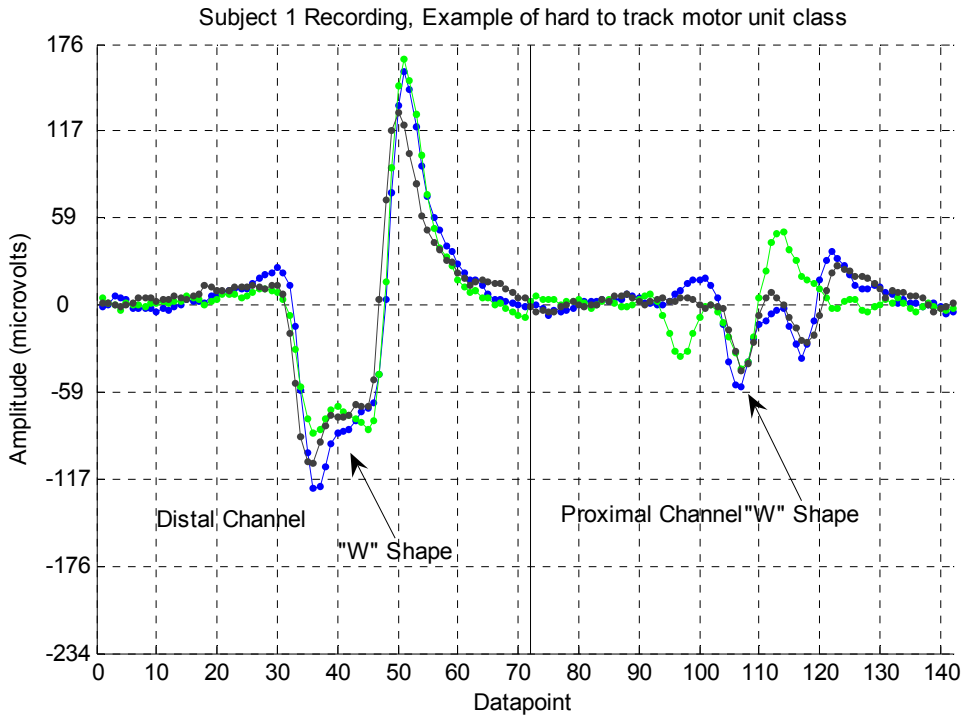

Figure 6.7 Hard to track potential. The left hand side of the figure shows the distal channel waveform, while the right hand side shows the proximal channel waveform for 3 individual potentials occurring at times that differ by more than a few hours. The "W" shape in these potential representations make it hard to track because either side of the "W" can be the most negative point in the potential at different times, even within the same 3-minute segment. Individual data points are also shown. There are only about 6 or so data points in each negative peak.

All potentials shown originate from the same motor unit, even though all look slightly different. The individual data points that comprise the waveforms are also shown. The "w" shape on the negative phase of the potential, in both channels, could not be consistently recorded by the data logger when sampling at 3.2 kHz. Thus, one explanation for the varying shape could be sampling error – the logger could not sample fast enough to keep the "w" shapes in the same

relative positions over time so that they could be grouped correctly and classified. For this global class, the accuracy was 88%. Alignment of these potentials was also problematic because either of the negative points on the “w” could be the most negative point in the potential at different times, even within the same 3-minute segment of EMG. If the alignment problem were circumvented by segmenting the potentials by aligning them in time, or in other words segmenting the same data points from both the distal and proximal channels, the effects of the low sampling rate could be reduced. Another possibility is to align by the largest positive peak of a potential when the negative phase of that potential has a complex shape. Unfortunately, this approach would increase complexity and could possibly make alignment problems worse. The relative shapes of these potentials do change somewhat with time, however. Thus the limits placed on the distance metrics to achieve accurate classification may still be met, making it difficult for the algorithm to recognize that these kinds of potentials belong to the same global class.

Tracking problems can also arise when changes in motor unit template shapes occur in one channel, but not the other (Figure 6.8).

Figure 6.8 Motor unit class template changes in one channel only. The left side of the figure is the distal channel representation of each potential, while the right side of the figure is the proximal channel representation. Both of these potentials occur within HR 17 MIN 6 of the subject 1 recording. It appears that both of these potentials belong to the same motor unit because the distal channel representations are almost identical and there are no other similarly shaped motor unit template potentials throughout the entire recording. The proximal channel representations could be different because a potential that has extremely low amplitude in the distal channel could be superimposed with the original waveform.

Both the distal channel (left side) and proximal channel (right side) representations of 2 potentials occurred in the same 3-minute EMG portion. These potentials appear to belong to the same global class because of the striking similarity of the potentials in the distal channel. In fact, this distal channel waveform shape is very unique and no other motor unit template shape is close to it over the entire 24-hour recording. One possible explanation for this obvious change in the proximal channel representations of this class is that the red potential in Figure 6.8 is superimposed with some unknown class. The unknown class could have a very small amplitude potential in the distal channel. While no such potential was observed independently throughout this 24-hour recording,

these motor units do fire sporadically and sometimes for short periods making it difficult to exclude this possible explanation. When presented with these data, a person used to evaluating EMG signals would have to conclude that these two potentials are different. For this reason, accuracy was only 60% for this global class due to a high incidence of false positives. One possible way to have an algorithm emulate this same process better, and thus to reduce the false positive rate, is to include some metric of potential amplitude as a criterion for acceptance of a global class. The impact that such changes have on the template shape also depends on the frequency with which the changes occur. If infrequent, then the template shape, which is an average, will not change markedly. However if common, the average template shape will change, inducing tracking and classification errors. Thus, the motor unit potential classification algorithm is designed based on the idea that the template shape of a global class is stable from one 3-minute EMG portion to the next. Instability, within limits, will cause classification and tracking errors.

Changes in the shapes of global classes over a 24-hour recording may also result from alterations in the conductive properties of the electrodes or electrode movement. Electrodes were taped down onto the skin to ensure that they did not move. The maximal M-waves that were recorded before and after the 24 hour recording differed by an average of 10% for the distal EMG and by 7% in the proximal channel. These data illustrate that electrodes do not necessarily behave like matched pairs over time and that the signals recorded by both channels can change by varying amounts over time. Even so, only a 10 %

change in potential amplitude can result from electrode issues. Changes in global template amplitude that exceed this level must arise from other sources.

Another source of error for tracking motor unit classes was time alignment for potentials of similar amplitude in both the distal and proximal channels. In time alignment (section 4.3.7), the window of the channel that has the potential with the larger peak to peak value is retained, while the opposite channel is re-segmented to have the same endpoints in time as the unchanged potential. When the peak to peak amplitudes of the distal and proximal channel representations are almost the same, the representation that is re-segmented can be that of either channel due to fluctuations in the amplitudes of both potential representations (Figure 6.9).

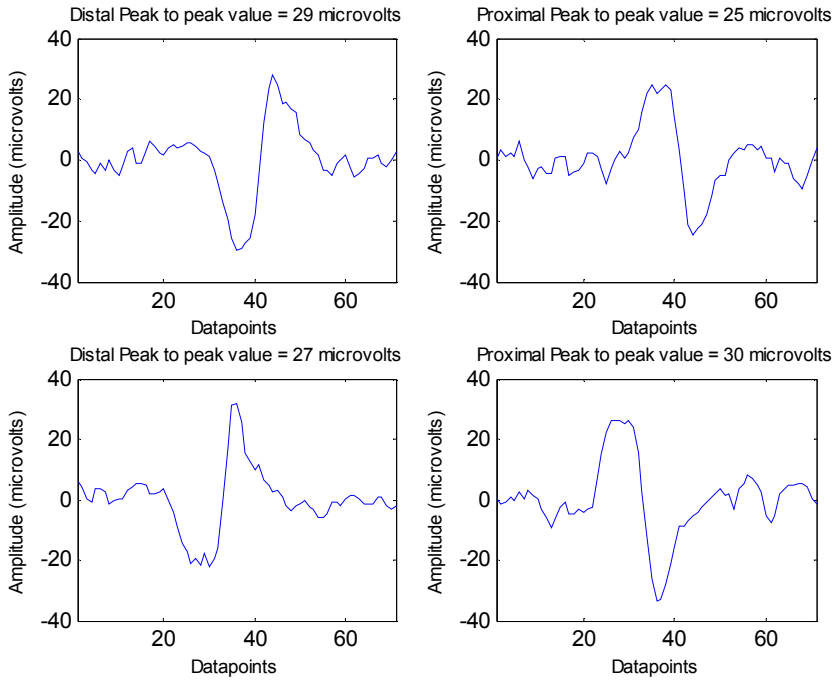

Figure 6.9 Time misalignment example. Two different potentials of the same class are shown. The left panes represent the distal channel and the right panes represent the proximal channel. The top panes illustrate one case where the distal channel potential's peak to peak value was greater than that of its proximal channel representation. The bottom panes show a different potential of the same class whose peak to peak value of the proximal channel is greater than that of the distal channel representation.

This issue is one explanation for obtaining lower accuracy for tracking compared to classification of some global classes.

Even though a different channel is chosen to do the time alignment, the relative timing between these potentials still remains constant and the resolution of superpositions is unaffected. This can be a problem for the first stage of the motor unit template uniting procedure. In this stage, all local templates over the entire recording are clustered. This time alignment error can cause templates that are in fact identical to not be combined at all, and a trackable global class may not be found. The peak to peak value fluctuations between channels most likely occur with motor unit classes with small amplitude templates like the one in Figure 6.9 and they are generally harder to follow in any case.

In the third stage of the motor unit template uniting procedure, additional errors may have resulted from the use of nearest neighbor templates in global class tracking. In order to verify if a particular global class was present in a 3-minute EMG segment in which it was not originally found, the nearest neighbor template was employed. If the nearest neighbor template happened to be incorrect, the wrong template would be utilized for comparisons. This error would propagate through the entire motor unit template uniting procedure, generating more mistakes. This results because the wrong template was utilized for comparisons. This situation could possibly be remedied by using some type of weighted average involving known templates for given global classes. This means the use of the direct output of the first stage of the motor unit template uniting procedure. Unfortunately, this method may only reduce the number of

erroneous matches made (false positives) which would be useful in improving overall accuracy. It may not improve the correct percentage.

Splitting error, or the error arising when a global class was not recombined during the third stage of the motor unit template uniting procedure, impacted the number of potentials missed by the algorithm. This is shown by Figure 5.18 in the results. Splitting error could result when local class templates were not mathematically similar enough to be grouped into the same global class in a given 3-minute EMG portion during the third stage of the motor unit template uniting procedure. It could be remedied by lowering the thresholds for classification, but since the impact of this error was minimal (an average of only 2.5%), any attempt to correct it may cause larger error.

6.4 Comparison of Individual Classification and Tracking Performances

While most global classes were well classified and tracked, the classification performance of some global classes was found to be independent of the tracking performances achieved by the motor unit template uniting procedure in section 5.5.1. These differences can occur because tracking and individual potential classification are different tasks performed using different methods.

The tracking procedure is also a task where potentials are clustered and classified, but in this case the clustered potentials are actually local class templates. Stage 2 of the motor unit template uniting procedure performs the same function as the final unsorted analysis in individual potential classification,

but there are implementation differences. In the final unsorted analysis distance metrics in addition to a superposition resolution algorithm are used to obtain the final set of classified potentials. The aforementioned stage 2 operates in a much simpler fashion, using fuzzy membership function values from individual potentials to determine which local templates belong to which global class. Stage 3 of the motor unit template uniting procedure does not classify local templates as global classes, but actually classifies individual potentials as global classes through the similar use of fuzzy membership values. Even though fuzzy membership values are used in both stages 2 and 3, their implementations are different, so their performances can likewise be different. The stark differences between all three routines can explain how their performances are unrelated for some global classes.

6.5 Custom Designed GUI Interface

The GUI tools for classification made manual analysis feasible, although it was still a very time consuming process. It was more efficient than similar software produced by other authors. McGill K, Lateva ZC and Marateb HR [2005] designed a similar automated classification program that classified multi-unit recordings of able-bodied EMG recorded using needle and wire electrodes. The authors stated that 1 second of EMG from able-bodied individuals with 9-12 active motor units required at most 20 minutes to manually classify. If extrapolated, it would take them 240 hours to process 12 minutes of data. Even though spontaneous EMG from people with SCI is different than multi-unit

voluntary EMG recordings, a six-fold time savings of manual classification time is substantial.

6.6 Periodic Noise immunity

Figure 6.10 shows an example of cell phone noise.

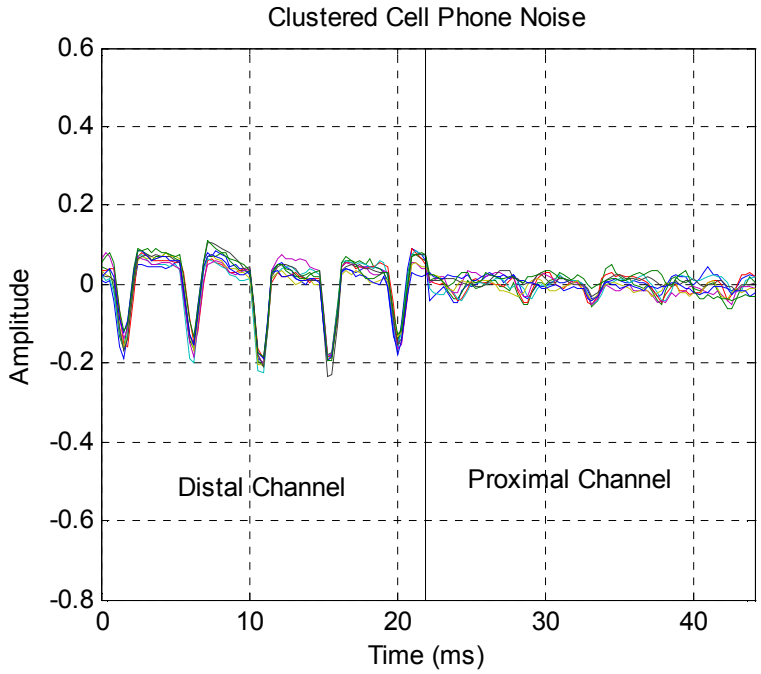

Figure 6.10 Clustered cell phone noise. The automatic motor unit classification algorithm is immune to periodic noise. It treats the noise just like it would potentials – by clustering them into independent classes. In this way, the clustered noise can be used in superposition resolution to "decontaminate" actual potentials.

The performance of the algorithm is unaffected by the presence of recurring or periodic noise. Periodic noise immunity is an important property of the automated motor unit classification algorithm because noise is treated just like a potential – it is clustered and grouped into its own independent class. The treatment of noise as potentials is beneficial. It can serve to "decontaminate" actual potentials if they form superpositions with the same type of noise that has

been clustered. The algorithm cannot tell noise classes from actual global classes, so it is the job of the human operator during processing to tell the algorithm which classes are noise. The immunity does not extend to sporadic or transient noise because this type of noise is unpredictable so it cannot be clustered as actual potentials are.

6.7 Applications of 24-hour classification

Automatically classifying 24 hours of EMG data at the motor unit level opens the door to automatically classifying other EMG properties and different physiological data. The high success rate of the automatic classification program proves that it is feasible to reliably identify motor unit potentials in long term surface EMG recordings that have an unknown number of classes. The firing rate histograms computed by the automatic classification algorithm can be used to help identify theoretical sources of the spontaneous motor unit activity. For example, the occasional firing of a motor unit at irregular rates make reflect activation of the motoneuron by synaptic noise [Matthews, 1996] whereas a train of motor unit potentials at a higher frequency may reflect the activation of a persistent inward current in the motoneuron [Heckman et al., 2005]. The automatic classification algorithm described in this research could also be applied in recognizing how motor unit activity changes during the time awake and the time asleep (Figure 5.25 in section 5.8), as well as before and after medication (Figure 5.26 in section 5.8). In both situations, this could be

investigated by looking for firing rate changes or changes in the number of firings of motor units before and after the administration of drugs.

Twenty-four-hour recordings have been done using various biosignals besides EMG, including neuronal activity [Mavoori et al., 2005], EEG [Velis D et al., 2007], blood oxygen saturation [O'Brien et al., 2000], and even signals from the taste receptors in the tongue [Shimatani et al., 2003]. The techniques used in this research could be applied to these other fields to classify data in long term recordings.

Chapter 7: Conclusion

An algorithm was designed to classify motor unit potentials automatically and was tested on 24-hour EMG recordings from individuals with paralyzed thenar muscles due to spinal cord injury. The classification algorithm performed well, achieving the classification accuracy performance of an expert classifier, or better, for more than 77% (n=41) of 53 global classes followed in four recordings. More than 94% (n=50) of the 53 global classes achieved the classification performance of a non-expert classifier.

The multi-step algorithm was able to reliably track an average of about 13 global classes over 24-hours (according to the expert results), accurately classify the potentials belonging to these classes, and determine their firing rates. The comprehensive software package used to view the data provided the necessary tools to investigate the output of the motor unit classification algorithm and to rate its performance.

The execution time of the automatic motor unit classification algorithm is up to three weeks. The first pass of the algorithm to determine the appropriate segmentation threshold takes approximately a day to execute and the second pass in which clustering is accomplished can take several days. The final classification pass may take upwards of a week or more to process. This is assuming the processing is being done on a moderately fast computer (2.8 GHz single core processor) and it is left on until all processing has finished. Although this execution time is long, the same procedure is unlikely to be accomplished manually (estimated time of two and a half years). Another benefit of the

automatic classification algorithm is that only minimal user intervention (half an hour at most) is required to set the globally tracked motor unit classes toward the end of the automatic classification procedure.

Before attempting to enhance the classification algorithm, the amplitude resolution of the EMG recordings must be increased so that the largest potential completely fills the entire 0V - 4V input range. Waveform stability would be increased with higher amplitude resolution, thus allowing smaller potentials to be more accurately classified and also more easily tracked over 24 hours. Baseline noise could be increased with a higher gain and some input signals are likely to overdrive the input range of the logger. Another possible way to improve classification performance would be to increase the sampling rate on the data logger. Unfortunately, it is not possible to increase the sampling rate for both channels of the data logger due to hardware limitations, but it may be possible to record only one channel with a much higher sampling rate. This would allow the peaks of potentials to be more faithfully represented, but would likely reduce the classification accuracy as well.

The classification algorithm could be improved in a number of ways. The superposition resolution routine needs the most improvement because it can impact the accuracy of all global classes. It could be enhanced by using a combination of Euclidean and correlation metrics, or even by finding a more robust distance metric than the correlation coefficient. An artificial neural network (ANN) approach may improve classification accuracy. An ANN offers the

flexibility to correctly classify superimposed potentials by using function approximation and pattern recognition abilities.

Among the globally tracked motor units, only 9 of 53 (15.0%) were always active throughout a 24-hour recording. Several classes exhibited regular firing behavior at different times (n=13, 24.5%) possibly due to activation of persistent inward currents in the motoneurons. Most motor units fired irregularly and sporadically, behavior most likely due to synaptic noise. There was activity during both the awake and sleep hours, but generally more of the activity occurred during the awake hours than during the sleep hours.

In conclusion, the automatic motor unit classification algorithm performed well but could be improved by enhancing the superposition resolution routine. This algorithm is an excellent tool by which to determine the approximate firing behavior of involuntarily firing spontaneous motor units over 24-hours. It also establishes one of the first long-term data classification software packages that could be applied towards the analysis of different biological signals.

References

Alaimo MA, Smith JL, Roy RR, and Edgerton VR. 1984. "EMG Activity of Slow and Fast Ankle Extensors Following Spinal Cord Transection." Journal of Applied Physiology 56:1608-1613.

Alford EK, Roy RR, Hodgson JA, and Edgerton VR. 1987. "Electromyography of Rat Soleus, Medial Gastrocnemius, and Tibialis Anterior During Hind Limb Suspension." Experimental Neurology 96:635-649.

American Spinal Injury Association (ASIA). 2006. "Dermatome Chart." http://www.asia-spinalinjury.org/publications/2006_Classif_worksheet.pdf

Airaksinen MK, Kankaanp M, Aranko O, Leinonen V, Arokoski JPA, Airaksinen O. 2005. "Wireless On-line Electromyography in Recording Neck Muscle Function: A Pilot Study." Pathophysiology 12:303-306.

Basmajian J and De Luca C, 1985. Muscles Alive: Their Functions Revealed by Electromyography, Fifth Edition. Williams and Wilkins: Baltimore

Bekka RE, Boudaoud S, and Chickouche D. 2002. "The Use of a Neural Network System in the Identification of Motor Unit Characteristics From Surface Detected Action Potentials: A Simulation Study." Journal of Neuroscience Methods 116:89-98.

Bennett DJ, Li Y, Harvey PJ, and Gorassini M. 2001. "Evidence for Plateau Potentials in Tail Motoneurons of Awake Spinal Rats with Spasticity." Journal of Neurophysiology 86:1972-1982.

Blewett C and Elder GCB, 1993. "Quantitative EMG Analysis in Soleus and Plantaris During Hind Limb Suspension and Recovery." Journal of Applied Physiology 74:2057-2066.

Boose A, Spieker S, Jentgens C, Dichgans J. 1996 "Wrist Tremor: Investigation of Agonist-antagonist Interaction by Means of Long-term EMG Recording and Cross-spectral Analysis." Electroencephalography and Clinical Neurophysiology 101: 355-363.

Burke RE, Levine DN, Tsairis P, and Zajac FE. 1973. "Physiological Types and Histochemical Profiles in Motor Units of the Cat Gastrocnemius." Journal of Physiology 34: 723–748.

Chauvet E, Fokapu O, Hogrel J-Y, Gamet D, and Duchêne E. 2003. "Automatic Identification of Motor Unit Action Potential Trains From Electromyographic Signals using Fuzzy Techniques." Medical and Biological Engineering and Computing 41:646-653.

Christodoulou CI and Pattichis CS. 1999. "Unsupervided Pattern Recognition for the Classification of EMG Signals." IEEE Transactions on Biomedical Engineering 46:169-178

Day SJ and Hulliger M. 2001. "Experimental Simulation of Cat Electromyogram: Evidence For Algebraic Summation of Motor-unit Action Potential Trains." Journal of Neurology 86:2144-2158.

Edin BB, Bäckström A, and Bäckström LO. 1988. "Single Unit Retrieval in Microneurography: A Microprocessor-based Device Controlled by an Operator." Journal of Neuroscience Methods 24:137-144.

Eken T. 1998. "Spontaneous Electromyographic Activity in Adult Rat Soleus Muscle." Journal of Neurophysiology 80:365-376.

Fang J, Agarwal GC, and Shahani BT. 1999. "Decomposition of Multi-unit Electromyographic Signals." IEEE Transactions on Biomedical Engineering 46:685-697.

Farina D, Fosci M, and Merletti R. 2002. "Motor Unit Recruitment Strategies Investigated by Surface EMG Variables." Journal of Applied Physiology 92:235-247.

Fausett, L. Fundamentals of Neural Networks. Prentice Hall: New Jersey, 1994.

Florestal JR, Mathieu PA, and Malanda A. 2006. "Automated Decomposition of Intramuscular Electromyographic Signals." IEEE Transactions on Biomedical Engineering 53:832-839.

Fournier M, Roy RR, Perham H, Simard CP, and Edgerton VR. 1983. "Is Limb Immobilization a Model of Disuse?" Experimental Neurology 80:147-156.

Fuglevand AJ, Bilodeau M, and Enoka RM. 1995. "Short-term Immobilization Has a Minimal Effect on the Strength and Fatigability of a Human Hand Muscle." Journal of Applied Physiology 78:847-855.

Gorassini MA, Bennett DJ, and Yang JF. 1998. "Self-sustained Firing of Human Motor Units." Neuroscience Letters 247:13-16.

Gorassini M, Bennett DJ, Kiehn O., Eken T., and Hultborn H. 1999. "Activation Patterns of Hindlimb Motor Units in the Awake Rat and Their Relation to Motoneuron Intrinsic Properties." Journal of Neurophysiology 82:709-717.

Gorassini M, Bennett DJ, Kiehn O., Eken T., and Hultborn H. 1999. "Activity of Hind Limb Motor Units During Locomotion in the Conscious Rat." Journal of Neurophysiology 83:2002-2011.

Gorassini M, Knash ME, Harvey PJ, Bennett DJ, and Yang JF. 2004. "Role of Motoneurons in the Generation of Muscle Spasms After Spinal Cord Injury." Brain 127:2247-2258.

Florestal JR, Mathieu PA, and Malanda A. 2006. "Automated Decomposition of Intramuscular Electromyographic Signals." IEEE Transactions on Biomedical Engineering 53:832-839.

Guyton A and Hall J, 1996. Textbook of Medical Physiology. W. B. Saunders Co: Philadelphia.

Häger-Ross CK, Klein CS, and Thomas CK. 2006. "Twitch and Titanic Properties of Human Thenar Motor Units Paralyzed by Chronic Spinal Cord Injury." Journal of Neurophysiology 96:165-174.

Hassoun MH, Wang C, and Spitzer AR. 1994. "NNERVE: Neural Network Extraction of Repetitive Vectors for Electromyography – Part I: Algorithm." IEEE Transactions on Biomedical Engineering 41:1039-1052.

Haykin, S. Neural Networks: A Comprehensive Foundation, 2nd Edition. Prentice Hall Inc.: New Jersey, 1999.

Heckman CJ, Gorassini M, and Bennett DJ. 2005. "Persistent Inward Currents in Motoneuron Dendrites: Implications for Motor Output." Muscle and Nerve 31:135-156.

Hennig R and Lomo T. 1985. "Firing Patterns of Motor Units in Normal Rats." Nature 314:164-166.

Hensbergen E and Kernell D. 1992. "Task-related Differences in Distribution of Electromyographic Activity Within Peroneus Longus Muscle of Spontaneously Moving Cats." Experimental Brain Research 89:682-685.

Hensbergen E and Kernell D. 1997. "Daily Durations of Spontaneous Activity in Cat's Ankle Muscles." Experiments in Brain Research 115:325-332.

Hertz J, Krogh A, and Palmer RG. Introduction to the Theory of Neural Computation. Addison-Wesley: New York, 1991.

Henneman, E, Somjen G, and Carpenter DO. 1965. "Functional Significance of Cell Size in Spinal Motoneurons." Journal of Neurophysiology 28:560-580.

Hoffer JA, Sugano N, Loeb GE, Marks WB, O'Donovan MJ, and Pratt CA. 1987. "Cat Hind Limb Motoneurons During Locomotion. II. Normal activity patterns." Journal of Neurophysiology 57:530-553.

Hodgson JA, Roy RR, Higuchi N, Monti RJ, Zhong H, Grossman E, and Edgerton VR. 2005. "Does Daily Activity Level Determine Muscle Phenotype?" Journal of Experimental Biology 208:3761-3770.

Hodgson JA, Wichayanuparp S, Recktenwald MR, Roy RR, McCall G, Day MK, Washburn D, Fanton JW, Kozlovskaya I, and Edgerton VR. 2001. "Circadian Force and EMG Activity in Hind Limb Muscles of Rhesus Monkeys." Journal of Neurophysiology 86:1430-1444.

Jackson A, Mavoori J, and Fetz E. 2007. "Correlations between the Same Motor Cortex Cells and Arm Muscles During a Trained Task, Free Behavior, and Natural Sleep in the Macaque Monkey." Journal of Neurophysiology 97:360-374.

Jain AK and Dubes RC. Algorithms for Clustering Data. Prentice Hall: New Jersey, 1988.

Kapit W and Elson LM. The Anatomy Coloring Book. Harper and Row: New York, 1977. Plate 36.

Kawamura J, Ise M, and Tagami M. 1989. "The Clinical Features of Spasms in Patients With a Cervical Cord Injury." Paraplegia 27:222-226.

Kern DS, Semmler JG, and Enoka RM. 2001. "Long-term Activity in Upper- and Lower-limb Muscles of Humans." Journal of Applied Physiology 91:2224-2232.

Kernell D, Hensbergen E, Lind A, and Eerbeek O. 1998. "Relation between Fibre Type Composition and Daily Duration of Spontaneous Activity in Ankle Muscles of the Cat." Archives Italiennes de Biologie 136:191-203.

Kiehn O and Eken T. 1997. "Prolonged Firing in Motor Units: Evidence of Plateau Potentials in Human Motoneurons?" Journal of Neurophysiology 76:3061-3068.

Kravitz HM, Corcos DM, Hansen G, Penn RD, Cartwright RD, Gianino J. 1992. "Intrathecal Baclofen: Effects on Nocturnal Leg Muscle Spasticity." American Journal of physical and Medical Rehabilitation 71:48-52.

Kukulka CG and Clamann PH. 1981. "Comparison of the Recruitment and Discharge Properties of Motor Units in Human Brachial Biceps and Adductor Pollicis During Isometric Contractions." Brain Research 219:45-55.

Lee RH and Heckman CJ. 1998. "Bistability in Spinal Motoneurons In Vivo: Systematic Variations in Persistent Inward Currents." Journal of Neurophysiology 80: 583-593.

Little JW, Micklesen P, Umlauf R, and Britell, C. 1989. "Lower Extremity Manifestations of Spasticity in Chronic Spinal Cord Injury." American Journal of Physical and Medical Rehabilitation 68:32-36.

Loeb GE and Gans C. Electromyography for Experimentalists. University of Chicago Press: Chicago, 1986.

Looney, CG. Pattern Recognition Using Neural Networks. Oxford University Press: New York, 1997.

Maglaveras N, Stamkopoulos T, Diamantaras K, Pappas C, and Strintzis M. 1998. "ECG Pattern Recognition and Classification Using Non-linear Transformations and Neural Networks: A Review." International Journal of Medical Informatics 52:191-208.

Mark RG and Moody GB. "ECG Arrythmia Analysis: Design and Evaluation Strategies." In: Advances in Processing and pattern Analysis of Biological Signals. Gath, I and Inbar G.F. (eds.) pp 251-272, 1996.

Mavoori J, Jackson A, Diorio C, and Fetz E. 2005. "An Autonomous Implantable Computer for Neural Recording and Stimulation in Unrestrained Primates." Journal of Neuroscience Methods 148:71-77.

Matthews PBC. 1996. "Relationship of Firing Intervals of Human Motor Units to the Trajectory of Post-spike After-hyperpolarization and Synaptic Noise." Journal of Physiology 492:597-628.

McGill KC. 2002. "Optimal Resolution of Superimposed Action Potentials." IEEE Transactions on Biomedical Engineering 49:640-650.

McGill K, Lateva ZC and Marateb HR. 2005. "EMGLAB: An Interactive EMG Decomposition Program." Journal of Neuroscience Methods 149:121-133.

Monster WA, Chan HC, and O'Connor D. 1978. "Activity Patterns of Human Skeletal Muscles: Relation to Muscle Fiber Type Composition." Science 200:314-317.

Mork PJ and Westgaard RH. 2004. "The Association Between Nocturnal Trapezius Muscle Activity and Shoulder and Neck Pain. European Journal of Applied Physiology 92:18-25.

Merletti R, Knaflitz M, and DeLuca CJ. 1992. "Electrically Evoked Myoelectric Signals." Critical Reviews in Biomedical Engineering 19:293-340.

O'Brien LM, Stebbens VA, Poets CF, Heycock EG, and Southall EP. 2000. "Oxygen Saturation During the First 24 Hours of Life." Archives of Disease in Childhood - Fetal and Neonatal Edition 83:F35-F38

Pedersen E, Klemar B, and Torring J. 1979. "Counting of Flexor Spasms." Acta Neurologica Scandinavica 60:164-169.

Pozzo M, Bottin A, Ferrabone R, and Merletti R. 2004. "Sixty-four Channel Wearable Acquisition System for Long-term Surface Myoelectrogram Recordings with Electrode Arrays." Medical and Biological Engineering and Computing 42:455-466.

Principe JC, Lefebvre WC, and Euliano NR. Neural and Adaptive Systems: Fundamentals Through Simulations. John Wiley and Sons: New York, 2000

Riley DA, Slocum GR, Bain JL, Sedlak FR, Sowa TE, and Mellender JW. 1990. "Rat Hind Limb Unloading: Soleus Histochemistry, Ultrastructure, and Electromyography." Journal of Applied Physiology 69:58-66.

Roy RR, Zhong H, Khalili N, Kim SJ, Higuchi N, Monti RJ, Grossman E, Hodgson JA, and Edgerton VR. 2007. "Is Spinal Cord Isolation a Good Model of Muscle Disuse?" Muscle and Nerve 35:312-321.

Schalk G, Carp JS, and Wolpaw JR. 2002. "Temporal Transformation of Multiunit Activity Improves Identification of Single Motor Units." Journal of Neuroscience Methods 114: 87-98.

Sheean G. 2002. "The Pathophysiology of Spasticity." European Journal of Neurology 9 (supplement 1):3-9.

Sherrington CS. 1929. "Some Functional Problems Attaching to Convergence." Proceedings of the Royal Society of London, Series B 105:332-362.

Shimatani Y, Nickles SA, Najafi K, and Bradley RM. 2003. "Long-term Recordings From Afferent Taste Fibers." Physiological Behavior 80:309-315.

Sporrong HK, Sandsjo JK, Kadefors R, and Herberts P. 1999. "Assessment of Workload and Arm Position During Different Work Sequences: A Study with Portable Devices on Construction Workers." Applied Ergonomics 30: 495-503.

Stashuk DW. 1999. "Decomposition and Quantitative Analysis of Clinical Electromyographic Signals." Medical Engineering in Physics 21:389-404.

Stashuk DW. 2001. "EMG Signal Decomposition: How Can It Be Accomplished and Used?" Journal of Electromyography and Kinesiology 11: 151-173

Stein RB, Brucker BS, and Ayyar DR. 1990. "Motor Units in Incomplete Spinal Cord Injury: Electrical Activity, Contractile Properties, and the Effects of Biofeedback." Journal of Neurology, Neurosurgery, and Psychiatry 53-880-885.

Taricco M, Pagliacci MC, Telabo E, and Adone R. 2006. "Pharmacological Interventions For Spasticity Following Spinal Cord Injury: Results of a Cochrane Systematic Review." Eura Medicophys 43:5-15.

Tepavac D, Swenson JR, Stenehjem, J, Saranovic I, and Popovic D. 1992. "Microcomputer-based Portable Long-term Spasticity Recording System." IEEE Transactions on Biomedical Engineering 39:426-431.

Thomas CK, Johansson RS, Westling G, and Bigland-Ritchie B. 1990. "Twitch Properties of Human Thenar Motor Units Measured in Response to Intraneural Motor-axon Stimulation." Journal of Neurophysiology 64:1339-46.

Thomas CK, Johansson RS, and Bigland-Ritchie B. 1991. "Force-frequency Relationships of Human Thenar Motor Units." Journal of Physiology 65:1509-16.

Thomas CK. 1997. "Contractile Properties of Human Thenar Muscles Paralyzed by Spinal Cord Injury." Muscle and Nerve 20:788-799.

Thomas CK and Ross BH. 1997. "Distinct Patterns of Motor Unit Behavior During Muscle Spasms in Spinal Cord Injured Subjects." Journal of Neurophysiology 77:2847-2850.

Westling G, Johansson RS, Thomas CK, and Bigland-Ritchie B. 1990. "Measurement of Contractile and Electrical Properties of Single Human Thenar Motor Units in Response to Intraneural Motor-axon Stimulation." Journal of Neurophysiology 64:1331-1338.

Wise. 2004. "Spinal Cord Injury Levels and Classification." http://carecure.rutgers.edu/Spinewire/Articles/SpinalLevels/SpinalLevels.html.

Velis D, Plouin P, Gotman J, and da Silva FL. 2007. "Recommendations Regarding the Requirements and Applications for Long-term Recordings in Epilepsy." Epilepsia 48:379-384.

Zennaro D, Welley P, Koch VM, Moschytz GS, and Laubli T. 2003. "A Software Package for the Decomposition of Long Term Multichannel EMG Signals Using Wavelet Coefficients." IEEE Transactions on Biomedical Engineering 50:58-69.

Zijdewind I and Thomas CK. 2001. “Spontaneous Motor Unit Behavior in Human Thenar Muscles after Spinal Cord Injury.” Muscle and Nerve 24:952-962.

Zijdewind I, Peterson L, and Thomas CK. 2004. “Firing Patterns of Spontaneously Active Motor Units in Spinal Cord Injured Subjects.” Abstract presented at the Active Dendrites in Motor Neurons Conference.

Zouridakis G and Tam DC. 2000. “Identification of Reliable Spike Templates in Multi-unit Extracellular Recordings Using Fuzzy Clustering.” Computer Methods and Programs in Biomedicine 61:91-98.

Zurada JM. Introduction to Artificial Neural Systems. West Publishing: New York, 1992.